27715

NATIONAL LIBRARY
OTTAWA

BIBLIOTHÈQUE NATIONALE
OTTAWA

NAME OF AUTHOR....DAVID STEPHEN NASH......

TITLE OF THESIS.....WEB SLENDERNESS..........
LIMITS FOR NON-COMPACT
BEAM-COLUMNS...............

UNIVERSITY....UNIVERSITY OF ALBERTA......

DEGREE FOR WHICH THESIS WAS PRESENTED..M.Sc. (CIVIL ENGINEERING)

YEAR THIS DEGREE GRANTED......1976......................

Permission is hereby granted to THE NATIONAL LIBRARY OF CANADA to microfilm this thesis and to lend or sell copies of the film.

The author reserves other publication rights, and neither the thesis nor extensive extracts from it may be printed or otherwise reproduced without the author's written permission.

(Signed)..Stephen Nash.......

PERMANENT ADDRESS:

575 GEORGE ST,
BUCKINGHAM, QUEBEC
....

DATED.....Feb 6........1976

NL-91 (10-68)

INFORMATION TO USERS

THIS DISSERTATION HAS BEEN
MICROFILMED EXACTLY AS RECEIVED

This copy was produced from a micro-fiche copy of the original document. The quality of the copy is heavily dependent upon the quality of the original thesis submitted for microfilming. Every effort has been made to ensure the highest quality of reproduction possible.

PLEASE NOTE: Some pages may have indistinct print. Filmed as received.

Canadian Theses Division
Cataloguing Branch
National Library of Canada
Ottawa, Canada K1A 0N4

AVIS AUX USAGERS

LA THESE A ETE MICROFILMEE
TELLE QUE NOUS L'AVONS RECUE

Cette copie a été faite à partir d'une microfiche du document original. La qualité de la copie dépend grandement de la qualité de la thèse soumise pour le microfimage. Nous avons tout fait pour assurer une qualité supérieure de reproduction.

NOTA BENE: La qualité d'impression de certaines pages peut laisser à désirer. Microfilmée telle que nous l'avons reçue.

Division des thèses canadiennes
Direction du catalogage
Bibliothèque nationale du Canada
Ottawa, Canada K1A 0N4

THE UNIVERSITY OF ALBERTA

WEB SLENDERNESS LIMITS FOR NON-COMPACT BEAM-COLUMNS

©

by

DAVID STEPHEN NASH

A THESIS
SUBMITTED TO THE FACULTY OF GRADUATE STUDIES AND RESEARCH
IN PARTIAL FULFILLMENT OF THE REQUIREMENTS
FOR THE DEGREE OF MASTER OF SCIENCE

DEPARTMENT OF CIVIL ENGINEERING

EDMONTON, ALBERTA, CANADA
SPRING, 1976

THE UNIVERSITY OF ALBERTA

THE FACULTY OF GRADUATE STUDIES AND RESEARCH

The undersigned certify that they have read, and recommend to the Faculty of Graduate Studies and Research for acceptance, a thesis entitled WEB SLENDERNESS LIMITS FOR NON-COMPACT BEAM-COLUMNS submitted by DAVID STEPHEN NASH in partial fulfillment of the requirements for the degree of Master of Science.

G. L. Kulak
....
G. L. Kulak
Supervisor

D W Murray
....
D. W. Murray

Peter F Adams
....
P. F. Adams

J Kennedy
....
J. S. Kennedy

Dated: February 6, 1976.

DEDICATION

To Linda

ABSTRACT

This investigation was established in an attempt to determine more rational web slenderness limitations for non-compact beam-columns. The present limits, as set forth in the CSA S16.1 and S16.2 Standards, distinguish between compact and non-compact cross-sections only in the range of beam-column design of $0 \leq P/Py \leq 0.15$. This results in a limit which is too conservative, as non-compact sections are not required to deform to the same extent as compact sections.

The results of six beam-column tests, along with the test results from another investigation on non-compact beams are presented. Utilizing these results, this study indicates a safe limit to which the web slenderness limitation for non-compact beam-columns may be raised.

ACKNOWLEDGEMENTS

The author would like to express his appreciation to the following persons for their invaluable assistance during the experimental program and preparation of the thesis:

To the Canadian Institute of Steel Construction Council, for the financial support of this project,

To Professor Kulak, for his supervision and guidance,

To Professors Adams, Murray, and Kennedy, for serving on the examination committee,

To Mr. Alastair Dunbar, for programming the minicomputer, and subsequent assistance with the data reduction,

To Mr. Michael Perlynn, for his frequent explanations and clarifications of his thesis,

To Mr. Richard Helfrich, whose help during the experimental program made it a pleasure,

To Mr. Larry Burden, for taking care of many details during the experimental program,

To Mr. Roy Gitzel and Mr. Sheldon Lovell, for constructing the deflection measuring device and associated electronic control equipment,

To Mr. Robert Billey, for conducting the coupon tests,

To Mr. Armand Cadieux, for machining the trolley,

To Mr. Al Muir, for machining the coupons,

To Mr. Joe Rogers, for taking the photographs,

and

To Mrs. Doreen Wyman, for typing the symbols.

TABLE OF CONTENTS

TOPIC PAGE

RELEASE FORM i

TITLE PAGE ii

ACCEPTANCE FORM iii

DEDICATION iv

ABSTRACT v

ACKNOWLEDGEMENTS vi

TABLE OF CONTENTS viii

LIST OF TABLES xi

LIST OF FIGURES xii

CHAPTER I INTRODUCTION

1.1 General 1

1.2 Definition of the Problem 2

1.3 Objectives of the Research Proposal 4

CHAPTER II LITERATURE SURVEY

2.1 Previous Investigations 7

2.2 Development of CSA S16-1969 Code Requirements 9

2.3 Recent Code Revisions 12

CHAPTER III EXPERIMENTAL PROGRAM

3.1 Scope 17

3.2 Specimen Description 18
3.3 Test Arrangement 21
3.4 Testing Procedure 27

CHAPTER IV TEST RESULTS

4.1 Coupon Tests 39
4.2 Description of the Actual Test Procedure 40
4.3 Specimen Moment-Rotation Behaviour 42
4.4 Specimen Buckling Behaviour 45
4.5 Initial Deflections and their Effects 51
4.6 Second-Order Considerations 53

CHAPTER V THEORETICAL ANALYSIS

5.1 Analysis of CSA S16-1969 Specification Requirements 68
5.2 Investigation Leading to Recent CSA Standard Revisions 81
5.3 Analysis of Present Investigation Test Results-Method I 89
5.4 Analysis of Present Investigation Test Results-Method II 93
5.5 Discussion of Analytical Results 97

CHAPTER VI SUMMARY, CONCLUSIONS, AND RECOMMENDATIONS

6.1 Summary 116
6.2 Conclusions 117
6.3 Recommendations 119

NOMENCLATURE 122
REFERENCES 125
APPENDIX I DESIGN OF THE TEST SPECIMENS 129
APPENDIX II THE DEFLECTION MEASURING DEVICE
A2.1 Introduction 134
A2.2 The Trolley 134
A2.3 The Apparatus 136

LIST OF TABLES

No.	TITLE	PAGE
3.1	Proportions of Test Specimens	30
4.1	Specimen Moment and Failure Data	54
4.2	Initial Web Deflection Data	55
5.1	Specimen Test Data	103

LIST OF FIGURES

No. TITLE PAGE

1.1 Moment-Rotation Behaviour of Beam-Columns 5

1.2 Present CSA S16-1969 Flange Slenderness Requirements 5

1.3 Present Web Slenderness Requirements 6

2.1 Haaijer and Thurlimann's Inelastic Plate Buckling Curve 16

3.1 Details of Beam-Column Test Specimens 31

3.2 The Various Currently-Used Web Slenderness Limitations and the Test Specimens . 32

3.3 Idealized Test Setup 33

3.4 Test Setup 34

3.5 Instrumentation 35

3.6 Deflection Device Measuring Web 36

3.7 Deflection Device Measuring Flange 37

3.8 Mounting of Strain Gauges at Specimen Mid-Height 38

4.1 Determination of Coupon Static Yield Stress 56

4.2(a) Moment-Rotation Relationship - Specimen 1 57

4.2(b) Moment-Rotation Relationship - Specimen 2 57

4.2(c) Moment-Rotation Relationship - Specimen 3 58

4.2(d) Moment-Rotation Relationship - Specimen 4 58

4.2(e) Moment-Rotation Relationship - Specimen 5 59

4.2(f) Moment-Rotation Relationship - Specimen 6 59

4.3 Portion of Specimens Monitored
for Plate Deflections 60

4.4(a) Web and Flange Deflections - Specimen 1 61

4.4(b) Web and Flange Deflections - Specimen 2 62

4.4(c) Web and Flange Deflections - Specimen 3 63

4.4(d) Web and Flange Deflections - Specimen 4 64

4.4(e) Web and Flange Deflections - Specimen 5 65

4.4(f) Web and Flange Deflections - Specimen 6 66

4.5 Web and Flange Buckle (Specimen 6) 67

5.1 Idealized Stress-Strain Diagram 104

5.2 Plate Buckling Model 105

5.3 Plate Coefficient of Fully-Plastified
Wide-Flange Sections Subjected
to Axial Load and Moment 106

5.4 The Theoretical Limit of Web Slenderness
for Compact Members 107

5.5 Actual Stress Distribution
Including Residual Stresses 108

5.6 Typical residual Stresses for
Rolled and Welded Members 109

5.7 y/h as a Function of P/Py
(Compact and Non-Compact) 110

5.8 y/h as a Function of $\frac{h}{w}\sqrt{Fy}$ (Compact and Non-Compact) 111

5.9 K' as a Function of $\frac{h}{w}\sqrt{Fy}$ (Compact and Non-Compact) 112

5.10 The Theoretical Compact and Non-Compact Beam-Column Web Slenderness Limitations 113

5.11 Alpha as a Function of $\frac{h}{w}\sqrt{Fy}$ 114

5.12 Test Specimens and the Non-Compact Web Slenderness Limitation 115

6.1 The Bi-Linear Design Approximation 121

A1.1 Location of the Test Specimens 133

A2.1 Block Diagram of the Deflection Measuring Device 139

CHAPTER I

INTRODUCTION

1.1 General

According to the Canadian Standards Association Specification S16-1969(1), members subjected to combined axial load and bending moment (beam-columns), are classified as either non-compact, compact, or suitable for plastic design. The web and flange slenderness limitations set forth in the standard have been chosen so that a non-compact section can just reach the yield moment, a compact section can just reach the plastic moment, and a section suitable for plastic design can both reach the plastic moment and undergo sufficient rotation so that the moments can be redistributed before local buckling occurs. These requirements are shown in Figure 1.1.

It has been well established that the critical buckling stress of a plate loaded in uniform edge compression is a function of its width-to-thickness ratio(2),

$$\sigma_{cr} = \frac{K \pi^2 E}{12 (1 - \nu^2) (h/w)^2}$$

It follows, therefore, that the flange and web plate components of a beam or a beam-column must become progressively stockier in order that buckling be precluded as the deformation demands on the cross-section increase. Thus, in order to prevent the possibility of local buckling, the limiting flange and web slenderness ratios must be decreased for a given grade of steel as the member classification goes from non-compact to compact to plastic design.

Deformation requirements increase also as the yield strength of the material increases. More member deformation is required to develop the higher critical buckling stress. As a result, the critical plate slenderness ratios for higher strength steels must be less than those for lower strength steels. The present CSA requirements take this into account (Figures 1.2 and 1.3).

1.2 Definition of the Problem

The CSA S16-1969 Standard established one set of critical web slenderness limitations for all three classifications: non-compact, compact, and suitable for plastic design. The only difference in design was that non-compact sections involve a factor of safety against reaching the yield moment (reduced for axial load) and the compact and suitable for plastic design sections involve a factor of safety against reaching the plastic moment (reduced for axial load). If the stipulated web slenderness limitation was satisfactory for plastically designed members, then it must be conservative for compact members, and even more conservative for non-compact members where the deformation and strength requirements are less severe.

According to the web slenderness limits in CSA S16-1969, for values of P/Py (ratio of actual load to yield load) less than 0.28, the critical web slenderness ratio for a beam-column is linearly reduced as the applied axial load increases. For all values of P/Py greater than or equal to 0.28, the critical web slenderness ratio is constant for a given grade of steel. This is illustrated in Figure 1.3.

Both the CSA S16-1969 Standard and the American Institute of Steel Construction Specification(3) have based their web slenderness limitations primarily on a series of tests conducted by Haaijer(4) in 1956 on stub columns and short beam specimens of ASTM-A7 steel. In only three of the tests was failure associated with web buckling, and each of these occurred in the stub column (pure compresion) tests.

Recently, Perlynn and Kulak(5) have shown that a substantial relaxation of the web slenderness requirements can safely be implemented for compact beam-columns, and their recommendations for both non-compact and compact beam-columns have been introduced into the CSA Standard S16.1(6) on limit states design and S16.2(7) on working stress design (Figure 1.3).

1.3 Objectives of the Research Proposal

The objectives of this investigation are threefold:

1. To examine the present and proposed web slenderness limitations for non-compact beam-columns by means of a suitable testing program,
2. To examine existing theories, and to develop, if necessary, additional theories to adequately describe the behaviour of web plate buckling under combined axial load and bending,
3. To suggest revisions for the web slenderness limitations for non-compact beam-columns, if appropriate.

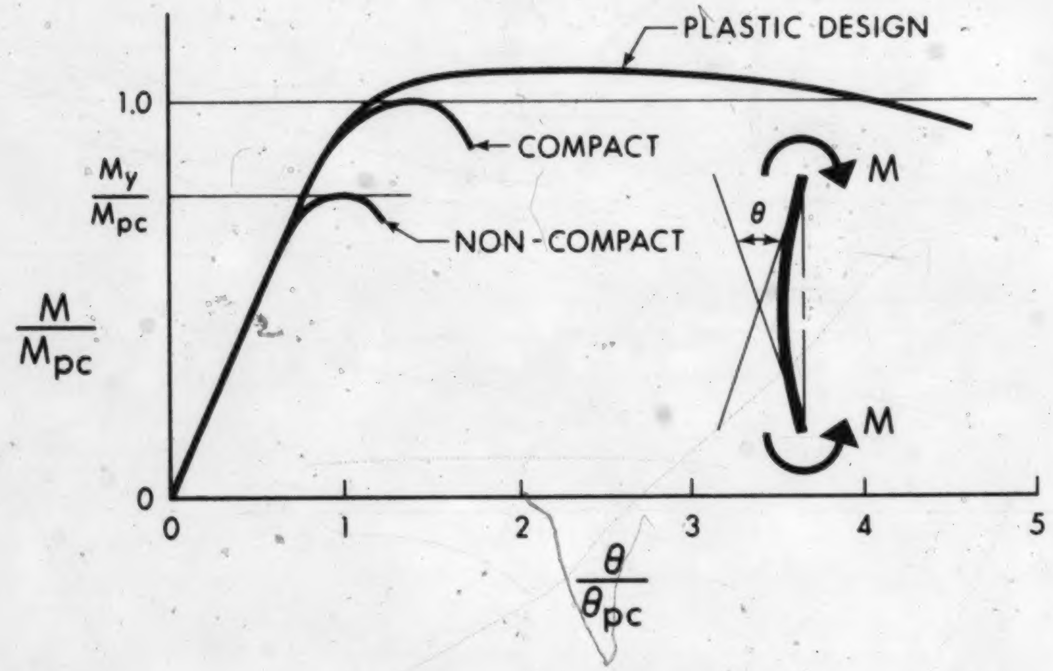

FIGURE 1.1

MOMENT-ROTATION BEHAVIOUR OF BEAM-COLUMNS

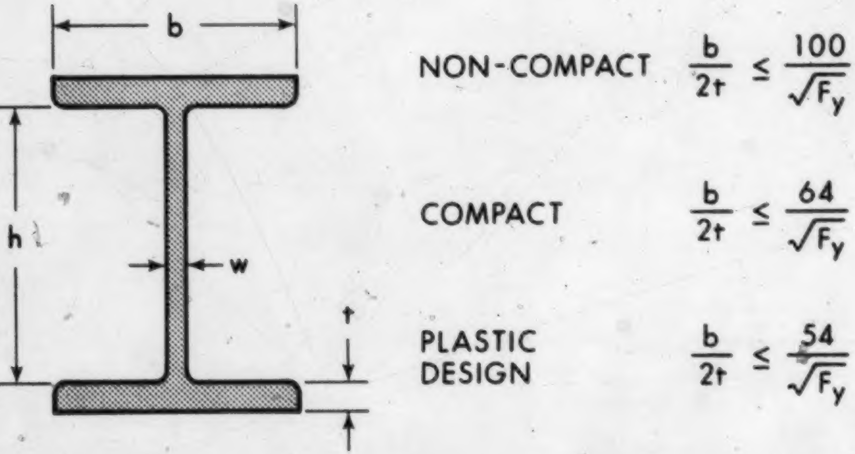
b
h
w
t
NON-COMPACT $\frac{b}{2t} \le \frac{100}{\sqrt{F_y}}$
COMPACT $\frac{b}{2t} \le \frac{64}{\sqrt{F_y}}$
PLASTIC DESIGN $\frac{b}{2t} \le \frac{54}{\sqrt{F_y}}$

FIGURE 1.2

PRESENT CSA S16-1969 FLANGE SLENDERNESS REQUIREMENTS

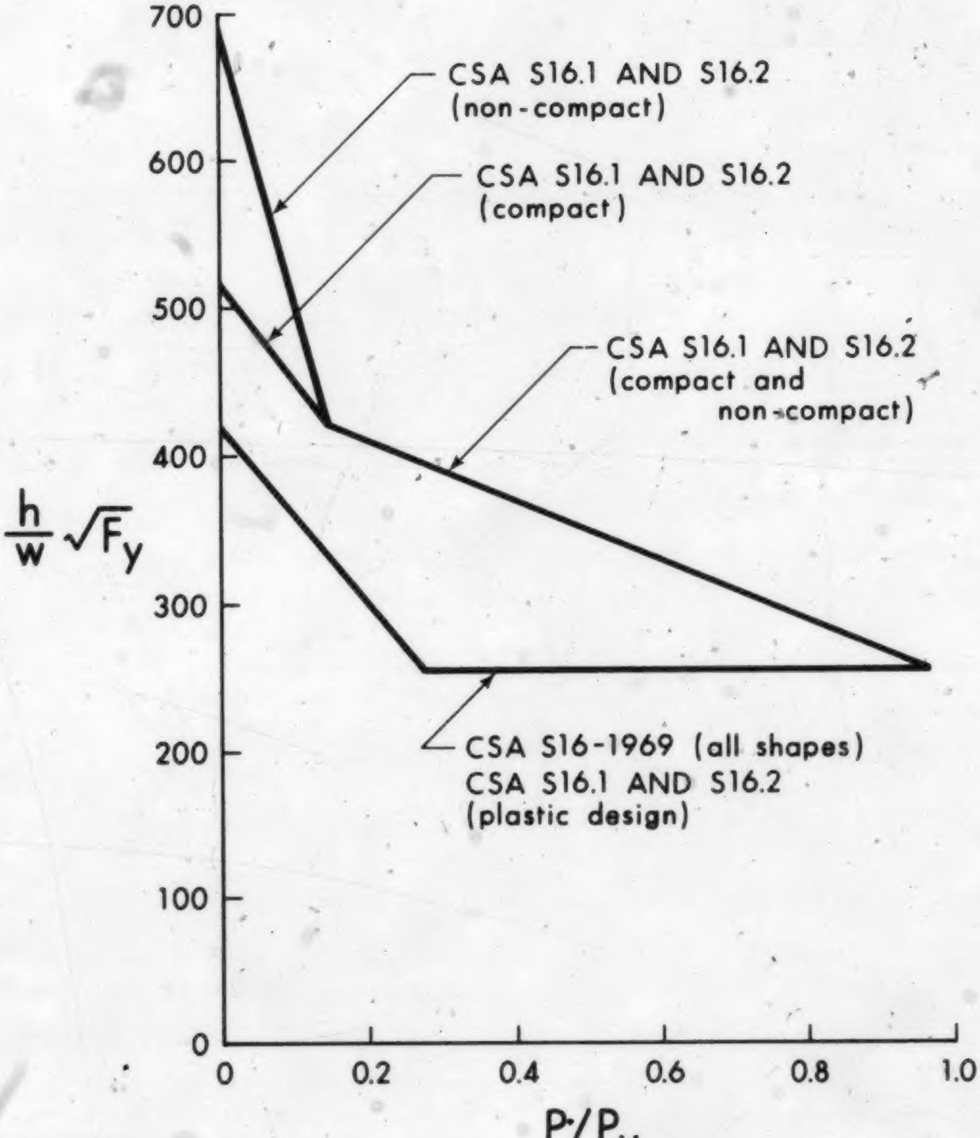

FIGURE 1.3

PRESENT WEB SLENDERNESS REQUIREMENTS

CHAPTER II

LITERATURE SURVEY

2.1 Previous Investigations

Comparatively only a small amount of research has been conducted into the problem of web buckling in beam-columns. Although buckling problems in general have been investigated over a long period of time, and plate buckling problems for the past half-century, it is only relatively recently that web buckling problems have been examined.

From the following fourth-order partial differential equation:

$$\frac{\partial^4 u}{\partial x^4} + 2\frac{\partial^4 u}{\partial x^2 \partial y^2} + \frac{\partial^4 u}{\partial y^4} = -\frac{w\sigma_x}{D}\frac{\partial^2 u}{\partial x^2} \qquad (2.1)$$

Timoshenko(2) derived the solution for the critical buckling stress in an isotropic simply-supported flat rectangular plate acting elastically under uniform edge loading in the longitudinal direction:

$$\sigma_{cr} = \frac{K\,\pi^2\,E}{12\,(1-\nu^2)\,(h/w)^2} \qquad (2.2)$$

where: σ_{cr}= elastic critical buckling stress,

E = Young's modulus,

ν = Poisson's ratio,

h = width of plate,

w = thickness of plate,

D = $EI/(1-\nu^2)$,

K = plate buckling coefficient.

The plate buckling coefficient, "K", was introduced into the equation to account for various ratios of length to width (the aspect ratio). Timoshenko showed that the minimum critical buckling stress for a plate simply-supported on all four sides could be found using $K = 4.0$ in Equation 2.2. This he showed to be valid for all length-to-width ratios.

This major development by Timoshenko opened the field of plate buckling to investigation by others. Of the many plate buckling models developed, some are concerned with plates subjected to loading conditions similar to those which web plates in a wide-flange member are required to withstand. The following two investigators have written comprehensive reviews:

Bleich(8) reviewed the literature dealing with elastic plate buckling under various edge support conditions, including the effects of various types of stiffeners. He also developed a method whereby inelastic plate buckling could be accounted for by varying the effective modulus of elasticity in the strain-hardening range.

McGuire(9) reviewed both elastic and inelastic plate buckling for plates by themselves and for plates making up various types of structural members. The differences between various codes and theories are also illustrated.

2.2 Development of the CSA S16-1969 Code Requirements

It was not until 1956 that a specific study into inelastic plate buckling was carried out(4). Prior to this it was generally accepted that when the yield stress of the material was reached, the element (column or plate) would buckle(10). Haaijer(4) investigated both flange and web plate buckling, accounting for both the inelastic behaviour of the material and the restraint against rotation provided at the web-to-flange junction. Good correlation was found to exist between Haaijer's web buckling theory and the results of his pure bending and pure compression tests on ASTM-A7 steel ($^{\sigma}$y=33ksi) wide-flange shapes. Some of the pure compression tests established that both web and flange plates were capable of reaching strain-hardening before the occurrence of buckling. Haaijer did not, however, consider the effects of residual stresses or the combined loading of in-plane bending and axial compression on web plates.

In 1958, Haaijer and Thurlimann(10) proposed a plate buckling relationship (Figure 2.1) which included an empirical transition curve for the inelastic range between the proportional limit and the point of strain-hardening. For prediction of web buckling, they also developed a web plate buckling equation based on Timoshenko's elastic plate buckling equation (Equation 2.2) for combined axial compression and in-plane bending. The result was an expression:

$$\alpha = \frac{h}{\pi w}\sqrt{\frac{12\,\sigma_y\,(1 - \nu^2)}{K\,E}} \qquad (2.3)$$

where: α = plate buckling modulus,

$\frac{1}{\alpha^2} = \frac{\sigma_{cr}}{\sigma_y}$

σ_{cr} = elastic critical buckling stress,

σ_y = yield strength of the material,

K = plate buckling coefficient for a fully-plastified wide-flange section.

They used this modified "K", the plate buckling coefficient, to account for inelastic plate behaviour, and showed that this procedure adequately described their three test results of failure due to web buckling in stub columns.

For a member that may be required to deform plastically, the following assumptions were made to develop a web buckling curve for design purposes:

1. $A/Aw=2.0$ (ratio of total area of wide-flange section to total area of web)
2. $h_t/h=1.05$ (ratio of total depth of wide-flange to clear depth of web)
3. $\varepsilon_m/\varepsilon_y=4.0$ (ratio of maximum strain in compression flange to yield strain)

Using these assumptions (taken as valid for an average wide-flange section), it followed that the neutral axis in a beam-column subjected to Mpc (plastic moment reduced for axial load) and $P/Py=0.28$, would have just reached the tension flange. Thus the whole web would be in compression, but not necessarily in uniform compression.

A theoretical design curve was first established, then approximated by two straight lines. The design curve has since been modified to make the web slenderness limitations applicable to steels of various yield strengths, and it is this representation that forms the basis for the AISC

Specification and CSA S16-1969; and also CSA S16.1 and S16.2 for plastic design sections. Figure 1.3 shows this limit.

It should be noted that no tests on specimens subjected to combined axial load and bending were done by Haaijer and Thurlimann, hence the theory was not experimentally verified for this mode of loading.

2.3 Recent Code Revisions

By conducting tests on nine beam-column specimens under different combinations of axial load and moment, Perlynn and Kulak(5) have shown that the previously-used web slenderness limitations(1,3) for compact beam-columns were too conservative. For their tests, they chose flanges which just met the S16-1969 requirements for compact flanges (Figure 1.2). By testing specimens with this flange proportion, it was known that if the flange buckled, the web was too stocky to be on the limit of web slenderness for a compact section. Similarly if the web buckled, it was too slender. By testing more than one specimen at each value of P/Py, they were able to determine quite closely where the limit would be when the flange and web would buckle simultaneously at the various P/Py ratios. This limit would then be the maximum web slenderness a compact beam-column should have in order to guarantee web buckling will not occur before flange buckling.

Perlynn and Kulak, however, were not able to satisfactorily correlate their results with Haaijer and Thurlimann's web buckling theory. Consequently, they developed two methods for predicting web buckling. In these, the effects of reasonable assumed residual stresses were included. Comparison between their methods and the results from three other testing programs (including Haaijer's) showed both methods capable of giving valid predictions of the occurrence of web buckling.

Using the limit of simultaneous web and flange failure which they established experimentally, Perlynn and Kulak developed a theoretical limit for maximum web slenderness ratios as a function of P/Py for compact beam-columns. The equation for the curve is:

$$\frac{h}{w}\sqrt{Fy} = 520\sqrt{1 - 0.695(P/Py)^{0.3846}} \qquad (2.4)$$

where: P = axial load,

Py= yield load of section,

Fy= yield stress of material,

h = clear web height,

w = web thickness.

This theoretical limit was then approximated for design purposes by a bi-linear expression:

(a) For $P/Py \leq 0.15$

$$\frac{h}{w}\sqrt{Fy} = 520\,[1 - 1.28(P/Py)]$$

(b) For $P/Py > 0.15$

$$\frac{h}{w}\sqrt{Fy} = 450\,[1 - 0.43(P/Py)]$$

These expressions have been incorporated into the CSA Standard S16.1 on limit states design and S16.2 on working stress design. Using the results of a testing program of non-compact beams(11), Perlynn and Kulak have also recommended the following bi-linear approximation to be used for the design of non-compact beam-columns:

(a) For $P/Py \leq 0.15$

$$\frac{h}{w}\sqrt{Fy} = 690\,[1 - 2.60(P/Py)]$$

(b) For $P/Py > 0.15$

$$\frac{h}{w}\sqrt{Fy} = 450\,[1 - 0.43(P/Py)]$$

where $\frac{h}{w}\sqrt{F_y} = 690$ was found to be a reasonable web slenderness limit for non-compact beams. This bi-linear approximation is different from that for compact beam-columns only in the region $0 \le P/P_y \le 0.15$. It was felt that since non-compact beam-columns do not have to undergo the same degree of deformation as compact beam-columns, a safe approximation would be to linearly reduce the slenderness limit from $\frac{h}{w}\sqrt{F_y} = 690$ at $P/P_y = 0$ to the junction of the linear approximations for compact members at $P/P_y = 0.15$. For $P/P_y \ge 0.15$, the web slenderness limitation for non-compact members was set at the same value as those for compact members pending a study into the possible limit to which the web slenderness of non-compact beam-columns may be raised. Figure 1.3 illustrates this approximation.

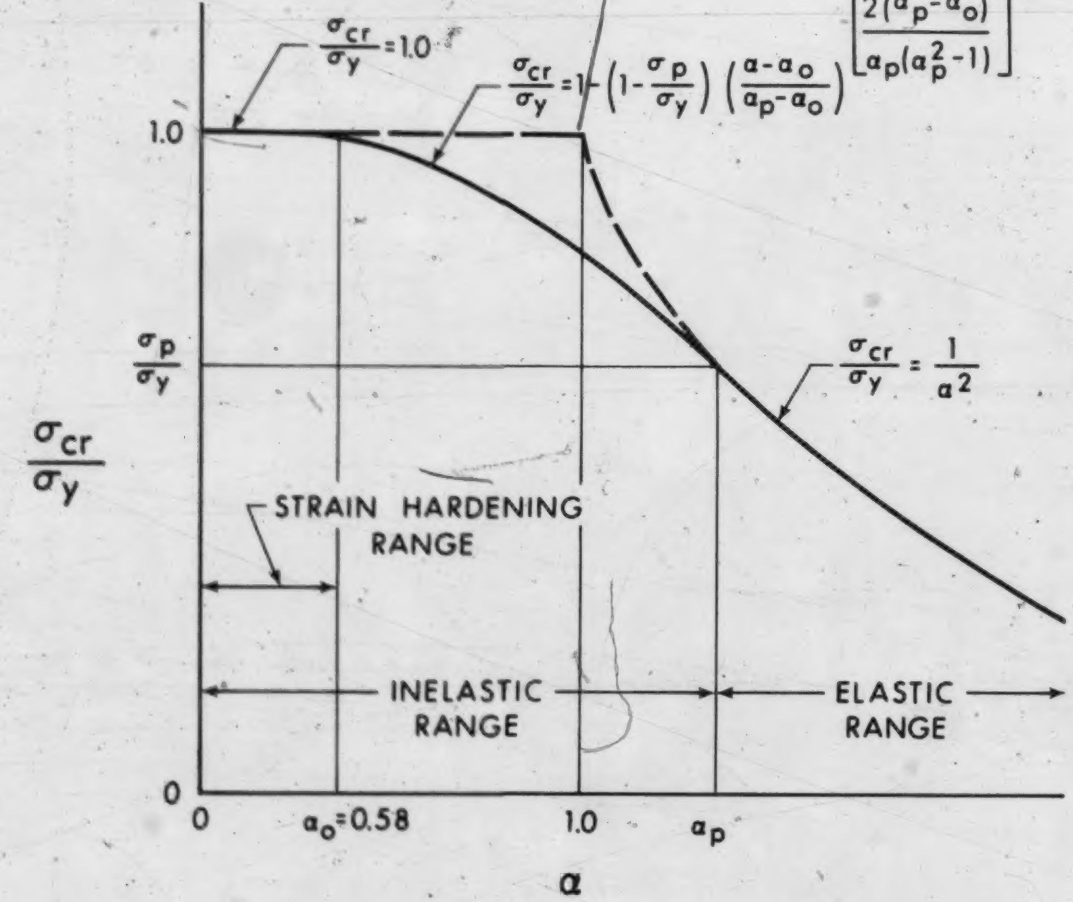

FIGURE 2.1

HAAIJER AND THURLIMANN'S INELASTIC PLATE BUCKLING CURVE

CHAPTER III

EXPERIMENTAL PROGRAM

3.1 Scope

For the purpose of examining the present non-compact web slenderness limitations (Figure 1.3), a total of six wide-flange specimens subjected to combined axial load and moment were tested. A flange shape common to all the specimens was established that just met the non-compact limitation of the CSA Standard S16 (i.e., $b/2t = 100/\sqrt{Fy}$). The webs of all the specimens were more slender than that allowed by the present CSA Standards[6,7] for non-compact members. The web depth (h) of the specimen was varied to produce the different web slenderness ratios desired (Table 3.1). For the six specimens tested, all had similar cross-sectional shapes with webs of the same thickness (Figure 3.1).

Tests were conducted at P/Py ratios of 0.15, 0.3, and 0.7 in order to obtain results representative of a wide range of beam-column design. A second consideration was to have the P/Py ratios slightly different from those in Perlynn and Kulak's testing program. It was hoped that by doing this, it would be possible to gain further understanding of general beam-column behaviour when the results of both investigations were studied. Two tests were conducted at each ratio of P/Py. The location of the test specimens relative to the various currently-used web slenderness limits is indicated in Figure 3.2 and their design is discussed in Appendix I.

It was felt that observation of the failure modes of the specimens would help to determine the web slenderness limit at which simultaneous web and flange buckling would occur. This limit would then be the maximum web slenderness that a non-compact beam-column could have in order to preclude local web buckling as the mode of member failure for loads up to the yield moment (reduced for axial load).

3.2 Specimen Description

The specimens were tested while simply-supported at their ends and with the moment applied by means of a concentrated load (P_2) placed eccentrically (Figure 3.3). A second axial load (P_1) was applied in such a way as to uniformly load the specimen over its cross-section. Thus the total axial load (P) acting on the specimen was the sum of the two individual loads and the applied moment (M) was the product of the eccentric load (P_2) and its eccentricity (e) from the centreline of the specimen. Because of the manner in which the concentrated loads were applied, the beam-column was essentially subjected to uniform compression and constant moment throughout its length, without the presence of shear. It was, therefore, theoretically possible that buckling could occur at any point along the length of the specimen. If the strong-axis deflections became significant during testing, however, the axial load acting through the deflection might increase the moment at mid-height enough to initiate buckling at this location.

The moment produced by the eccentrically placed concentrated load was transmitted to the beam-column specimen by means of reusable arms fabricated from back-to-back channels and cover plates. These arms were bolted to the cap plates at the ends of the specimens (Figure 3.3). It was felt that the connection would be stronger than the specimen, and buckling would not occur at either end of the specimen because of the presence of the cap plate. The arms were designed to withstand the maximum moment (Specimen 1), and the maximum load P (Specimen 5). They were checked against premature failure in bending, shear, and web crippling. It was considered that potential lateral-torsional buckling of the specimen, and lateral buckling of the moment arms would be resisted because the eccentric load would be acting against any deflections caused by twisting of the specimen or moment arms.

The webs of the specimens were fabricated from 1/4 inch thick CSA G40.21 Grade 44W steel plate(12). The flanges and webs had been designed on the basis of a yield stress of 44 ksi, the nominal yield stress of G40.21 Grade 44W steel plate less than 1-1/2 in. thick. Because of supply problems, it was decided to use a particular piece of plate of ASTM-A36[13] (σ_y=36ksi) steel for the flanges on the basis of a mill report that the yield stress of this piece was approximately 44 ksi. The flanges of all the beam-column specimens had dimensions of 5/16in. by 9-1/2in., and all were fabricated from the same mill rolling in an effort to have constant material properties. The flange dimensions resulted in a width-to-thickness ratio of 15.20, which just meets the non-compact limitation of 15.08 as established by the CSA Standard S16 for 44 ksi yield strength steel. It was also specified that the individual web plates be all taken from the same piece.

The clear length of the beam-column was established at 45 inches. This length provided adequate room for the placement of required gauges and recording equipment. The clear length also provided sufficient span over which the local buckling could occur without being restricted by the boundary effects at the ends. However, the length was short enough to prevent premature overall member buckling about the strong axis during testing.

To prevent member buckling about the weak axis, lateral bracing was provided for the tension and compression flanges of each of the beam-columns. A bracing arrangement based upon Watt's straight line mechanism[14] was attached by threaded pins welded at mid-height to the centreline of the flanges. This produced a short beam in the weak axis direction which met the bracing requirements for plastic design.

Although the lateral bracing prevented movement perpendicular to the weak axis, no other movement was restricted. The beam-column was, however, torsionally restrained at its mid-height by the manner in which the braces were attached. The bracing did not interfere with lateral movements perpendicular to the weak axis, nor did it interfere significantly with the local buckling of the flanges and webs. Since the beam-column itself was torsionally stable, the torsional restraint offered by the bracing system was not expected to affect the test results. Perlynn and Kulak did note, however, with their similar testing arrangement, that because the threaded pins were welded at the mid-height of the specimen in the middle of the flange, the local buckle did not occur there(5).

The proportions of the beam-column test specimens, as received, are shown in Table 3.1.

3.3 Test Arrangement

The concentric concentrated load (P_1) was applied using an MTS (Material Testing System 908.14) testing machine, capable of applying 1400 kips in compression. The base and bottom loading surface of the testing machine is fixed to the laboratory floor, while the cross head, which contains the hydraulic ram, is movable to accept specimens of various heights (Figure 3.4). The magnitudes of the concentric load were measured from an electronic transducer connected to an oil pressure line located within the compression head of the testing machine. The accuracy of this system of measurement is considered to be ±0.5%.

The eccentric load (P_2) was applied using a hydraulic centrehole jack rated at 120 kips maximum capacity (Figure 3.5). A 1-1/8 in. diameter high-strength steel rod, threaded at the ends, was bolted into place, passing upward through the upper arm and the centrehole jack and downward through the lower arm and a load cell capable of measuring up to 100 kips. With the centrehole jack applying a tensile load to the rod the resulting reactions tended to pull the arms towards each other. The effect not only created a stable loading arrangement, but the beam-column was further restrained against torsional buckling.

Steel rockers were provided at reaction points of the concentric load (i.e., at the top and bottom of the specimen). These seven inch radius rockers acted as simple supports. The bottom rocker, fabricated to the shape of a half-cylinder, permitted rotations only about the strong axis of the beam-column. However, the top rocker, part of the compression head of the testing machine, had a ball and socket joint. This permitted rotations about both axes at the top of the specimen. Weak axis rotations were not expected to be present.

Steel rockers 1-1/2 in. thick and with a radius of curvature of 4-1/2 in. were provided at the reaction points of the eccentric load. These were drilled to provide passage of the tension rod and rotated about a line parallel to the strong axis of the beam-column.

As a result of the precautions taken as to the physical assembly, no overall instability problems of the setup were encountered during the testing program.

Rotations of the specimen were recorded by means of an apparatus consisting of two light channel sections securely clamped to small plates welded to the cap plates at the top and bottom of the specimen, where the specimen was bolted to the moment arms. Three rod-and-plunger type transducers were placed between the channel sections. Two of these were mounted at 21 inches and 42 inches respectively from the centreline of the beam-column. From the readings of these two transducers, an average rotation could be determined. The third transducer was mounted co-incident with the beam-column centreline and recorded the axial shortening due to the loads. This was applied as a correction to determine the actual rotations.

Out-of-plane web and compression flange deflections were measured using a device which was originally developed to measure the depth of a stream bed in a hydraulics testing flume. This apparatus was modified so it would measure semi-automatically a series of web deflections on a predetermined grid size. This was done by means of a motorized trolley running along the tension flange which moved a depth-measuring probe over the flange and web of the specimen. The probe itself operates on optical principles and nothing physically touches the surface being monitored. This device is illustrated in Figure 3.6 in position to measure one vertical line of web deflections. It is also shown in Figure 3.7 in position to measure the compression flange deflections. This apparatus is discussed in greater detail in Appendix II. The compression flange deflection was measured about 1/2 in. from the outer edge of the flange. The accuracy of the readings taken by this device was considered to be about ±0.002 inch.

Since it was desired to keep the positions of the grid fairly constant with respect to the edges of the web (i.e., have each reading taken at the same place as the last time the apparatus measured the deflection at that grid point), it was decided to use the tension flange as datum for the measurements of web and compression flange deflections. Using the tension flange as datum would also give good measurements for the compression flange deflections as the readings would be automatically compensated for the effects of strong axis deflection and specimen rotation.

Using the tension flange as datum, however, loses its usefulness when the specimen's rotation (tension flange curvature) increases beyond a token amount, as when a buckle forms. When this occurs, the trolley following the tension flange would no longer be able to guide the probe device to the same grid locations for each set of readings. The deflections were of interest only up to the point in the test where the buckle became visible. The readings were taken mainly to determine or predict whether the web or the flange buckled first, and the trolley was removed before the curvature of the tension flange became excessive.

The strong axis deflections of the specimen were measured by six rod-and-plunger type transducers (Figure 3.5). Five of these were connected at approximately equal increments along the 45 inch length of the specimen. Because the bottom rocker support, unlike the top one, tended to travel as it rotated, the sixth transducer was mounted so as to monitor its translation. These readings were taken in case the buckle appeared at mid-height of the specimen, so that P-Δ effects could be incorporated into the analysis.

The strain distribution at the mid-height of the specimen was measured by means of a set of fourteen electric resistance strain gauges placed at the mid-height of the specimen (Figure 3.8). Four of these were placed on the inside face of the flanges, 1-3/4 in. from the flange edges. Because some of the wheels of the trolley ran on the inside of the flange, it was necessary to position the gauges this far from the edge of the flange. To obtain useful readings, all the gauges had to be the same distance from the edge of the flange. The remaining ten gauges were placed on the web, four 1-1/4 in. from the inside flange faces, and six at the three locations that divide the web into four equal increments. At each of the web locations, one gauge was placed on either side of the web in order to obtain an average reading. If web buckling was occurring at this location, (i.e., at the mid-height of the specimen) it would be noticed before any visual observation because of the marked increase in difference between the two strain readings. The four gauges closest to the inside flange faces were placed near the two positions along the web where the assumed residual strain distribution was zero.

All measurements were recorded on a Data General Nova 2 minicomputer serving as a data acquisition device. The analog measurements were converted to digital readings by the minicomputer's analog-to-digital converter, and the necessary data adjustments done at a later time on the minicomputer with prepared programs. The data was then transmitted via a tape device to the University of Alberta's main computer where the plots and other output were produced. The minicomputer made it possible to take many readings effortlessly, and hence very comprehensive web and flange deflection readings were taken during the tests.

Prior to testing, each specimen was whitewashed on the side not used for deflection measurements in order to aid in the observation of yield patterns. The other surfaces were painted flat white to enable the deflection apparatus to operate properly.

3.4 Testing Procedure

Although the top and bottom ends of the specimen were to be prepared square and true, imperfections were considered inevitable. As a result, before a specimen could be tested, it had to be aligned(15). The specimen was first centered between the head of the testing machine and the floor roller. Alignment was then accomplished by loading the specimen concentrically to 4 kips, and then to 50 kips with the testing machine, and reading the four strain gauges mounted near the flange tips for each load. Care was taken not to exceed the proportional limit of the material and cause premature yielding. The minicomputer was programmed to calculate the net eccentricities in the two directions of the horizontal plane for each of the testing machine loads. To do this, it used the four flange strain gauge readings as well as some specimen properties. The specimen was then unloaded, and shims were placed between the head of the testing machine and the top of the specimen, such that the eccentricities were reduced to less than 0.25 in. from the specimen cross-sectional centroid in both directions.

Once the specimen had been aligned, the concentric load was reduced to 4 kips to hold the specimen in position and all initial readings were taken. At this point in the test, the deflection device was installed and initialized.

To begin testing, the concentric load was applied in increments of approximately one-fifth of the total axial load P, with some readings taken after each increment. Upon reaching the total axial load P, moment application was started. Because the moment was applied by means of the eccentric load, an increase in moment was accompanied by an increase in eccentric load. To keep the total axial load constant, it was necessary to reduce the axial load applied by the testing machine by the same amount as the eccentric load was increased. The net effect was to apply moment to the specimen while the axial load remained constant. No attempt was made to lower the MTS load and increase the eccentric load simultaneously. This was not expected to affect the test results.

After each increment, and while holding the loads constant, all deformations were allowed to stabilize before a set of readings was taken. When failure was imminent, however, it became difficult to maintain the eccentric load at the value desired. Hence it was allowed to drop off, and when the readings were stable, they were taken. The maximum drop in a particular test was typically 2% of the maximum eccentric load, and hence was not expected to affect the readings significantly.

Strain gauge, rotation meter, strong-axis deflection readings, and the load readings were taken every load increment. Web and flange deflection readings were taken at intervals depending upon the slope of the moment-rotation curve and the amount of load present at that increment. These readings were taken at least every third increment, and as failure was pending, they were taken more often. Throughout the test the behaviour of the specimen was monitored by plotting the moment-rotation relationship.

Prior to the start of the beam-column tests, two series of standard coupon tests were conducted to determine the material behaviour and strength. Eight coupon tests were performed on the flange plate material, and six were performed on the web plate material. These were done on pieces of plate supplied by the specimen fabricator and taken from the same rollings as the web and flange materials.

SPECIMEN	P/Py	h (inches)	(h/w) $\sqrt{Fy}$
1	0.15	24.01	639.4
2	0.15	20.06	534.2
3	0.30	22.18	590.7
4	0.30	18.33	488.2
5	0.70	18.82	501.2
6	0.70	15.06	401.1

TABLE 3.1

PROPORTIONS OF TEST SPECIMENS

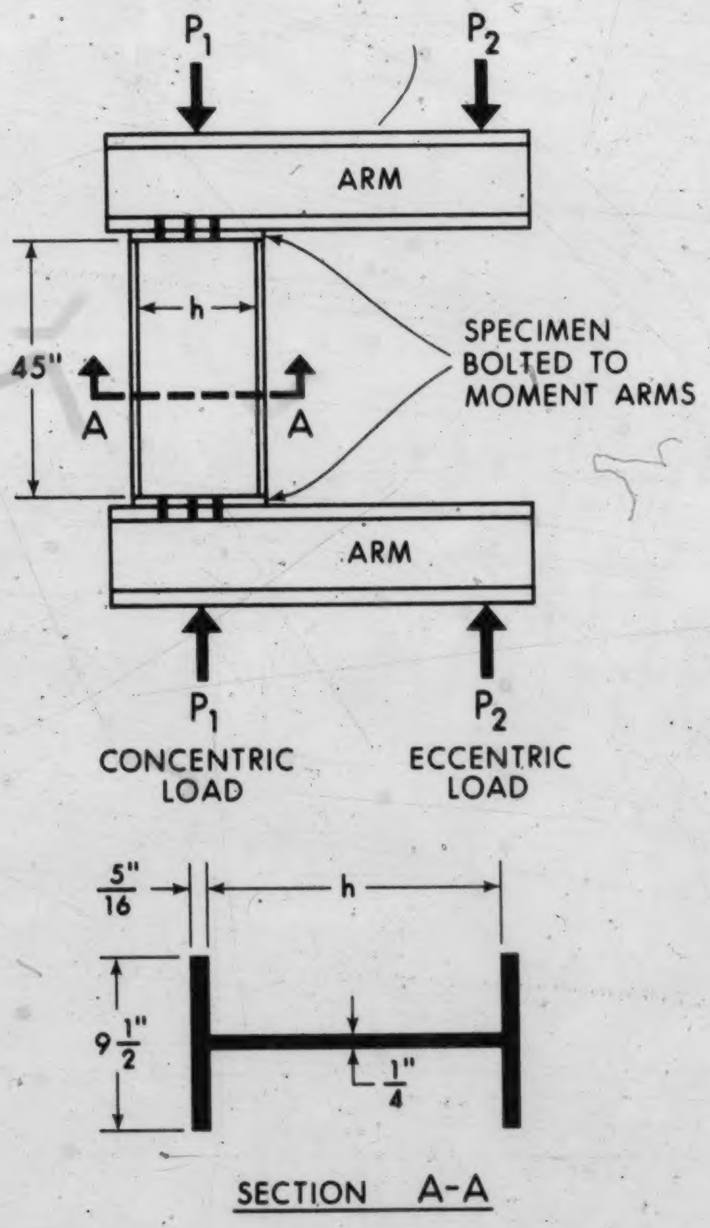
P1
P2
ARM
h
45"
A
A
SPECIMEN BOLTED TO MOMENT ARMS
ARM
P1
CONCENTRIC LOAD
P2
ECCENTRIC LOAD
5"/16
h
9 1"/2
1"/4
SECTION A-A

FIGURE 3.1

DETAILS OF BEAM-COLUMN TEST SPECIMENS

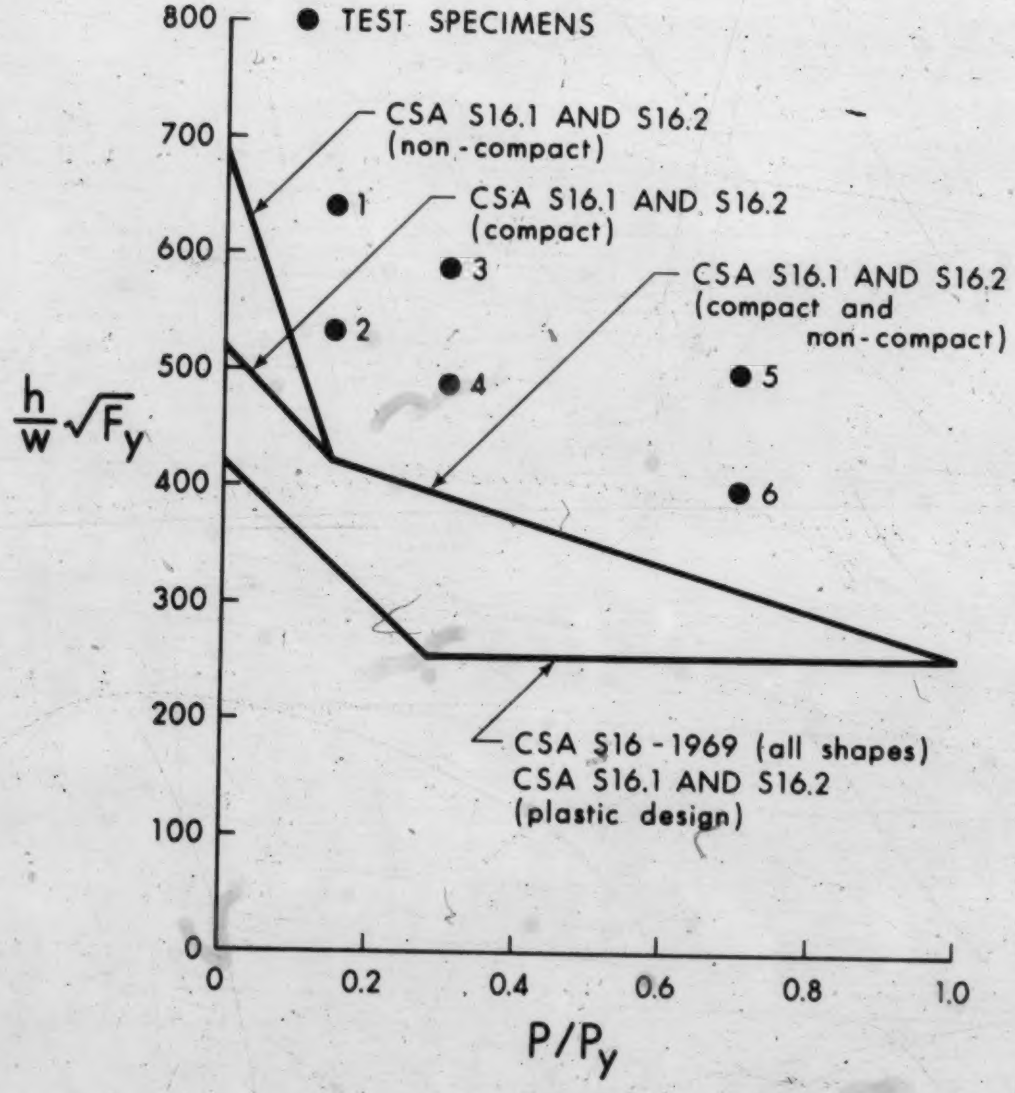

FIGURE 3.2

THE VARIOUS CURRENTLY-USED WEB SLENDERNESS LIMITATIONS AND THE TEST SPECIMENS

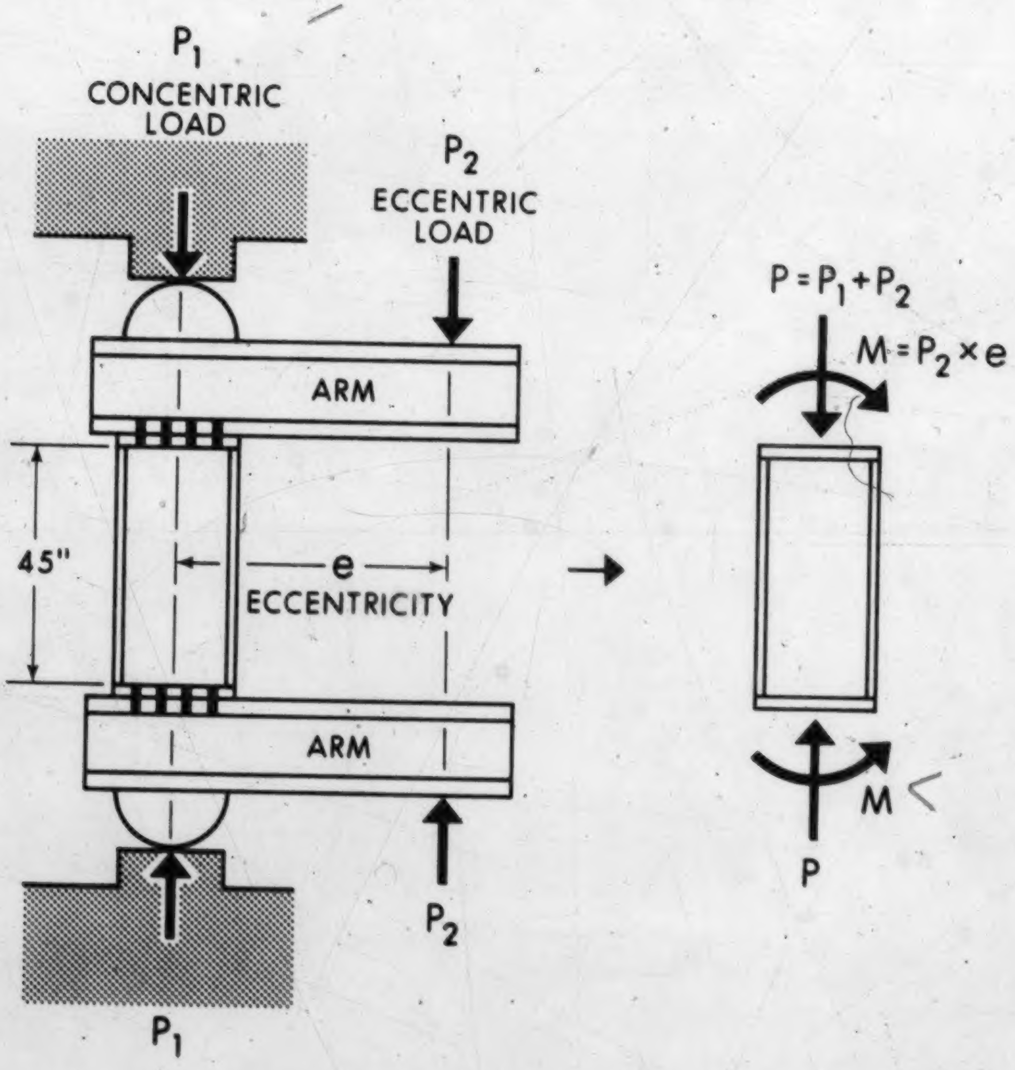
P_1
CONCENTRIC LOAD
P_2
ECCENTRIC LOAD
ARM
45"
e
ECCENTRICITY
ARM
P_1
P_2
$P = P_1 + P_2$
$M = P_2 \times e$
M
P

FIGURE 3.3

IDEALIZED TEST SETUP

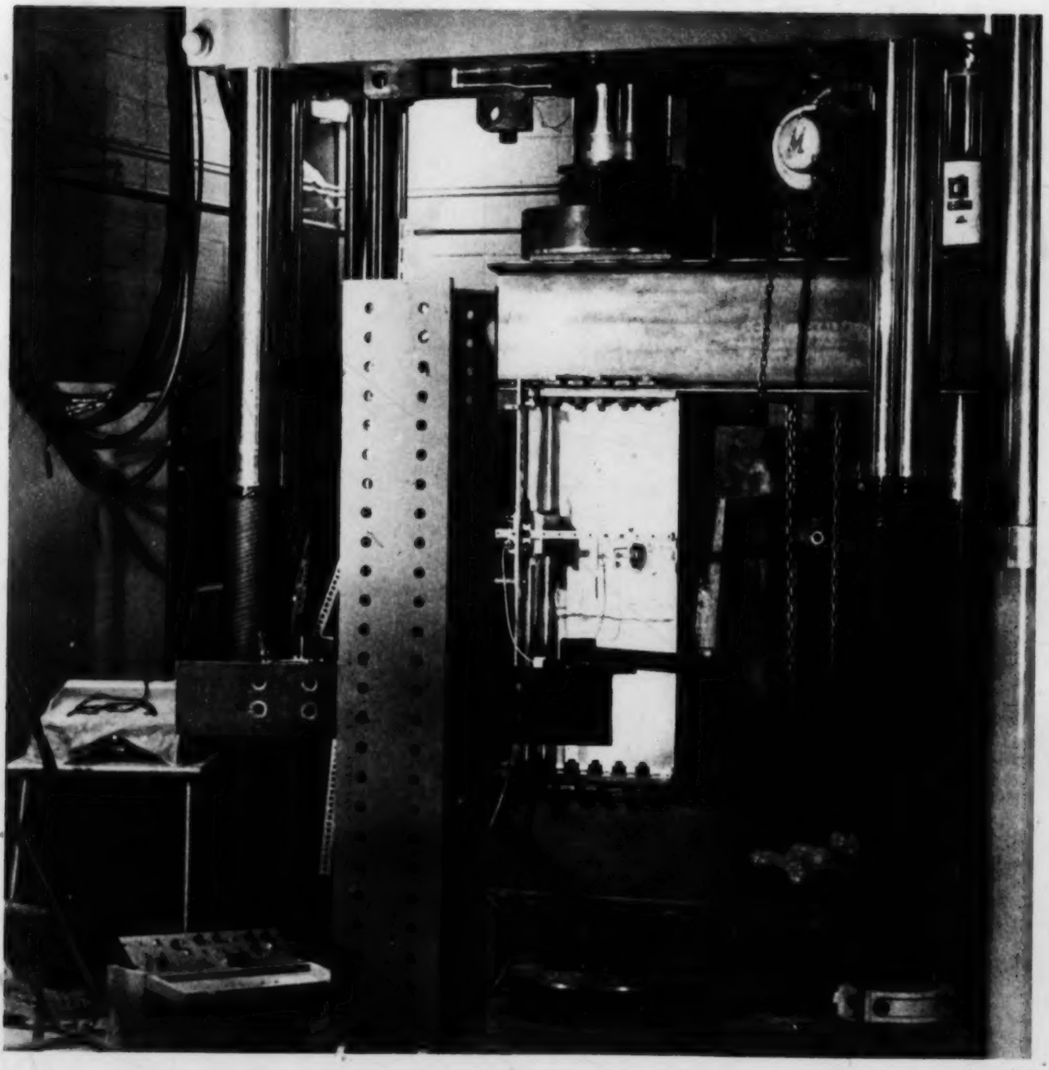

FIGURE 3.4

TEST SETUP

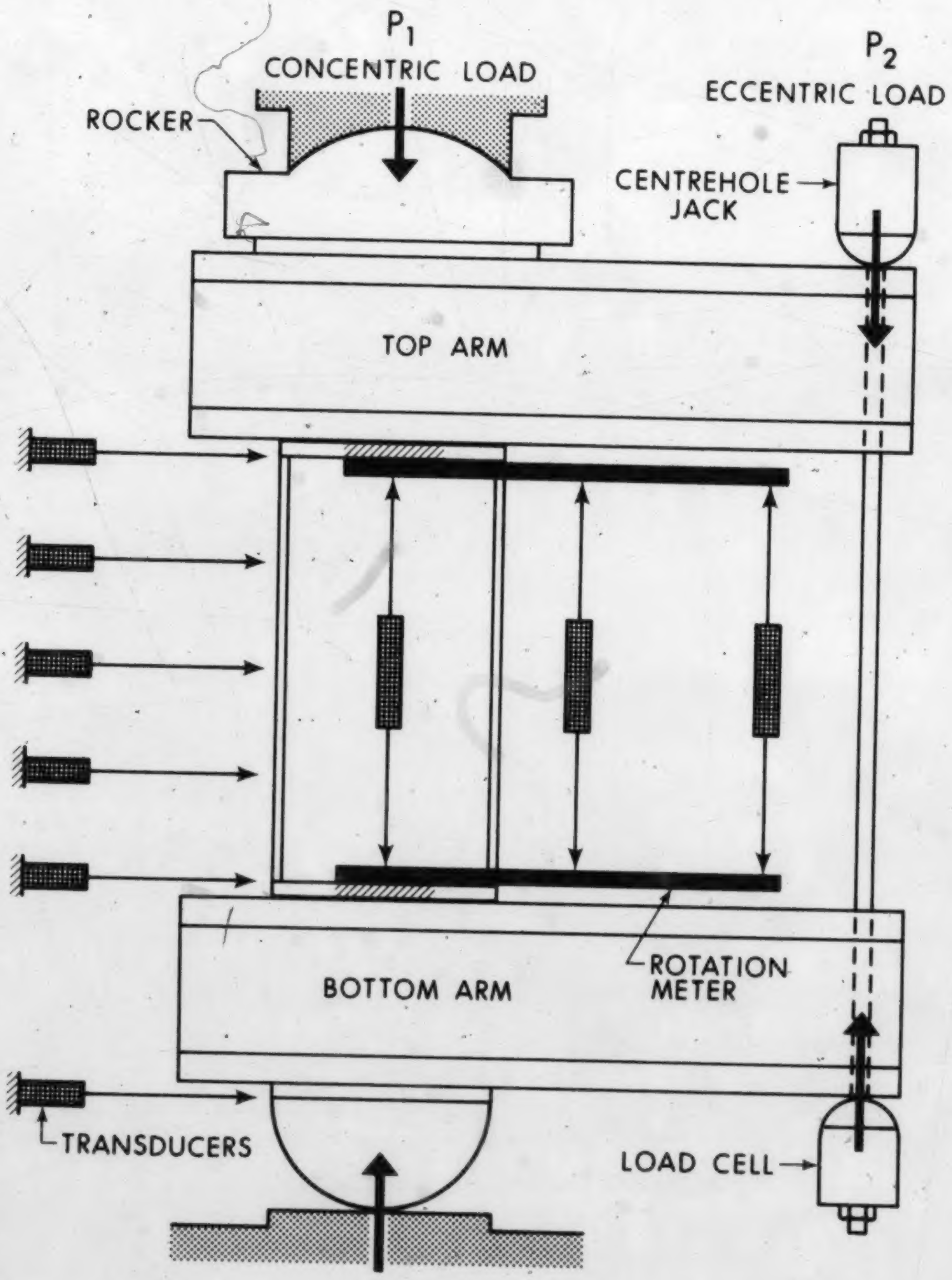
P$_1$
CONCENTRIC LOAD
P$_2$
ECCENTRIC LOAD
ROCKER
CENTREHOLE JACK
TOP ARM
BOTTOM ARM
ROTATION METER
TRANSDUCERS
LOAD CELL

FIGURE 3.5

INSTRUMENTATION

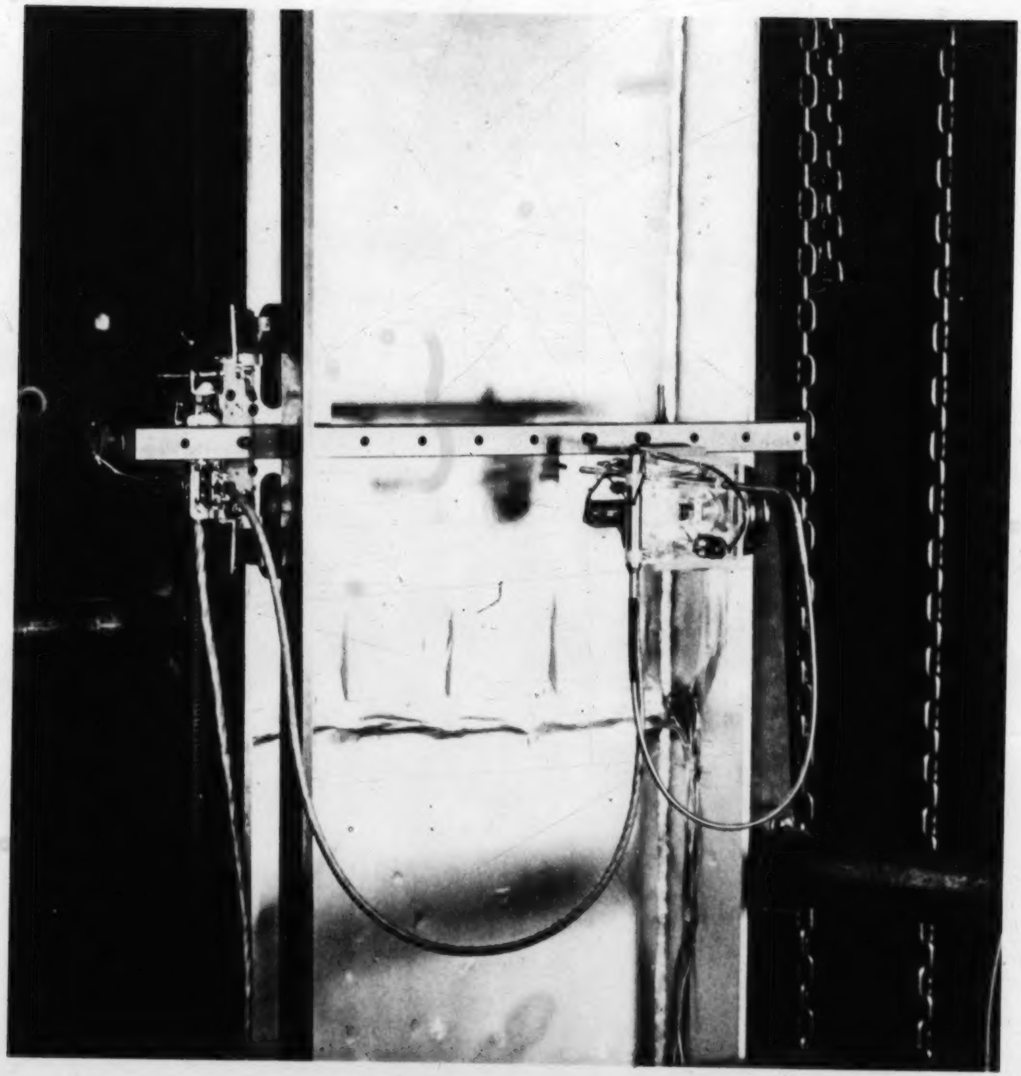

FIGURE 3.6

DEFLECTION DEVICE MEASURING WEB

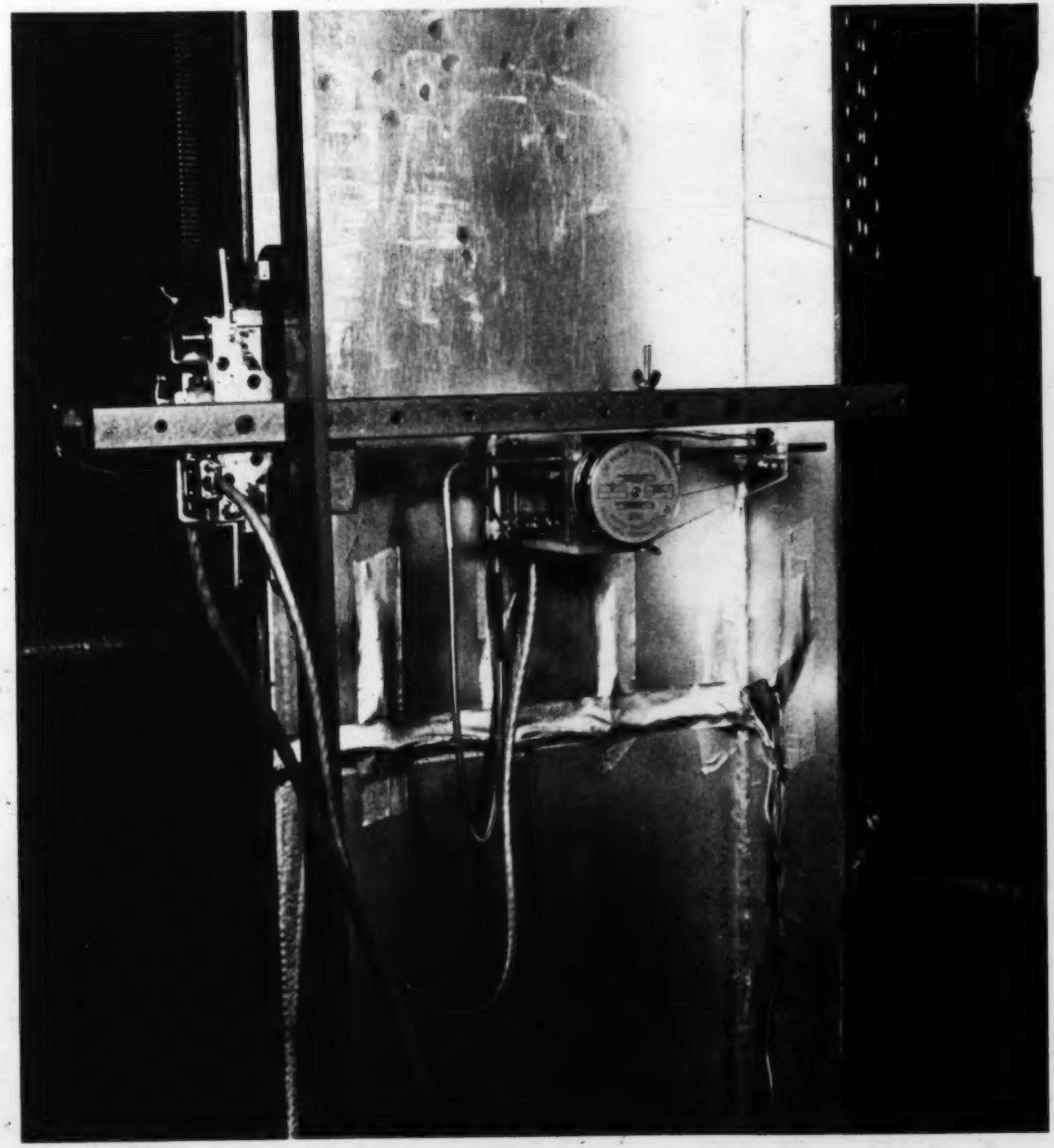

FIGURE 3.7

DEFLECTION DEVICE MEASURING FLANGE

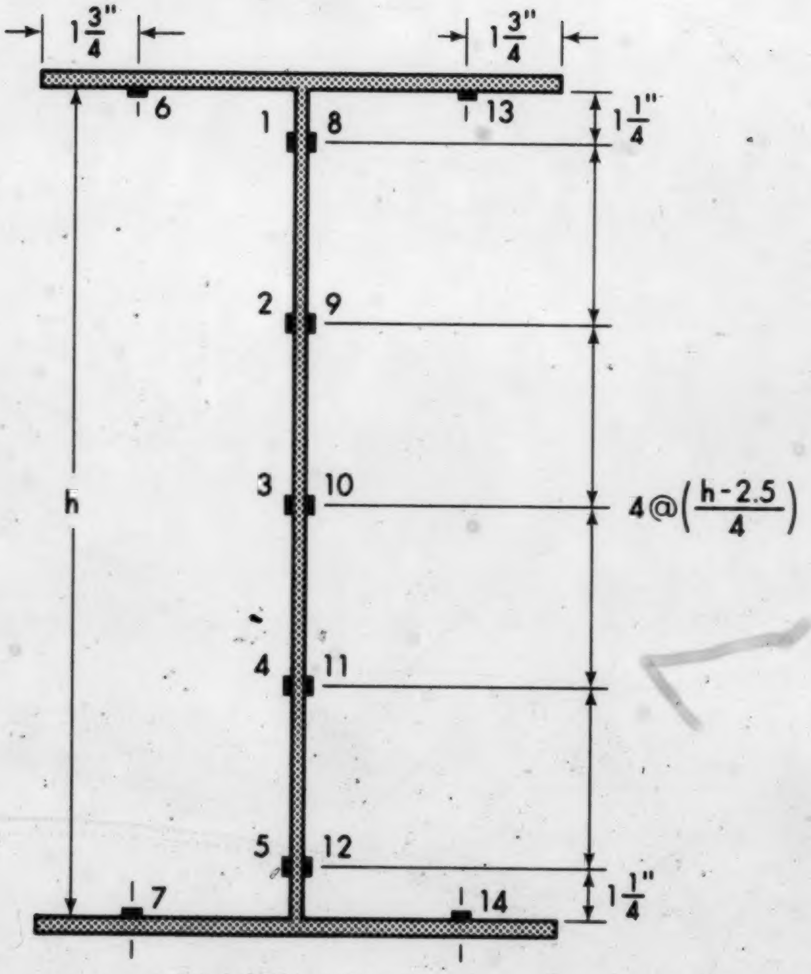

$1\frac{3}{4}''$
$1\frac{3}{4}''$
6
13
1
8
$1\frac{1}{4}''$
2
9
3
10
h
$4@\left(\frac{h-2.5}{4}\right)$
4
11
5
12
7
14
$1\frac{1}{4}''$

FIGURE 3.8

MOUNTING OF STRAIN GAUGES AT SPECIMEN MID-HEIGHT

CHAPTER IV

TEST RESULTS

4.1 Coupon Tests

From two series of tension tests done on standard coupons it was determined that the average static yield strength of the flange material was 44.53 ksi, and that of the web was 44.33 ksi. These values corresponded very closely to the nominal yield stress of 44.00 ksi, on which the specimen design was based. This was convenient for the analysis, and made easier the prediction of specimen behaviour before the tests were performed.

The coupons were sawed and milled from plates supplied by the specimen fabricator. The web coupon plate material was specified to be from the same rolling as the plate from which all the specimen webs had been fabricated. An identical procedure was followed for the flange plate material.

In all, fourteen coupon tests were performed. Six of these were on the web plate material, and the other eight on the flange plate material. Since the flange plate material was A36 steel, it was felt that the two extra tests would make any major differences between it and G40.21 Grade 44W steel more noticeable. The steel behaved satisfactorily, and its yield point was found to be very close to that specified for G40.21 Grade 44W steel.

Each coupon was loaded until the material had just entered the range of yielding as observed on a stress-strain diagram. At this point in the test, the coupon was allowed to relax by shutting off the hydraulic valve of the testing machine. The result was a slight change in strain, and this was carefully watched as the load slowly decreased. At the point when the slope of the stress-strain curve was starting to become parallel to the linear-elastic portion of the curve and was no longer vertical, the load was again applied. This process of coupon relaxation was repeated two or three times. A value of the static yield point was obtained by averaging the stresses corresponding to the points where the coupon was stable (Figure 4.1).

It was hoped that since all of the beam-column specimens had been fabricated from steel of the same rollings as the coupon plate materials, the yield strength and behaviour of the materials in the specimens would be known and uniform throughout the test series.

4.2 Description of the Actual Test Procedure

Since the yield strengths of both the web and flange plate materials were found to be very close to the nominal yield stress of 44 ksi for G40.21 Grade 44W steel, the difference between the actual and the nominal yield strengths was neglected. This meant that the design properties of the specimens were expected to be close enough to the actual properties. Therefore any loads such as expected yield moment and load were not recalculated.

Before testing, the test specimens were first aligned. This included alignment of both the concentric load with the centroid of the specimen and the eccentric load such that it would act in the same plane as the web.

A load of 4 kips was then put on the specimen (as indicated by the digital readout on the MTS control console) by the testing machine, and the initial readings were taken. It should be noted that the minicomputer obtained the MTS load from a transducer output on the MTS control console. This output read slightly lower than the digital readout. The testing machine load was taken to be the amount indicated by the digital readout for adjustment of the load. For any computations, however, the minicomputer utilized the MTS reading from the transducer output.

The moment was increased until either the specimen failed and it became impossible to maintain the eccentric load, or until the yield moment was reached. If the yield moment was reached, the test was continued in the same fashion. If the specimen had not failed by the time two further load increments had been applied to the specimen, the test continued except that the MTS load was no longer decreased.

A problem arose which had not been anticipated when it was decided to use the tension flange as datum for the deflection measuring device. It was noticed for specimens at high P/Py values, and in particular specimen 5, that the tension flange was beginning to twist and buckle at the full axial load before moment application was started. Hence, the trolley was not able to maintain its alignment from one load increment to the next as it moved up and down the tension flange. As application of moment proceeded, the tension flange began to straighten, and for the last couple of sets of web and compression flange readings was considered straight enough to make the readings accurate.

It was noticed that because of a large amount of grinding done by the fabricator, the mill scale had been removed over a large portion of the specimens. Hence the whitewash could not flake off in the usual manner, and it was difficult to detect and interpret the yield patterns.

4.3 Specimen Moment-Rotation Behaviour

The specimens were loaded at least until the ultimate moment was reached. This was indicated by either a zero or a negative slope of the moment-rotation curve. The moment-rotation curves for the specimens are shown in Figures 4.2(a) through 4.2(f). These curves were adjusted to account for initial curvatures that were present under full axial load only.

All but two of the specimens reached the expected yield moment, reduced for axial load, before failure. Specimen 2 reached 99% of its yield moment, and specimen 5 reached 79% of its yield moment. These data are tabulated in Table 4.1.

In general, the form of the moment-rotation curves is consistent with what was expected. In particular, the specimens with low axial load were able to withstand substantially larger rotations before failure than did the specimens with higher axial load. Furthermore, the specimens under high axial load tended to fail much more suddenly than did the specimens under lower axial load.

Specimen 1 appears to have behaved more like a plastic design section than a non-compact section. It underwent large rotations before failure, while sustaining a moment approximately equal to the plastic moment. This specimen was the only one not to have shown a decrease of moment capacity within the range of data taken. It was tested until the rotation was approximately seven times the yield rotation, and the moment-rotation plot was still horizontal when the test was stopped.

Specimen 2 also underwent a large rotation before failure occurred, although the moment was not as great. Because it is more likely for a stocky specimen to fail at a larger moment relative to its yield moment (i. e., a larger Mu/My ratio) than a slender section, it was expected that specimen 2 would fail at a higher Mu/My ratio than specimen 1. This, however, was not the case and no apparent reason seems to exist for this discrepancy.

Specimen 3 exceeded the yield moment and exhibited a more sudden failure than either specimens 1 or 2. The specimen rotation at failure was less than the failure rotations exhibited by either specimens 1 or 2.

Specimen 4 behaved in much the same way as specimen 3. It was noted for specimens 3 and 4, that the stockier one (specimen 4) failed at the larger Mu/My ratio.

Specimen 5 failed suddenly at a moment considerably less than the yield moment, and had a smaller rotation at failure than did any of the other specimens. It is possible that the high axial load caused the specimen to fail prematurely as it interacted with initial deflections in the flange and the web.

Specimen 6 also failed suddenly, although it had the largest Mu/My ratio of all the specimens. Its failure rotation was greater than that of specimen 5.

4.4 Specimen Buckling Behaviour

In Perlynn and Kulak's investigation(5), the identification of which plate element (web or flange) buckled first had been very helpful in the analysis of the test results. Unfortunately, and in spite of the large amount of data on web and flange movements collected in the present tests, it was frequently not apparent which plate element buckled first.

Because the deflection readings of the web were taken at grid points whose locations were known and constant (having been adjusted for specimen curvature and shortening), it became possible to plot contours of the deflections of the web, and a single line graph of compression flange deflections for each load increment. Because of the varying reflectivity of the paint and the variance of the ambient light at the different grid points, changes in deflections were plotted rather than absolute values as contour intervals. Using changes in deflections would cancel out any undesired effects due to these variations.

Deflection readings on specimen 1 were taken with a grid size of 4 in. by 4 in. on the web, and linearly every 4 in. on the flange. For the remaining specimens, a grid size of 2 in. by 2 in. was used for the web and readings every 2 in. were taken along the flange.

All the specimens had deflection measurements taken over the central 32 in. length of the beam-columns. This meant that no deflection data were taken for the top and bottom 6-1/2 in. of the specimen (Figure 4.3). This was unfortunate in the case of specimen 2, because the web movements which eventually caused specimen failure occurred very close to the cap plate of the specimen, and no readings were recorded near this location. Other specimens also had yield lines and significant deflections near the cap plates where no deflection readings were taken. Because the total grid size was an integral number of 2 in. or 4 in. grid points, the portion of the web monitored for deflections varied from specimen to specimen and did not encompass the entire distance "h" between the flanges (Figure 4.3).

The contour values used in plotting the web deflections were chosen on the basis of the intervals that would encompass most of the greatest deflection changes for all the load increments of a particular specimen. In the end, ten contour values were chosen for each specimen. Often, not all of the ten contour values existed for a particular plot. This was deliberate. If, at a later load increment in a test, a new contour value of a larger deflection change is plotted, the web is known to be moving.

The flange deflections were plotted as a straight line graph of deflections over the flange length.

Determination of the buckling behaviour was accomplished by superimposing three contour plots on a graph, each having a reduced number of contour values. A similar procedure was followed for the flange plots.

By noting the movement of a particular section of the flange or a contour value over the web, it is possible to gain insight into the buckling of the plate element. Comparison between web and flange plate movements helped determine how the specimens failed.

The contour and deflection plots are shown in Figures 4.4(a) through 4.4(f). The load increments and the respective contour values for each load increment are indicated on the plots for each specimen. The solid lines represent the web contours and the flange deflections at the first load increment plotted; the dashed lines, the intermediate load increment; and the dotted lines, the highest load increment. A negative contour value or flange deflection value indicates that the plate element is moving away from its initial position and the deflection device. The size of the contour plots in these figures are drawn to an approximate scale of 1:5.33. The load increments plotted were chosen so that one would be at a low load in order to provide a basis for web and flange plate movements at the higher load increments. The other two load increments plotted are at high loads, usually one at the load increment nearest the failure load for which the web and compression flange deflection readings were taken, and the other load increment immediately preceeding it for which these deflections were taken.

Since it was not definitely clear in most cases whether the first plate element to buckle was the web or the flange, judgement was used to provide a decision. In view of the uncertainties this was generally such that the most conservative prediction of behaviour would result.

Figure 4.4(a) shows that specimen 1 underwent a substantial amount of movement in the web as the load was increasing, while the flange movements were much smaller. In fact, the flange appears to be almost straight except for part near mid-height where the deflections are noticeable. It appears that this specimen failed by web buckling. The strain gauge readings (not presented) do not indicate a web buckle, but the contour plots show that the largest movements do not occur at mid-height, where the strain gauges were located.

It was more difficult to determine the failure mode for specimen 2 (Figure 4.4(b)). Substantial flange movements occurred near the bottom of the specimen at the higher load increments. The web was also moving, both at the top and the bottom of the specimen, and hence appears as if it could have caused the failure. It apparently had twisted; the top is closer and the bottom farther away than at the first load increment. It was judged that the web caused the specimen failure. Unfortunately, the buckle of this specimen formed very close to the cap plate at one end of the specimen, and no deflection readings were taken in the immediate vicinity of the buckle. Hence the determination of which plate element caused this specimen to fail was difficult. At the higher load increments, the strain gauges indicate some web movement, but, as was the case for specimen 1, the large deflections did not occur where the strain gauges were located.

As shown in Figure 4.4(c), specimen 3 showed substantial movements of both the flange and the web. It was apparent that as one plate element failed, the other one was close to failure itself. It appears as though the flange was deflecting more at the first load increment, but the web deflected as much as the flange did as the loads were increased. The buckle formed just above mid-height, and appears to have been caused by a simultaneous web and flange failure. The strain gauges indicate some web movement.

Specimen 4 had substantial web movements at the top and bottom with the mid-height remaining relatively stable. Figure 4.4(d) shows that the flange exhibited large movements at the same heights as the web deflections were occurring. The flange moved a substantial amount more than the web, so it appears as if the specimen failed by flange buckling. The strain gauge readings indicate some movement of the web.

Specimen 5 appears to have substantial movement of both the web and the flange. In Figure 4.4(e), it can be seen that, for low load, the web and flange moved approximately the same amount. Because of the high axial load involved, it was noticed that the tension flange was beginning to twist before the application of moment was started. Hence, the deflection readings for the intermediate load increments were not considered to be accurate, and could not be used. For the higher load increments, the flange appeared to be moving a very large amount while the web was not moving to such a great extent. The strain gauges showed, however, that a web buckle was forming. Hence it appears as if the specimen failed by simultaneous web and flange buckling.

Figure 4.4(f) shows that specimen 6 had reasonably large movements at the low load increment for both the web and the flange. However, for the higher load increments, it appears as if the flange moved more than the web. Hence, it was concluded that this specimen failed by flange buckling. The strain gauges do not indicate any substantial movement of the web at mid-height.

It was also noted that specimens 1, 2, and 4 had substantial movements of the web and flange near the top and bottom of the specimen, but much smaller deflections at the mid-height of the specimen. This is thought to be due to the presence of the studs welded to the specimens for the lateral bracing system.

A web and flange buckle (shown well after the ultimate moment had been attained) is given in Figure 4.5, and a summary of how each specimen is considered to have failed is included in Table 4.1.

4.5 Initial Deflections and their Effects

Relatively light steel plate was used in order to fabricate reasonable cross-sectional shapes for testing. It is probable that, as a result of residual stresses resulting from the welding of these thin plates and from normal shop fabrication procedures, initial deflections of both the flanges and web were present.

It was noted after three tests, (4, 5, 6), had been completed that the deflection device did not give a reliable evaluation of initial deflections because of changes in ambient light and reflectivity of the painted surface at the various grid points. The relative differences, which are the ones of primary interest in this investigation, are still useful because the point to point variations cancel each other out when the differences are used. Hence, for specimens 1, 2, and 3 a bridge device using three dial gauges was used to take readings of the initial web deflections. For specimens 4, 5, and 6 an estimate was made of the initial web deflections. This was done by assuming that the first line of web readings nearest the tension flange had zero net deflection and the other readings along the row in question were compared to it. The readings near locations where the strain gauges were mounted were ignored because of the wiring of the gauges. The maximum net deflection change between the tension flange reading and the respective web deflection readings was then taken to be the maximum out-of-straight of the specimen (Table 4.1). Using this procedure, it was determined that the maximum relative out-of-straight (δ/h) for the specimens was 0.005 (specimen 2). This is 74.7% of the allowable limit according to CSA Standard W59.1(16).

It is also possible to estimate the initial out-of-straight of the compression flange using the readings from the deflection device, provided the tension flange is assumed straight and not twisted. This assumes that the reading taken closest to the top of the specimen is at zero net deflection. These readings have not been presented due to the uncertainty of the straightness of the tension flanges.

The effects of initial out-of-straightness of the plate elements in non-compact beam-columns is not obvious from the tests. However, it may be reasonably assumed that if the compression flange has an initial large out-of-straightness compared to the web any axial load or moment application will tend to increase this out-of-straightness. A similar situation exists for the web. For non-compact beam-columns, the effect of the initial out-of-straight of the flanges has perhaps as profound an effect as that of the web, because the flanges are so slender.

It was noted that the high axial load specimens were more susceptible to out-of-straightness effects, and hence sudden failures.

4.6 Second-Order Considerations

It was noted that the maximum second-order moment due to the interaction between strong-axis deflections and axial load at ultimate moment was 3% (Specimen 5). Hence it appears to be reasonable to neglect these second-order P-Δ effects.

SPECIMEN	P/Py	$\frac{h}{w}\sqrt{Fy}$	Mu/My	FAILURE
1	0.15	639.4	1.16	W
2	0.15	534.2	0.99	W
3	0.30	590.7	1.12	W&F
4	0.30	488.2	1.20	F
5	0.70	501.2	0.79	W&F
6	0.70	401.1	1.53	F

TABLE 4.1

SPECIMEN MOMENT AND FAILURE DATA

SPECIMEN	HEIGHT (in)	δ (WEB) (in)	δ/h (WEB)	% (all.)
1	24.01	0.061	0.0025	37.5
2	20.06	0.100	0.0050	74.7
3	22.18	0.041	0.0018	27.0
4	18.33	0.071•	0.0038	57.0
5	18.82	0.081•	0.0043	64.5
6	15.06	0.057•	0.0038	57.0

•ESTIMATE ONLY

TABLE 4.2

INITIAL WEB DEFLECTION DATA

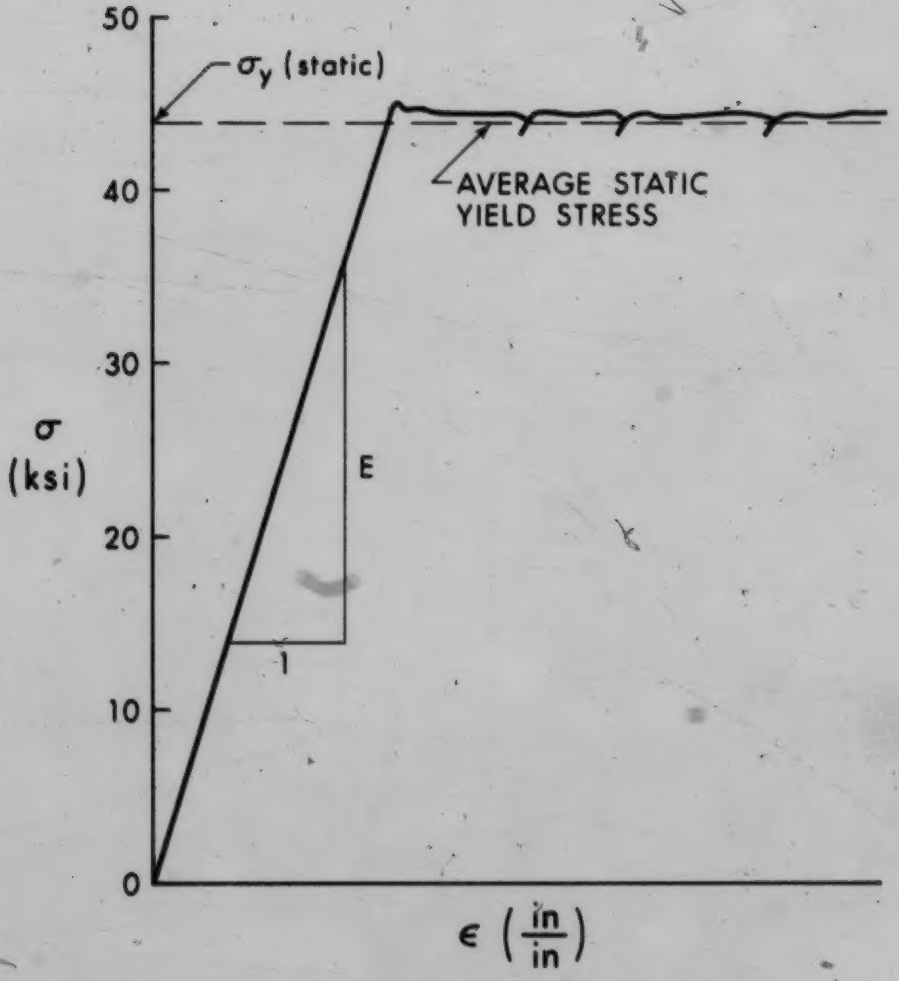

FIGURE 4.1

DETERMINATION OF COUPON STATIC YIELD STRESS

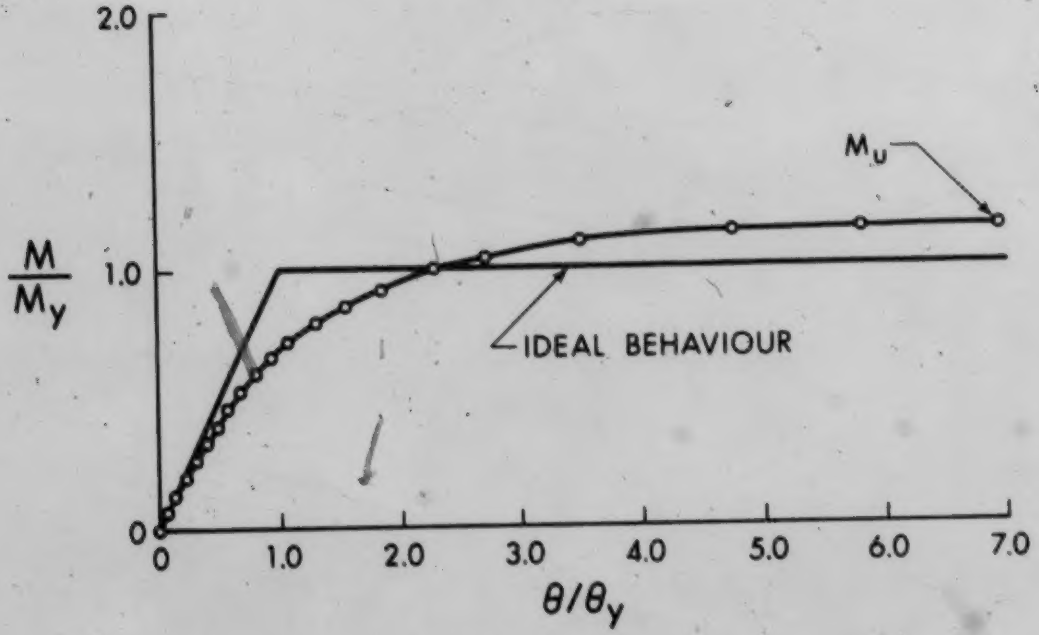

FIGURE 4.2(a)

MOMENT-ROTATION RELATIONSHIP - SPECIMEN 1

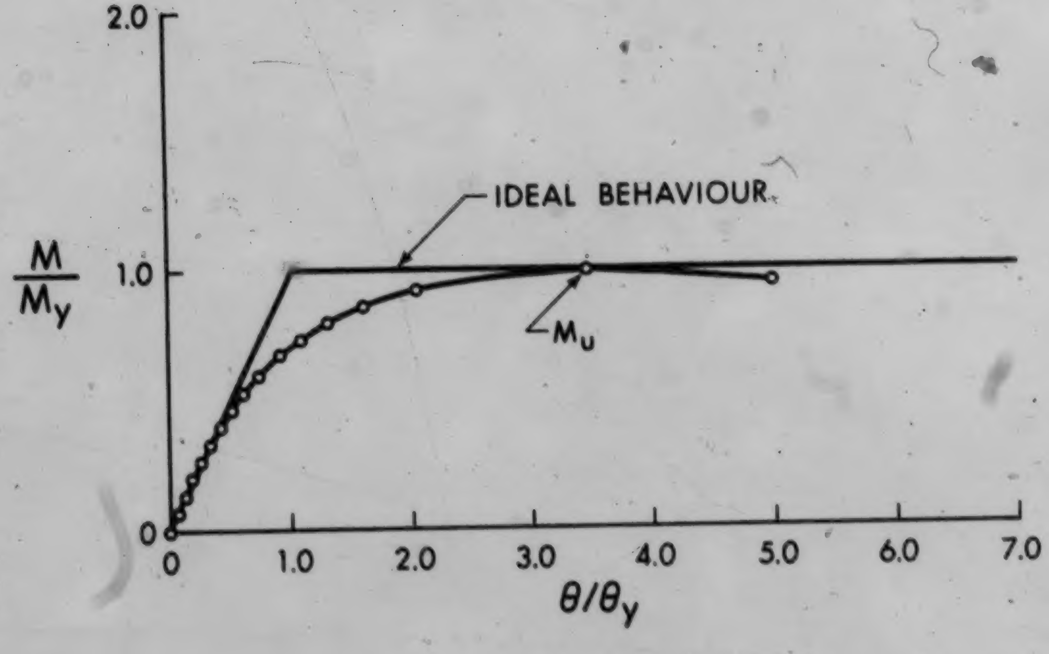

FIGURE 4.2(b)

MOMENT-ROTATION RELATIONSHIP - SPECIMEN 2

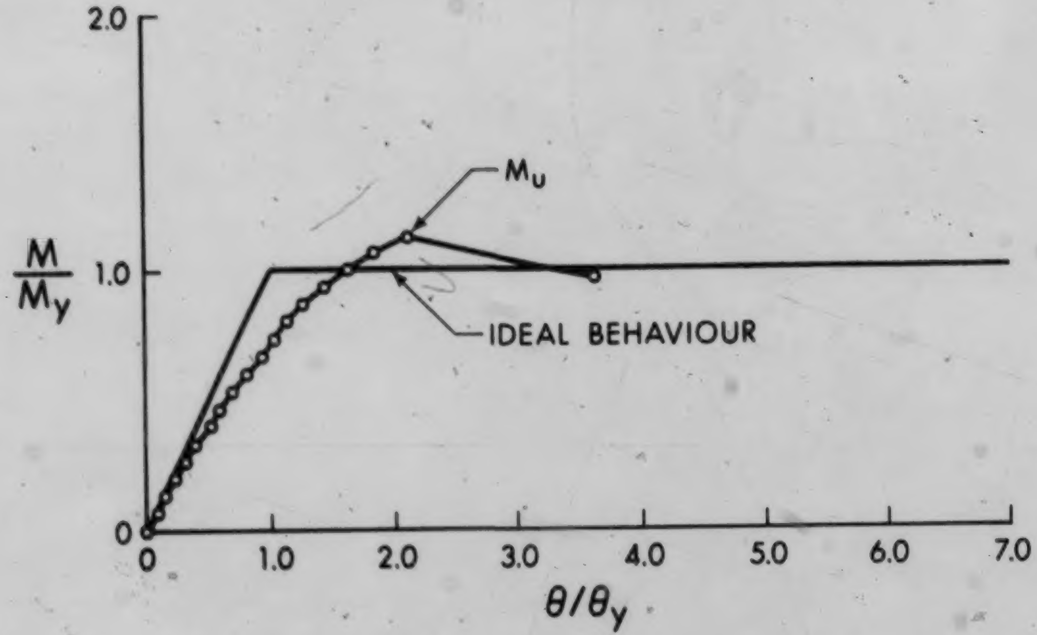

FIGURE 4.2(c)

MOMENT-ROTATION RELATIONSHIP - SPECIMEN 3

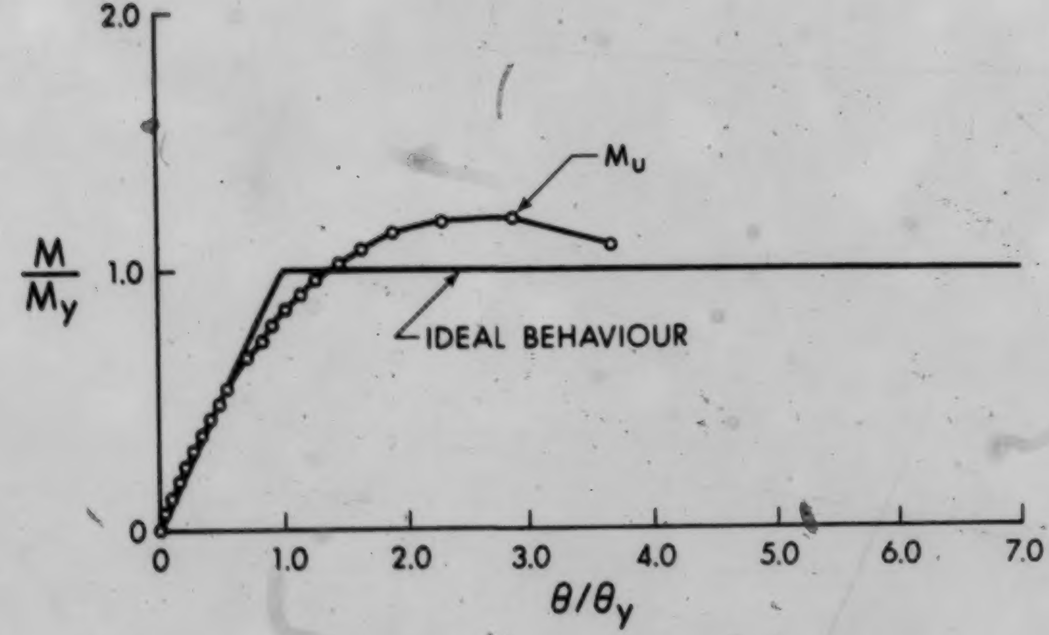

FIGURE 4.2(d)

MOMENT-ROTATION RELATIONSHIP - SPECIMEN 4

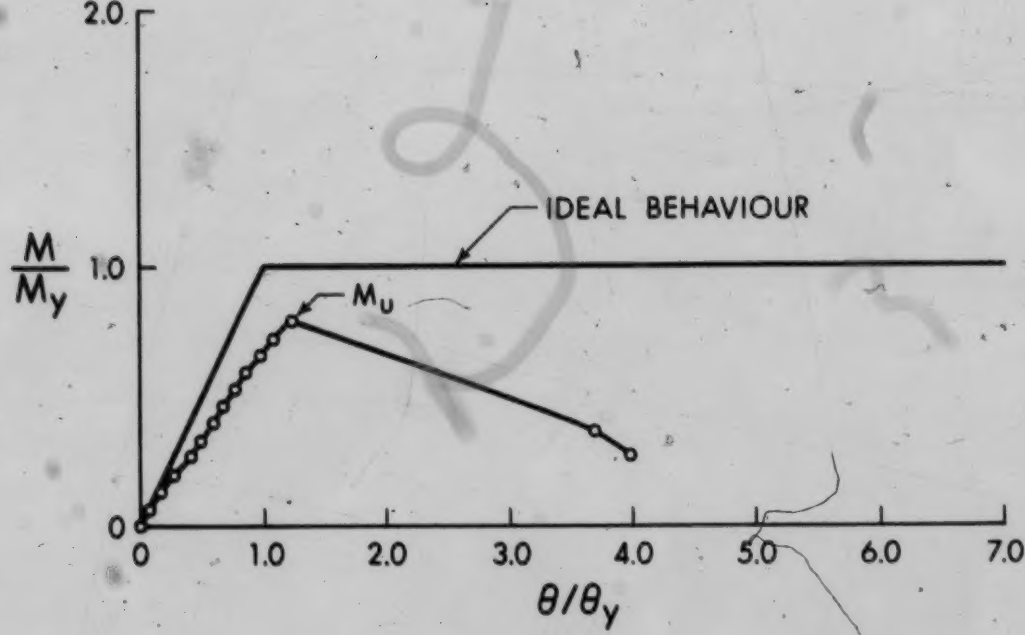

FIGURE 4.2(e)

MOMENT-ROTATION RELATIONSHIP - SPECIMEN 5

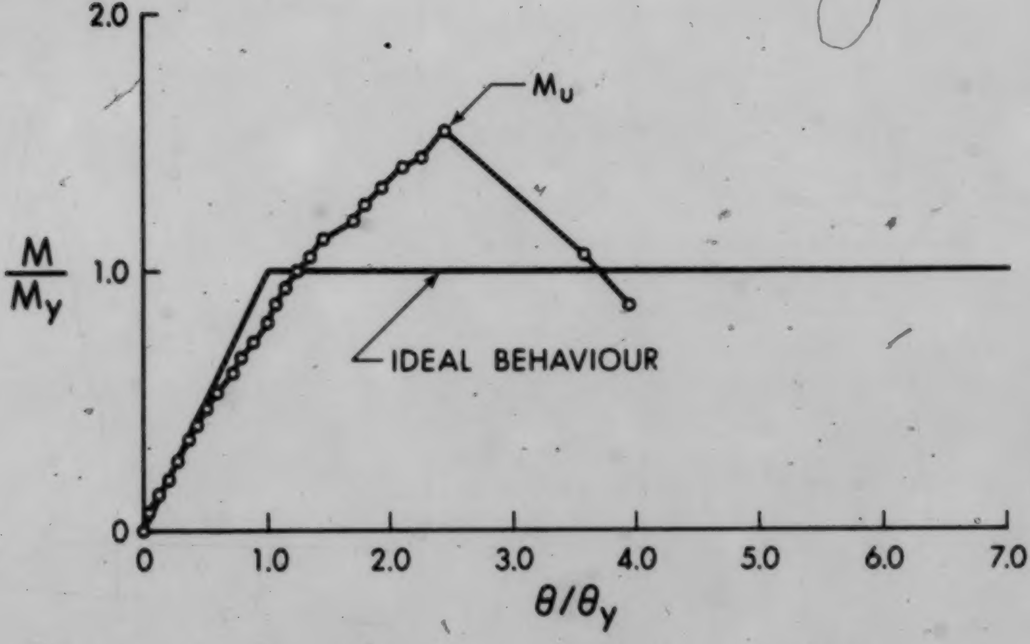

FIGURE 4.2(f)

MOMENT-ROTATION RELATIONSHIP - SPECIMEN 6

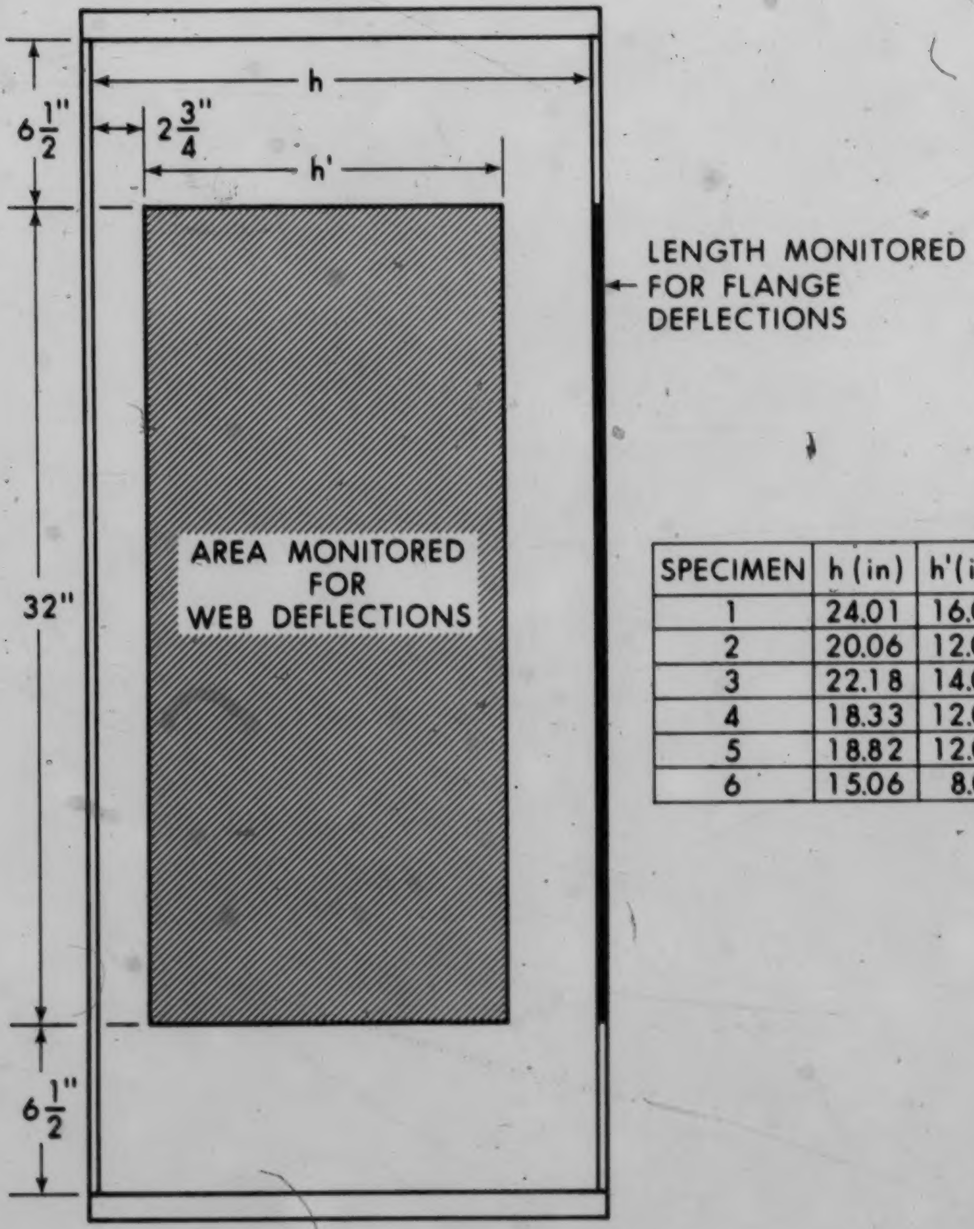
h
$6\frac{1}{2}$"
$2\frac{3}{4}$"
h'
LENGTH MONITORED FOR FLANGE DEFLECTIONS
AREA MONITORED FOR WEB DEFLECTIONS
32"
$6\frac{1}{2}$"

SPECIMEN	h (in)	h'(in)
1	24.01	16.00
2	20.06	12.00
3	22.18	14.00
4	18.33	12.00
5	18.82	12.00
6	15.06	8.00

FIGURE 4.3

PORTION OF SPECIMENS MONITORED FOR PLATE DEFLECTIONS

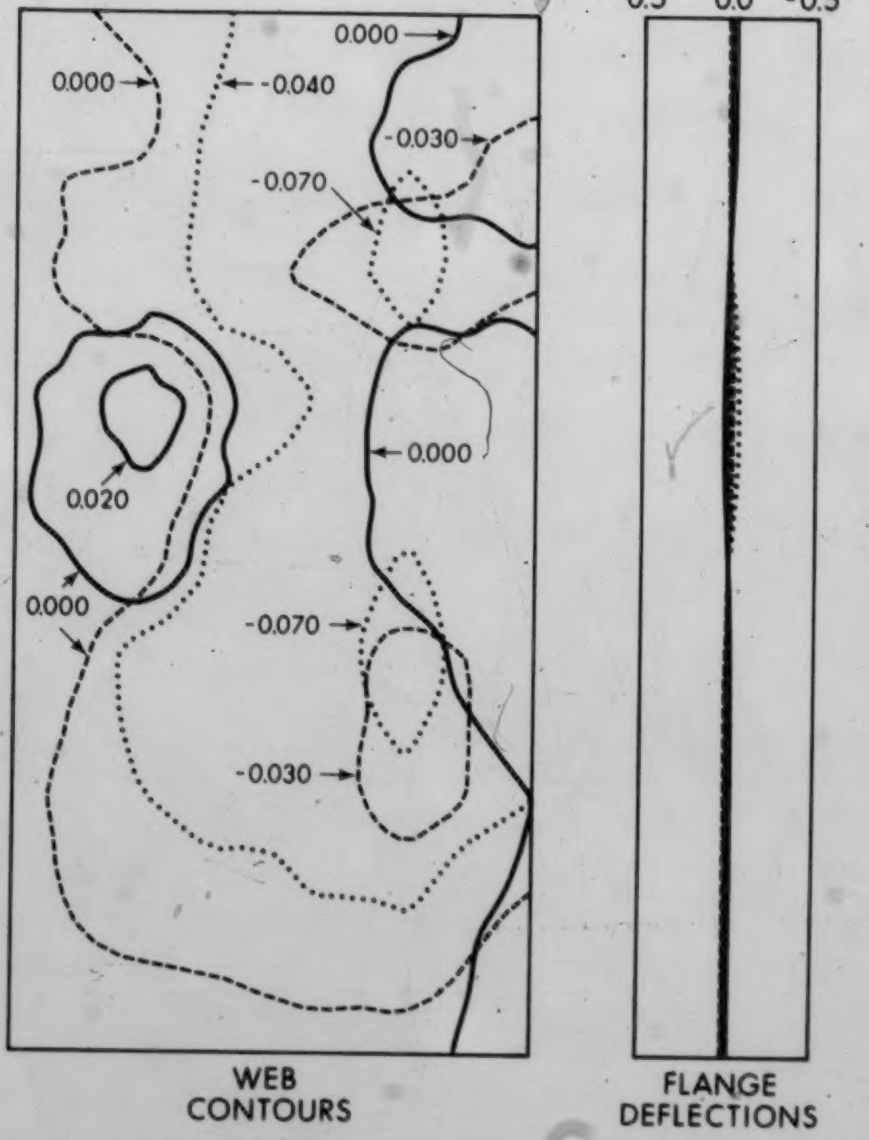

LINE	M (in-k)	P (k)
———————	709	78
- - - - - - - -	3260	78
···········	3555	78

FIGURE 4.4 (a)

WEB AND FLANGE DEFLECTIONS - SPECIMEN 1

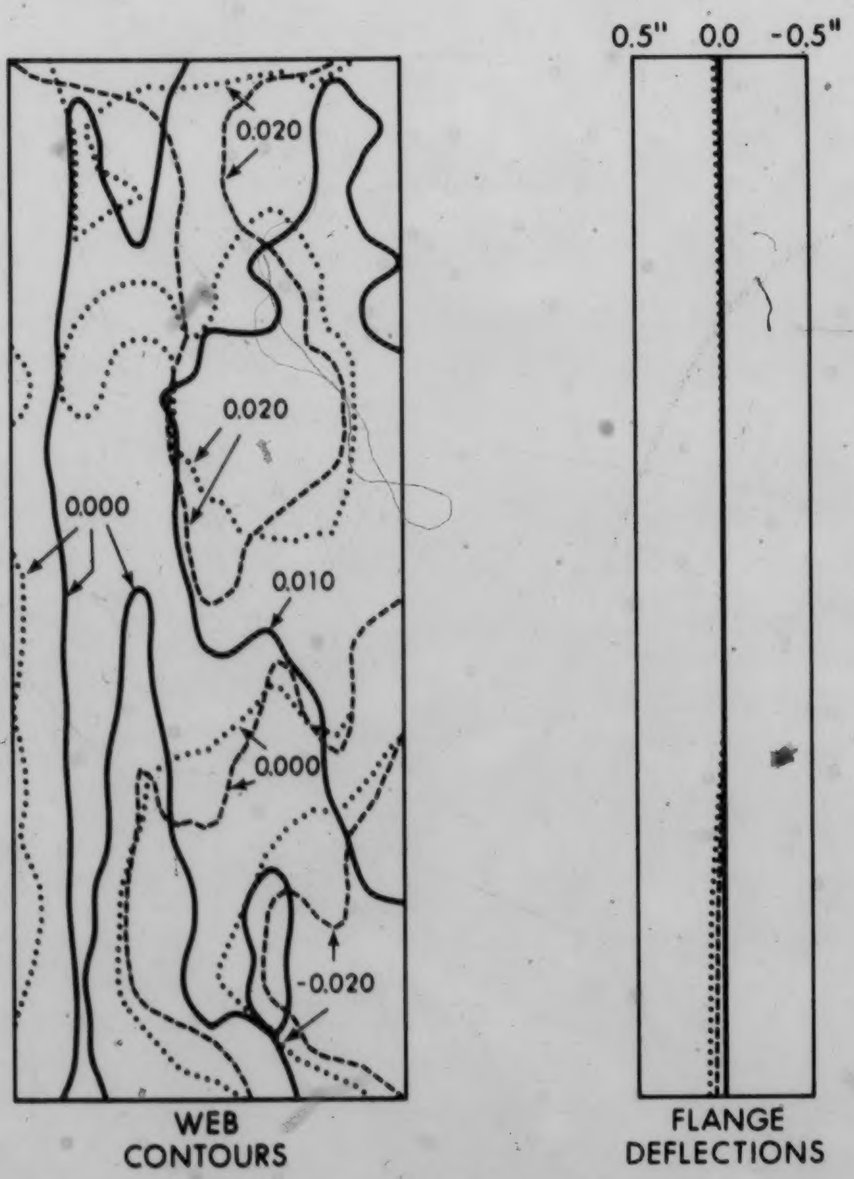

LINE	M (in-k)	P (k)
———————	380	72
--------	2446	72
....	2622	72

FIGURE 4.4(b)

WEB AND FLANGE DEFLECTIONS - SPECIMEN 2

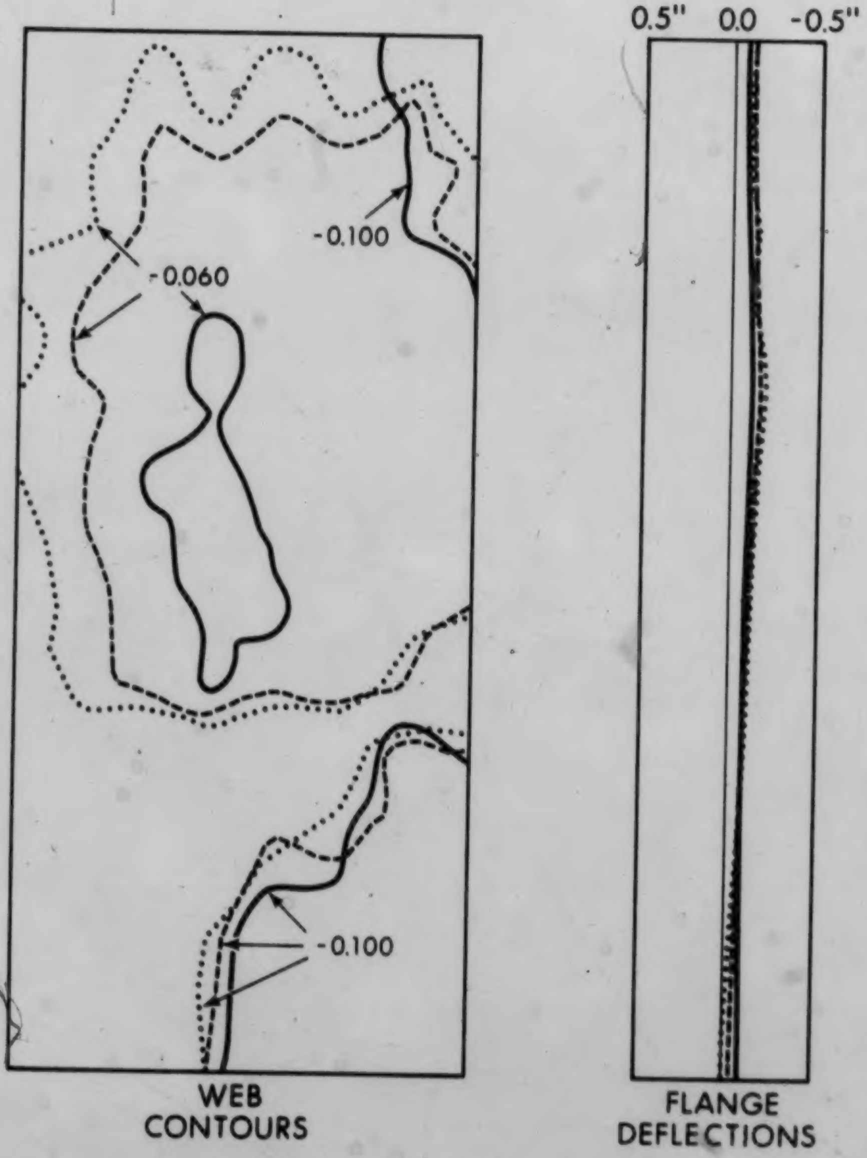

LINE	M (in-k)	P (k)
———————	532	150
--------	2300	150
··········	2650	150

FIGURE 4.4 (c)

WEB AND FLANGE DEFLECTIONS - SPECIMEN 3

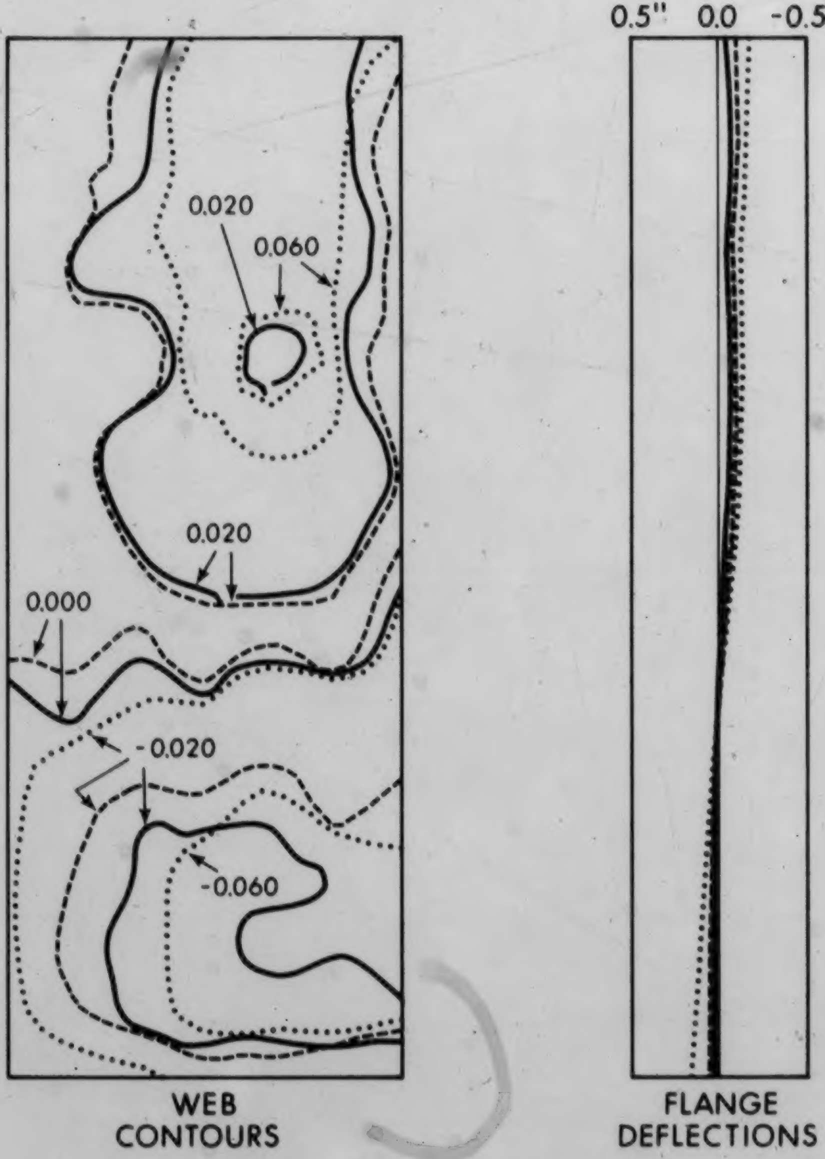

LINE	M (in-k)	P (k)
———	2024	138
- - - - -	2268	138
·········	2488	138

FIGURE 4.4(d)

WEB AND FLANGE DEFLECTIONS - SPECIMEN 4

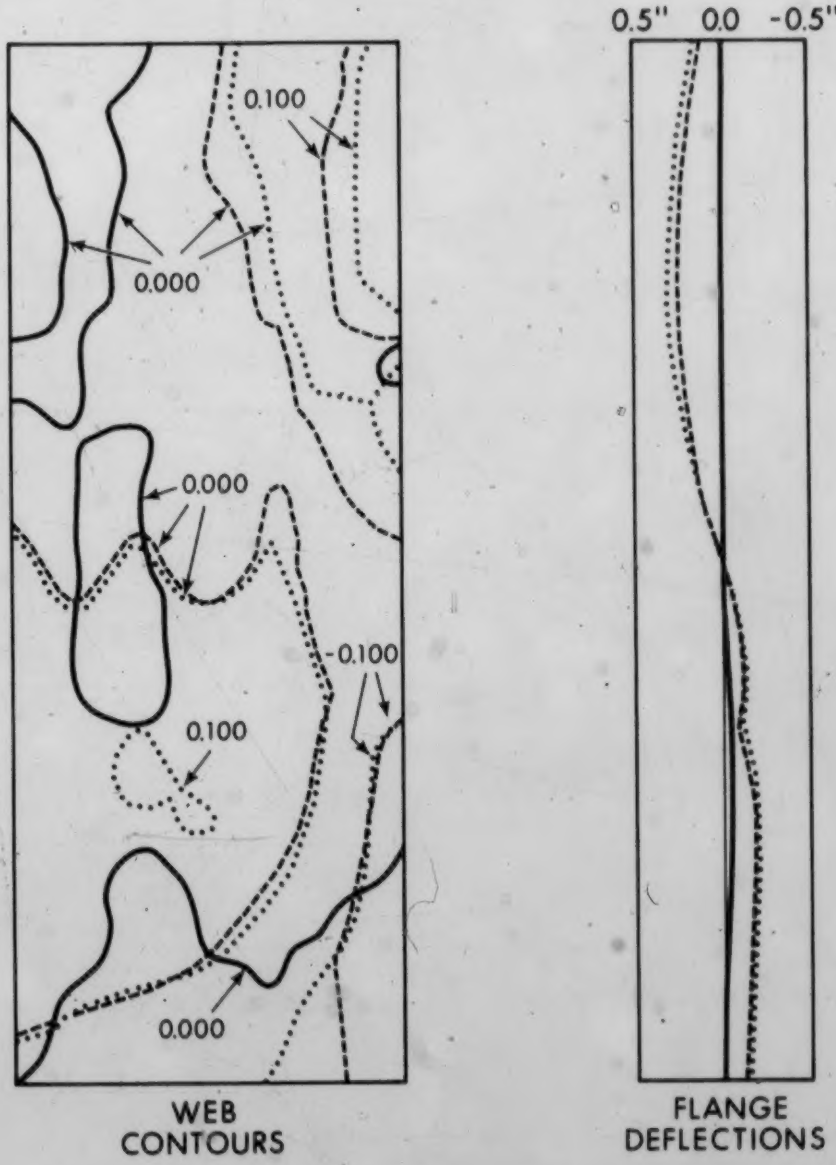

LINE	M (in-k)	P (k)
———	0	132
--------	487	325
··········	668	325

FIGURE 4.4(e)

WEB AND FLANGE DEFLECTIONS - SPECIMEN 5

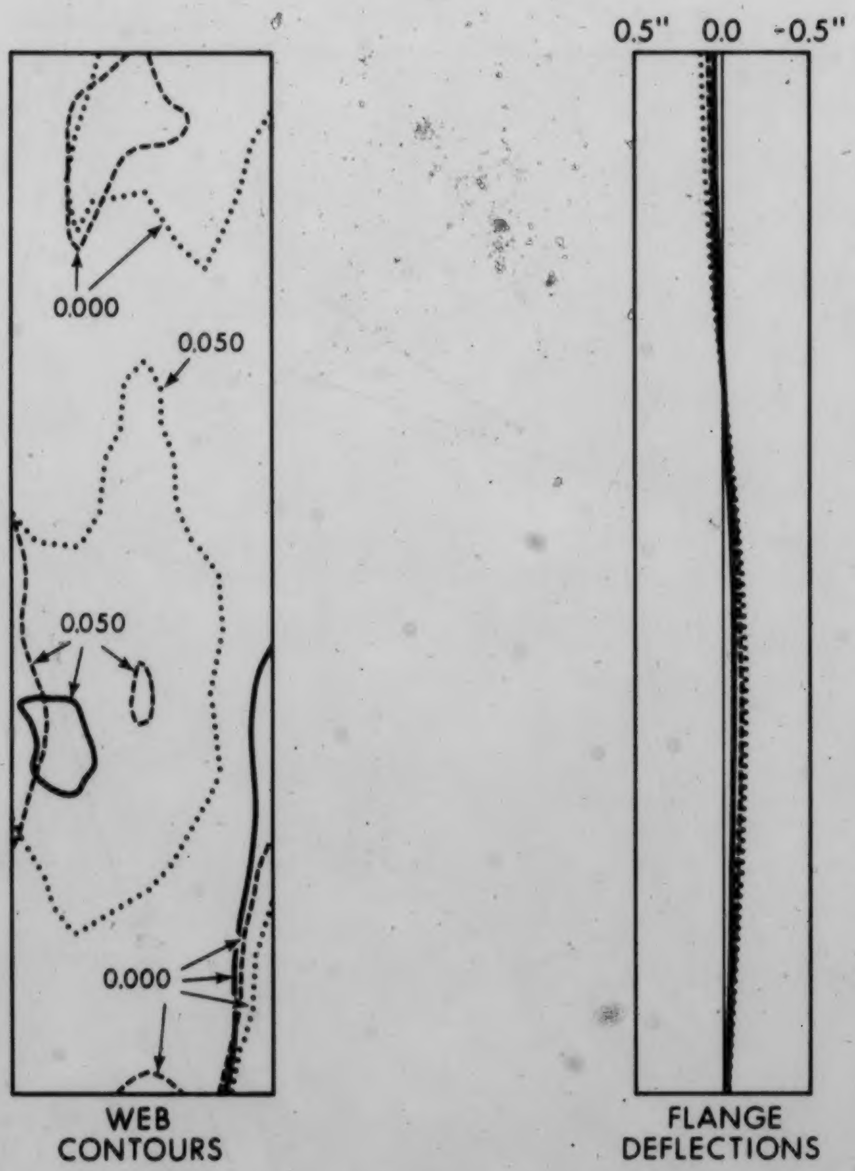

LINE	M (in-k)	P (k)
———	516	296
- - - -	997	296
········	1095	296

FIGURE 4.4(f)

WEB AND FLANGE DEFLECTIONS - SPECIMEN 6

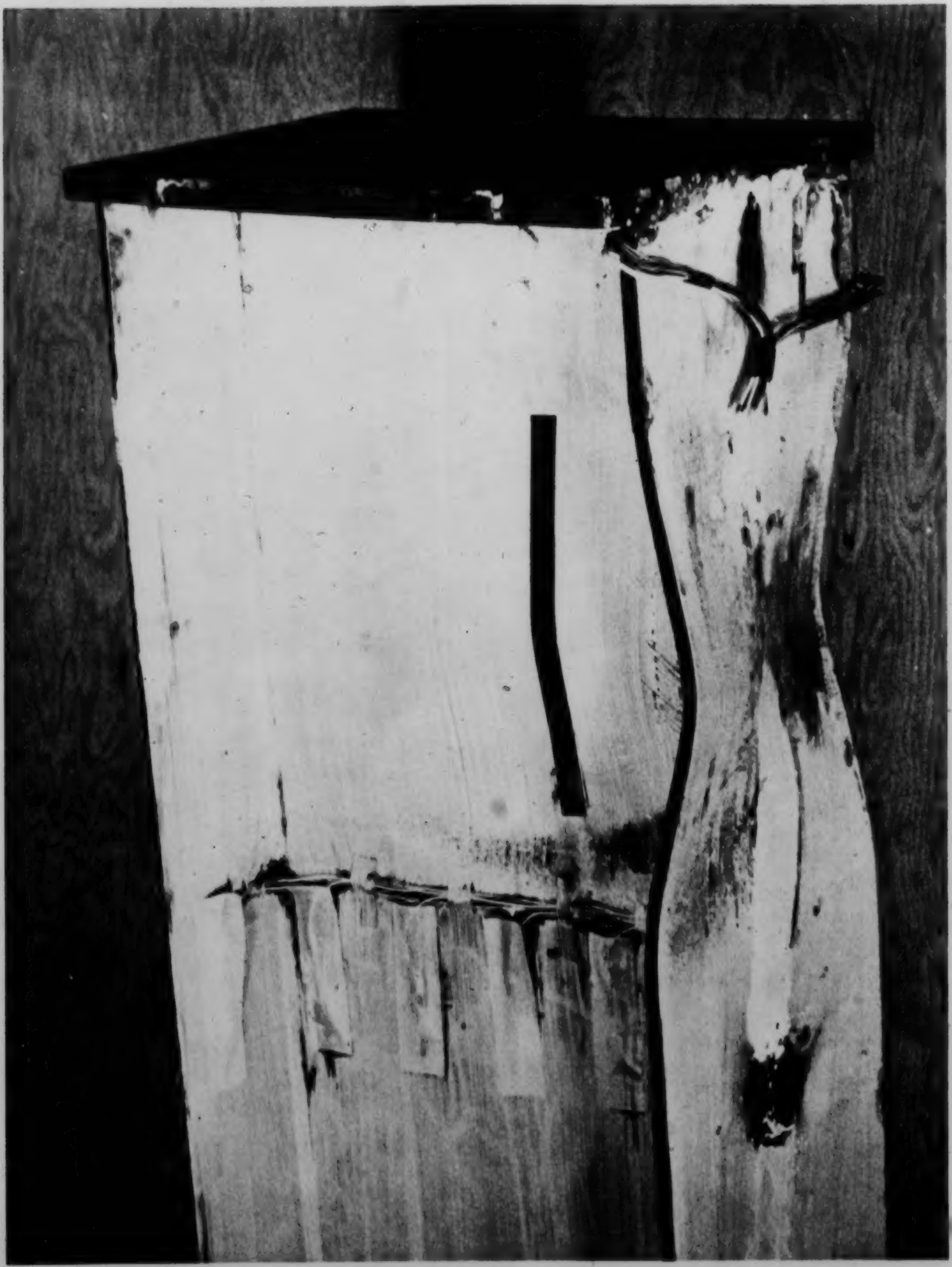

FIGURE 4.5

WEB AND FLANGE BUCKLE (SPECIMEN 6)

CHAPTER V

THEORETICAL ANALYSIS

5.1 Analysis of CSA S16-1969 Specification Requirements

The first major investigation into flange and web plate buckling was conducted by Haaijer(4). In his investigation, Haaijer accounted for the possibility that web and flange plates may reach strain-hardening before buckling. His analysis was based on the following assumptions:

1. An idealized stress-strain diagram can be used for the analysis of the test results (Figure 5.1).
2. Yielding occurs in slip bands(17), so that the material is either in the elastic range or in the strain-hardening range.
3. The material is homogeneous and isotropic in the elastic range, and homogeneous and orthotropic in the strain-hardening range.
4. The rotation interaction between the web and flange plates can be accounted for by using a coefficient of restraint (β).
5. Yielding starts at the loaded edges of a column specimen and progresses inwards, or starts at the centre and progresses outwards

towards the loaded edges. (Haaijer uses this assumption to show that columns can buckle at stresses above the yield stress, then assumes that this also holds true for plates.)

6. An incremental stress strain relationship(18) can be applied to the analysis. Initial imperfections of the plate are accounted for by the introduction of effective moduli for the strain-hardening range.
7. No strain reversal occurs for a plate supported along all four edges when it deforms to its buckled shape from its non-buckled shape.

Once the possibility of column buckling at stresses above the yield stress was established, Haaijer developed a plate buckling equation for the strain-hardening range.

Assuming that buckling occurs without strain reversal, it is possible for a web plate element of orthotropic material to be in equilibrium in the deformed position when subjected to uniform edge compression (Figure 5.2). This can be expressed mathematically by the following fourth-order partial differential equation:

$$D_x \frac{\partial^4 u}{\partial x^4} + 2H \frac{\partial^4 u}{\partial x^2 \partial y^2} + D_y \frac{\partial^4 u}{\partial y^4} = -\frac{\sigma_{cr} w}{I} \frac{\partial^2 u}{\partial x^2} \qquad (5.1)$$

where:

$$D_x = \frac{E_x}{1 - \nu_x \nu_y}$$

$$D_y = \frac{E_y}{1 - \nu_x \nu_y}$$

$$D_{xy} = \frac{\nu_y E_x}{1 - \nu_x \nu_y}$$

$$D_{yx} = \frac{\nu_x E_y}{1 - \nu_x \nu_y}$$

$2H = D_{xy} + D_{yx} + 4G_t$

G_t = tangent shear modulus

u = deflection of plate at centre

w = plate thickness

σ_{cr} = critical buckling stress

$$I = \frac{w^3}{12}$$

Equation 5.1 is similar to Equation 2.1, the only difference being in the coefficients used to describe the material behaviour. Equation 2.1 deals with isotropic material which requires only two independent parameters to describe the material behaviour, while Equation 5.1 deals with orthotropic material which requires five such parameters to describe it.

The condition that the in-plane and deformed positions of the plate are in equilibrium at the instant of buckling (the bifurcation point) can be expressed in terms of work. Any additional work done by the external forces in further bending the plate must equal the change in the internal energy of the plate. This yields the following integral equation:

$$\frac{\sigma_{crw}}{I} \iint \left(\frac{\partial u}{\partial x}\right)^2 dxdy = \iint \left[Dx\left(\frac{\partial^2 u}{\partial x^2}\right)^2 + Dy\left(\frac{\partial^2 u}{\partial y^2}\right)^2 + (Dxy + Dyx)\left(\frac{\partial^2 u}{\partial x^2}\right)\left(\frac{\partial^2 u}{\partial y^2}\right) + 4\,Gt\left(\frac{\partial^2 u}{\partial x\,\partial y}\right)^2 \right] dxdy \qquad (5.2)$$

This approximate work-energy approach was used because solutions to Equation 5.1 can be easily obtained only if $H^2 = DxDy$, an assumption made by Bleich(8). This assumption, however, was found not to be valid for Haaijer's experimental results. If the following constraint on Equation 5.1 is considered:

$$2H = Dxy + Dyx + 4Gt$$

and if $H^2 = DxDy$ is substituted for H in the constraint equality, the equality is not satisfied using the values of the constants determined from Haaijer's experimental results.

Equation 5.2 will give an approximate solution if an appropriate deflection surface is assumed. Although the degree of approximation depends upon the correctness of the assumed deflection surface, the result will be conservative in any case. For a rectangular plate supported along all four edges, with the loaded edges $x = 0$ and $x = l$ being hinged, and the edges $y = \pm h/2$ having equal restraint against rotation (Figure 5.2), Haaijer assumed the following deflected surface:

$$u = [\, B\pi((y/h)^2 - 0.25) + (A+B)\cos(\pi y/h)\,]\sin(\pi x/l) \qquad (5.3)$$

where:

A = constant

B = constant

$\beta = \dfrac{B}{A} = \dfrac{Mh}{2DyI}$ = coefficient of restraint against rotation

M = moment per unit length required for a unit rotation

h = width of plate

l = length of plate

(In fact, Haaijer misquoted his reference here, by not squaring the y/h term. The correct deflected shape, as written in Equation 5.3, was first suggested by Lundquist and Stowell(10). Perlynn and Kulak(5), by quoting Haaijer, also misquoted Lundquist and Stowell.)

Substituting Equation 5.3 into Equation 5.2 and integrating will give the critical buckling stress. In the limiting cases for a web plate subjected to uniform axial compression, when the unloaded edges $y = \pm h/2$ are hinged or fixed, the minimum values of the critical buckling stress are:

(a) For $y = \pm h/2$, hinged, $(\beta=0)$;

$$\sigma_{cr} = \frac{\pi^2}{12}\left(\frac{w}{h}\right)^2 [2\sqrt{DxDy} + Dxy + Dyx + 4\,Gt] \qquad (5.4)$$

(b) For $y = \pm h/2$, fixed, $(\beta=\infty)$;

$$\sigma_{cr} = \frac{\pi^2}{12}\left(\frac{w}{h}\right)^2 [4.554\sqrt{DxDy} + 1.237\,(Dxy+Dyx) + 4.943\,Gt] \qquad (5.5)$$

By substituting the appropriate values of the constants Dx, Dy, Dxy, Dyx, and Gt for the strain-hardening range, Equations 5.4 and 5.5 can be used to give the critical buckling stress of plates subjected to strains greater than or equal to the strain at the start of strain-hardening ε_{st} (Figure 5.1).

For the simplified stress-strain curve assumed, substitution of the elastic values of the constants in Equations 5.4 and 5.5 will give valid elastic buckling solutions for σ_{cr} less than σ_y. It is obvious that the lower critical buckling stress will occur for the case of the plate with all four edges hinged.

Haaijer conducted tests on wide-flange shapes of ASTM-A7 steel subjected to either pure bending or pure compression. He concluded that Equations 5.4 and 5.5 adequately described the test results. At the time, however, the behaviour of a web plate subjected to combined in-plane bending and uniform axial compression was not investigated.

Equations 5.4 and 5.5 pertain only to plate elements that are free of residual stresses, that is, annealed specimens. This is because of the simplified stress-strain diagram used (Figure 5.1). As-delivered specimens, however, generally contain residual stresses of a large enough magnitude to cause partial yielding to occur at an applied stress considerably less than the yield stress. The elastic solutions obtained from Equations 5.4 and 5.5 are valid only up to a limiting stress σ_p, where:

$\sigma_p = \sigma_y - \sigma_r$

σ_y = yield stress,

σ_r = residual stress.

A more realistic approach to the problem, for the range $\sigma_p < \sigma_{cr} < \sigma_y$, was proposed in 1958 by Haaijer and Thurlimann(10), when they suggested a plate buckling equation which took into account the effects of residual stresses. A plate buckling curve (similar to a column buckling curve) was developed which had an empirical transition curve to describe the buckling behaviour of a plate subjected to stresses between its proportional limit and its yield stress (Figure 2.1).

Dividing each side of Timoshenko's plate buckling relationship (Equation 2.2) by the yield stress results in:

$$\frac{\sigma_{cr}}{\sigma_y} = \frac{K \pi^2 E}{12 \sigma_y (1 - \nu^2) (h/w)^2} \tag{5.6}$$

Haaijer and Thurlimann defined:

$$\frac{1}{\alpha^2} = \frac{\sigma_{cr}}{\sigma_y} \tag{5.7}$$

to obtain:

$$\alpha = \frac{h}{\pi w} \sqrt{\frac{12 \sigma_y (1 - \nu^2)}{K E}} \tag{5.8}$$

which is the same as Equation 2.3.

Equation 5.7 is valid for values of α greater than some limiting value α_p (Figure 2.1). This corresponds to stresses below the proportional limit and α_p corresponds to the non-dimensionalized limiting stress σ_p/σ_y. From the point given by $(\sigma_p/\sigma_y, \alpha_p)$, some transition curve must be followed as progressively more of the material reaches the strain-hardening range, to the point at which the buckling stress equals the yield stress $(\sigma_{cr}/\sigma_y = 1.0, \alpha_o)$. A portion of a plate element reaching the latter point, has by definition, all of its material yielded and has reached the strain-hardening range. Haaijer and Thurlimann proposed the following transition curve for $\alpha_o \le \alpha \le \alpha_p$:

$$\frac{\sigma_{cr}}{\sigma_y} = 1 - \left(1 - \frac{\sigma_p}{\sigma_y}\right)\left(\frac{\alpha - \alpha_o}{\alpha_p - \alpha_o}\right)^n \qquad (5.9)$$

where:

σ_{cr} = critical buckling stress for uniform compression

$\sigma_p = \sigma_y - \sigma_r$

σ_p = stress at proportional limit

σ_r = maximum value of the plate compression residual stresses

$n = \dfrac{2(\alpha_p - \alpha_o)}{\alpha_p(\alpha_p^2 - 1)}$

$\alpha_p = \sqrt{\sigma_y/\sigma_p}$

Haaijer and Thurlimann suggested values for α_o for three types of compression elements and showed that they are nearly independent of the amount of rotation restraint offered along the unloaded edges. For hinged webs, they found $\alpha_o = 0.579$, and for fixed webs, $\alpha_o = 0.588$. For simplicity, they suggested using $\alpha_o = 0.58$ for web plates supported along all four edges. By definition, then, when $\alpha_o = 0.58$, the web plate in a wide-flange member may be uniformly compressed up to strain-hardening without the occurrence of local buckling.

Knowing the maximum residual compressive stress in a specimen, σ_r, it is possible using Equation 5.9 to plot σ_{cr}/σ_y versus α. Using Equations 5.7 and 5.8, it is also possible to determine the limiting value of h/w for any value of σ_{cr}/σ_y. Haaijer did this for his test results and found that good correlation existed for webs and flanges subjected to pure compression. However no tests were conducted to determine the behaviour of web plates subjected to combined in-plane bending and axial compression.

Haaijer and Thurlimann realized the importance of extending the previous considerations to cases of plates subjected to combined bending and axial load. The web of a wide-flange section, subjected to an axial load P and a bending moment M, presents such a case. Depending upon the ratio of axial load to moment, the neutral axis may lie inside or outside of the web.

For the case of combined in-plane bending and compression, Haaijer and Thurlimann suggested that Equation 5.8 could still be used to describe the behaviour of a web plate if an appropriate plate buckling coefficient "K" could be determined. This is because α is a function of the maximum critical strain in the web and the web slenderness ratio h/w.

The minimum values for "K" for a stress distribution of a fully-plastified wide-flange section are shown in Figure 5.3. For any loading condition except pure compression, attaining the necessary stress distribution would require that the ratio of the maximum compressive strain in the web to the yield strain be infinite. The values of K can be determined by equating the work of the external forces to the dissipation of the internal energy at the instant of buckling. In Figure 5.3, h is the clear depth of the web, and y_0 corresponds to the position of the neutral axis. For the two limiting cases, pure bending is represented by $y_0/h = 0.5$, and pure compression by $y_0/h = 1.0$.

For an expedient solution to the problem, Haaijer and Thurlimann plotted experimentally determined values of α as a function of the critical strain (ϵ_{cr}) for Haaijer's three pure compression tests failing by web buckling.

For a beam-column web, defining the maximum strain of the compression flange to be ϵ_m and assuming that the average strain over the compression zone in the web would be $\epsilon_m/2$, it was graphically determined that for web plates:

For $\varepsilon_m/\varepsilon_y = 12, \alpha = 0.58;$

$\varepsilon_m/\varepsilon_y = 8, \alpha = 0.60;$

$\varepsilon_m/\varepsilon_y = 4, \alpha = 0.69.$

Using the assumptions stated in Chapter 2, web slenderness limits were proposed by Haaijer and Thurlimann(10). These form the basis for the CSA S16-1969 web slenderness limitations. However, it should be noted that no tests on web plates subjected to combined axial load and moment were conducted for experimental verification.

Although good correlation was found to exist between Haaijer and Thurlimann's theory for plates in pure compression and their test results, in extending this same theory to apply to web plates subjected to combined axial load and moment, some assumptions of doubtful validity were used:

1. In determining the values of K for Equation 5.8 (Figure 5.3), a stress distribution corresponding to that of a fully-plastified wide-flange section was assumed. For all loading cases except pure compression, this would mean that the member would be required to deform until the condition $\varepsilon_m/\varepsilon_y = \infty$ had been reached.

2. The ratio of the maximum compression flange strain to the yield strain ($\varepsilon_m/\varepsilon_y$), would reach a value of four for members required to deform plastically.
3. It was also assumed that the maximum compressive strain in the compression flange would be ε_m and the average strain over the compression zone in the web would be taken as $\varepsilon_m/2$. This implies that the analysis is for a plate in uniform compression with a width equal to the depth of the compression zone of the web.

Since Perlynn and Kulak(5) were not able to satisfactorily correlate their test results for compact beam-columns with Haaijer and Thurlimann's web buckling theory, it was decided that this theory did not adequately describe beam-column behaviour. This was considered to be at least partly attributable to the assumptions used in the theory.

Based on their test results, and the test results from another investigation(11), Perlynn and Kulak recommended higher web slenderness ratios for both compact and non-compact beam-columns and these have been incorporated into the most recent CSA Standards(6,7).

5.2 Investigation Leading to Recent CSA Standard Revisions

Because of the proportions of their test specimens, Perlynn and Kulak(5) were able to closely establish experimentally the limit of web slenderness at which a compact member would have its compression flange and web buckle simultaneously (Figure 5.4). Having established this limit, they then developed two methods to predict the occurrence of web buckling.

Method I consisted of developing two relationships, one between the web slenderness h/w, and the ratio of the depth of the neutral axis to the web depth y/h, and the other between P/Py and y/h. By equating the two relationships, h/w can be obtained as a function of P/Py. Since residual stresses were expected to affect the test results, they were taken into account.

By addition of the strain diagrams for axial load, moment and residual stresses, it is possible to determine the location of the neutral axis as represented by the y/h ratio (Figure 5.5). Since only one of the investigators quoted by Perlynn and Kulak determined the residual stress patterns in his test specimens(20), they assumed typical residual stress patterns for both rolled and welded members(9,21) for the other investigators' test results (Figure 5.6).

For their test results, Perlynn and Kulak determined the y/h ratios by graphically determining the combined strain diagrams for each member at the applied load and ultimate moment. The resulting stress distributions were obtained from the superposition of the strain diagrams for axial load, ultimate moment (Mu), and the assumed residual stresses. They were able to show that at ultimate conditions, different assumed residual stress patterns do not greatly affect the resulting y/h ratio for a member, primarily because residual stress patterns possess symmetry and a certain degree of consistency in magnitude. In particular, the value of 15 ksi for the maximum compressive residual stress is considered to be typical for most deep rolled and welded wide-flange sections.

Perlynn and Kulak then plotted their test results, along with the test results of the three other investigations on a graph of y/h versus P/Py (Figure 5.7). It was noted that the resulting relationship was very nearly linear for P/Py < 0.8, and could be represented by:

$$\frac{y}{h} = 0.4463\,\frac{P}{Py} + 0.607 \qquad (5.10)$$

When P/Py = 1.0, y/h is theoretically infinite. It is not obvious how the function behaves for 0.8 ≤ P/Py ≤ 1.0. If a member that is loaded into the strain-hardening range (P/Py > 1.0) had a very small moment applied to its ends, the y/h ratio would quickly diminish from infinity. Hence Perlynn and Kulak assumed only that y/h starts to increase towards infinity for P/Py > 0.8.

For the second relationship, y/h versus h/w, test results were again plotted (Figure 5.8). This figure has been plotted as y/h vs $\frac{h}{w}\sqrt{Fy}$ so that the results of the present investigation could be plotted on the same graph. Only the points representing the specimens considered in this investigation have been plotted. At this point, it was realized that two boundaries describing member failure were possible. One of these describes the web slenderness limits at which flange buckling ceases to be critical and web buckling becomes the mode of member failure. For web slenderness ratios that plot on this line, $M/Mpc \geq 1.0$. The other boundary describes the web slenderness limits at which a member would cease to reach $M/Mpc = 1.0$, irrespective of the mode of failure. These boundaries were determined graphically by observation of the types of failures of the specimens and superimposed on the graph of $\frac{h}{w}\sqrt{Fy}$ versus P/Py. Since there were gaps in the slenderness ratio between specimens at each ratio of P/Py, some judgement was required in placing these curves, although they are thought to be on the conservative side.

The boundary of interest is the one that describes the web slenderness limits when flange buckling ceases to be the mode of member failure because it yields the more conservative web slenderness ratio. Simultaneous flange and web plate buckling was found to occur at:

$$\frac{y}{h} = \frac{(8.20 - 0.100(h/w))^{(2.6)} + 61}{100} \qquad (5.11)$$

By combining Equations 5.10 and 5.11, Perlynn and Kulak determined that the boundary describing simultaneous web and flange plate buckling was given by:

$$\frac{P}{Py} = \frac{(8.20 - 0.100(h/w))^{(2.6)} + 0.3}{44.63} \qquad (5.12)$$

Equation 5.12 gave reasonably good correlation with the test results.

Method II consists of finding $\frac{h}{w}\sqrt{Fy}$ as a function of P/Py by using a revised form of Equation 2.3 (Equation 5.8). Using the results of four different experimental programs, they were able to find values of α for the various specimens by using Equations 5.7 and 5.8.

Knowing these α values, it is possible to calculate a modified K value using Equation 5.8, designated K', for the test results. This K' parameter was then plotted against $\frac{h}{w}\sqrt{Fy}$ to obtain a relationship between $\frac{h}{w}\sqrt{Fy}$ and K'. Substitution of h/w as a function K' into Equation 5.12 from

Method I gives a relationship between K' and P/Py. This expression can then be substituted into Equation 5.8 to find the relationship between $\frac{h}{w}\sqrt{Fy}$ and P/Py.

Although this method utilizes the results of Method I, it is in fact a different procedure, and is based directly on Haaijer and Thurlimann's buckling theory. Because the experimental test results were used for the determination of the relationships used in this development, it is expected that K' will reflect the inelastic plate buckling properties of the members tested.

In determining the α values from Equations 5.7 and 5.8, it is necessary to calculate σ_{cr}/σ_y for the specimens. The maximum strain in the compression flange-to-web junction, at the ultimate moment, is determined from the experimental results. This is then converted to stress and divided by the yield stress of the specimen to give the σ_{cr}/σ_y ratio.

Of the four experimental programs considered, only Haaijer's(4) had specimens where $\sigma_{cr}/\sigma_y > 1.0$. Although many tests in the other investigations showed that the yield strains in the compression flange-to-web junction were surpassed, none had attained strain-hardening. Since Haaijer and Thurlimann's transition curve, described by Equation 5.9, is not valid for σ_{cr}/σ_y ratios greater than 1.0, Perlynn and Kulak assumed that if σ_{cr}/σ_y was greater than

1.0, then $\sigma_{cr}/\sigma_y = 1.0$. This is because Equation 5.9 implies that once a member reaches $\sigma_{cr}/\sigma_y = 1.0$, it is in the strain-hardening range and Equation 5.9 is no longer applicable.

Perlynn and Kulak then plotted the various transition curves corresponding to the four investigations under consideration. They noted that the residual stress distribution caused the steels with the lower yield stresses to reach the proportional limit at a lower applied load than the higher yield strength steels. Hence the transition curves were not coincident for the investigations they considered.

In order to plot the transition curves, Perlynn and Kulak assumed $\alpha_o = 0.58$, a value suggested by Haaijer and Thurlimann. Using Equation 5.9, they then calculated the corresponding value of α knowing σ_p, σ_y, σ_{cr}, α_o, and α_p. Invoking the mathematical convention that zero raised to a power greater than zero equals zero, they were able to prove that $\alpha = \alpha_o = 0.58$ when $\sigma_{cr}/\sigma_y = 1.0$. By doing this, it appeared that their specimens not failing by web buckling had $\alpha = \alpha_o = 0.58$. Since by definition, when $\alpha = \alpha_o$, the point of strain-hardening has been achieved, this in effect states that these particular specimens were able to reach strains greater than the yield strain before buckling occurred. Because the material yielded in slip-bands(17), some of the material reached strain-hardening. Perlynn and

Kulak, on the other hand, state that none of their specimens reached the point of strain-hardening, meaning that the specimens as a whole did not reach strain-hardening, but some of the material did.

Perlynn and Kulak then solved for K' using Equation 5.8 with the α values obtained. Following this they obtained a linear approximation to the relationship of K' vs $\frac{h}{w}\sqrt{Fy}$ (Figure 5.9);

$$K' = \frac{0.48\,(h/w)\,\sqrt{Fy}}{\sqrt{Fy}} - 9.6 \qquad (5.13)$$

Next, K' was found as a function of P/Py. Referring to Method I, substituting Equation 5.12 into Equation 5.13 results in:

$$K' = 29.76 - 20.68\,(P/Py)^{(0.385)} \qquad (5.14)$$

Finally, substitution of K' in Equation 5.4 for K in Equation 5.8 results in an expression relating $\frac{h}{w}\sqrt{Fy}$ to P/Py:

$$\alpha = \frac{h}{100w} \sqrt{Fy} \sqrt{\frac{0.01241}{1 - 0.695 \, (P/Py)^{0.385}}} \qquad (5.15)$$

where $E = 30 \times 10^6$ psi and $\nu = 0.3$.

From this, they assumed that since $\alpha = 0.58$ appeared to be the limiting value from their test results, they substituted this value into Equation 5.15 to obtain an expression between $\frac{h}{w}\sqrt{Fy}$ and P/Py. This limit was set to ensure that the web component part of a member will reach the yield stress of the material, to a depth of about h/4 below the compression flange-to-web junction before web buckling will occur. This depth of h/4 corresponds to $\varepsilon_m/\varepsilon_y = 2.0$ which is the maximum ratio of compressive web strain to yield strain recorded for their tests on compact beam-columns. The expression is:

$$\frac{h}{w}\sqrt{Fy} = 520 \sqrt{1 - 0.695 (P/Py)^{0.385}} \qquad (5.16)$$

which is the same as Equation 2.4. This expression is plotted in Figure 5.4.

This procedure was shown to give the same results as Method I, hence the usefulness of their results and procedures seems to be verified. Perhaps this is because uniform compression of a web plate up to strain-hardening (for which Haaijer and Thurlimann(10) recommended $\alpha = 0.58$) may be equivalent to combined axial load and bending moment up to the yield stress for an equivalent web depth of about h/4 (for which Perlynn and Kulak(5) used $\alpha = 0.58$). This could be reasoned by considering the extra rotational deformation and hence the additional strain the compression part of the web must undergo when bending is present, as compared with pure compression.

5.3 Analysis of Present Investigation Test Results-Method I

Method I of predicting web buckling is analogous to the Method I used by Perlynn and Kulak(5) in their investigation of compact beam-columns. It consists of the determination of the y/h ratios for the specimens, and then plotting them against P/Py in order to determine a relationship between y/h and P/Py. Then, y/h is plotted as a function of $\frac{h}{w}\sqrt{Fy}$ to find a relationship between y/h and $\frac{h}{w}\sqrt{Fy}$. The two relationships containing the y/h ratios are then equated to determine the allowable slenderness ratio $\frac{h}{w}\sqrt{Fy}$ for non-compact beam-columns as a function of P/Py.

In determining the y/h ratios to be used, it was necessary to decide whether or not to use theoretical calculations, or the results from strain gauge data. It was decided to use the theoretical stress determination, because the effects of an assumed residual stress distribution could be included. Since the strain gauges were mounted after the specimens were fabricated, the strain readings would not give an accurate indication of the effects of the residual stresses over the depth of the web. This assumed residual stress distribution is shown in Figure 5.6, and is identical to the one used by Perlynn and Kulak for welded members. The stresses were then added up, so that the total stress at different positions along the web would consist of the sum of the stresses due to axial load, the stress at that point due to moment, and the residual stress at that point (Figure 5.5).

After calculation of the total stress at a number of points over the depth of the web, the stress was plotted as a function of its position on the web. The y/h ratio was taken as the ratio of the distance to the point where the total stress was zero to the total web height.

In some cases, the yield stress was exceeded at points along the web. These points were quite far away from the location where the total stress was zero. This was not expected to affect the y/h ratio significantly, and was ignored.

Once the neutral axis had been located in this way for all the specimens in this test series, and for the non-compact beams tested previously(11), the y/h values were plotted as a function of P/Py (Figure 5.7). These data are also tabulated in Table 5.1. The relationship shown in Figure 5.7 follows the same general trend as that observed earlier for compact beam-columns. From the plot, it was determined that the relationship between the parameters for $P/Py < 0.8$ is:

$$\frac{y}{h} = 0.410 \frac{P}{Py} + 0.700 \qquad (5.17)$$

This relationship is considered to be valid for $P/Py < 0.8$. As was the case for compact beam-columns, it is not obvious how the function behaves for $P/Py > 0.8$. In theory, it is possible that it reaches infinity at $P/Py = 1.0$, and this is what has been indicated here. As a result of fabrication tolerances and imperfections, however, y/h will probably never be very large in practice.

In order to obtain the second relationship, y/h is plotted against the slenderness ratio $\frac{h}{w}\sqrt{Fy}$ (Figure 5.8). On this plot, the type of failures undergone by each specimen and their respective Mu/My ratios are also indicated. Judgement had to be used here to plot a reasonable curve for simultaneous web and flange buckling, as indicated by the failure mode of the specimens and their Mu/My ratios. The limiting web slenderness of interest is the one where the specimen will fail by simultaneous web and flange buckling and for which $Mu/My = 1.0$. Hence, the curve should pass between specimens 5 and 6 because specimen 5 failed by simultaneous web and flange buckling and specimen 6 failed by flange buckling. Moreover, the Mu/My ratios dictated than the curve pass somewhere near the mid-point between the two specimens, where linear interpolation indicated Mu/My = 1.0 should exist. A similar determination was made for specimens 3 and 4, and the curve was fitted to pass between the points representing these two specimens. The curve is felt to be conservative for P/Py > 0.2 because it indicates a less slender limit than the specimens which failed by simultaneous web and flange buckling and had Mu/My > 1.0 (Specimens 3 and 5). However for specimens 1 and 2, the curve appears to be unconservative because of both the Mu/My ratios and the mode of specimen failure. Because both specimens 1 and 2 failed by web buckling, the curve would normally be placed such that the expected maximum slenderness limit would be a lesser slenderness than specimen 2. However, because the Mu/My ratio was less for specimen 2 than specimen 1, the curve was placed near specimen 2 in the gap between specimens 1 and 2. This was done by judgement. Perlynn and Kulak's investigation offered some guidance as to the expected shape of the curve. From here, the curve was extended to reach approximately the mid-point of the gap between the beam specimens NC-1 and NC-2. The resulting curve is thought to be a conservative estimate of the limit of simultaneous web and flange failure for non-compact members. Even though specimen 2 did not appear to fit the test results perfectly, it was felt that this had more to do with errors of unknown magnitude in the test procedure rather than the analysis, and so the curve was considered to be a conservative estimate. The equation describing the relationship between y/h and P/Py is:

$$\frac{y}{h} = 1.578 \times 10^{-7}(690 - \frac{h}{w}\sqrt{Fy})^{2.6} + 0.70 \qquad (5.18)$$

Combining equations 5.17 and 5.18 results in a relationship between $\frac{h}{w}\sqrt{Fy}$ and P/Py. This estimate of the boundary of the failure limit due to simultaneous web and flange buckling is:

$$\frac{h}{w}\sqrt{Fy} = 690\,[1.0 - 0.425\ (P/Py)^{0.385}] \qquad (5.19)$$

This equation has been plotted in Figure 5.10, along with Perlynn and Kulak's theoretical prediction for compact members (Equation 5.16).

5.4 Analysis of Present Investigation Test Results-Method II

Analogous to Method I, Method II is similar to the second procedure used by Perlynn and Kulak(5) to determine the maximum web slenderness limits.

First, the values of α for the specimens (including the non-compact beams of Holtz and Kulak(11)) were calculated. For the beam-columns, this was done by calculating the average strain of the web strain gauge readings closest to the web to compression flange junction, and then converting this strain to stress using E = 29600 ksi. If the strain was greater than the yield strain, α was taken to be equal to 0.58. This procedure implicitly assumes the definition of raising zero to a positive power used by Perlynn and Kulak to determine the values of α when $\sigma_{cr}/\sigma_y = 1.0$. For the specimens where this averaged strain was less than the yield strain, the appropriate value of α was calculated using either Equation 5.7 or 5.8. It was felt that these strain readings would not be adversely affected by the presence of residual strains, because the assumed residual strain distribution is small where these two strain gauges were located on the web. For the beams, the values of α were calculated by choosing the maximum compressive stress in the web as obtained by adding up the total stress due to the sum of the assumed residual stress, the stress due to the moment, and the stress due to the axial load. Once the maximum stress in the web was determined, it was substituted into Equation 5.7 and the α value was calculated. These data are also tabulated in Table 5.1, and are plotted in Figure 5.11.

After the values of α were calculated, they were substituted into Equation 5.8 and a new value of K, called K', was calculated for each specimen. This K' parameter was then plotted against $\frac{h}{w}\sqrt{Fy}$, to obtain a relationship between these parameters. This relationship is also plotted in Figure 5.9. In this figure, the solid line represents the results of the present investigation (E = 29600 ksi), and the dotted line represents the test results considered by Perlynn and Kulak which did not fail by web buckling (E = 30000 ksi). The points plotted which are not near the curves are the four specimens considered in this investigation which buckled in the web. The remaining four specimens are plotted on the curve.

From this plot, it is possible to conclude two things. The first conclusion is that the plots for K' versus $\frac{h}{w}\sqrt{Fy}$ from the separate investigations are coincident within experimental error. This indicates that K' is not a function of the cross-sectional proportions of the specimens involved. Indeed, Perlynn and Kulak originally used the results from three other testing programs as well as their own to obtain the curve. The second thing of note is that any specimen which failed by web buckling plots above the curve. It is, for example, reasonable to assume that specimen 2 buckled in the web, because it is considerably above the curve. Perlynn and Kulak represented their test results with Equation 5.13, which is a linear approximation to the curved line they obtained by plotting the points corresponding to the specimens they were considering which did not fail by web buckling. Another representation of this curved line, incorporating a more precise parabolic approximation, is:

$$K' = 0.000111 \left(\frac{h}{w}\sqrt{Fy}\right)^2 \qquad (5.20)$$

It is considered that this curve represents a reasonable approximation to the maximum web slenderness which a specimen may have (in terms of K') before a specimen will fail by web buckling.

Next, substitution of the results of Method I (Equation 5.19) into Equation 5.20 will give a relationship between K' and P/Py:

$$K' = 0.000111 \left[690 - 293.1\,(P/Py)^{0.385}\right]^2 \qquad (5.21)$$

Substitution of Equation 5.21 into Equation 5.8 should result in another expression to determine the maximum limit of web slenderness, provided a suitable value for α can be chosen. Perlynn and Kulak had $\alpha = 0.58$ for all their specimens not failing by web buckling. For the present investigation, however, α varies, although it is equal to 0.58 for all the specimens not failing by web buckling. Hence, it was decided to use $\alpha = 0.58$, and see if the results would be meaningful. Assuming $\alpha = 0.58$, $E = 29600$ ksi, and $\nu = 0.3$, this results in:

$$\frac{h}{w}\sqrt{Fy} = 690\,[1.0 - 0.425(P/Py)^{0.385}] \qquad (5.22)$$

Note that this equation is identical to Equation 5.19, hence both methods yield the same result. This expression is thought to be a reasonable estimate of maximum web slenderness for non-compact beam-columns. The plot of this expression along with the test specimens is shown in Figure 5.12.

5.5 Discussion of Analytical Results

In spite of the difficulty of reducing the data obtained from specimen 2, which had a difficult failure mechanism to interpret, the analyses did indicate a reasonable prediction of the expected limit of simultaneous web and flange buckling.

Because the curve for K' vs $\frac{h}{w}\sqrt{Fy}$ corresponded to that of Perlynn and Kulak's(5), which in itself utilized data from four separate investigations, it was safe to assume that any points which plotted above this line failed by web buckling. This aided the analysis especially with regard to specimen 2, and substantiated the opinion that this specimen failed by web buckling.

Since the expressions for maximum web slenderness turned out to be identical using the two methods of analysis, it appears that a choice of $\alpha = 0.58$ in Method II for specimens not failing by web buckling is justified. Indeed, if Equation 5.20 is substituted into Equation 5.8 with $\alpha = 0.58$, $\nu = 0.3$, and $E = 29600$ ksi, Equation 5.8 reduces to the trivial identity $0 = 0$. Hence the results of Method I will always be the solution of Method II, provided $\alpha = 0.58$. Therefore Perlynn and Kulak's conclusion of having web buckling invariably occurring before flange buckling or simultaneous web and flange buckling if α is greater than 0.58 seems to be extendable to the case of non-compact beam-columns.

It should be noted that the curve determined by the analyses (Figure 5.12) appears to be slightly unconservative in the region of $P/P_y = 0.15$. In particular, it appears as if the curve is indicating that the limit for simultaneous web and flange failure is above a specimen known to have failed by web buckling. This is due to the shape of the curve used to predict simultaneous web and flange buckling (Figure 5.8). In this figure, the curve of expected simultaneous web and flange failure is on the unconservative side of specimen 2. Since both methods of analysis utilized the results of this plot, and its associated relationship (Equation 5.18), the results of the theoretical analyses will also appear unconservative in the region near specimen 2. The recommended design approximation should then be reduced slightly in this region to take care of this inconsistency.

The two methods used in the analysis portion of this investigation yield what appears to be identical results. Although Method II appears to be similar to Method I and utilizes the results from Method I, it is essentially based upon Haaijer and Thurlimann's web buckling theory(10).

During the tests, it was noted that the greatest value of the ratio of the averaged maximum strain to the yield strain ($\varepsilon_m/\varepsilon_y$) at the web to compression flange junction was 2.5 (Specimen 6). It appears as if the compression flanges strained approximately the same amounts as those in Perlynn and Kulak's investigation. Since α is a function of the critical strain (ε_{cr}), and the amount of straining is reasonably consistent in both investigations, it appears as if using $\alpha = 0.58$ can be justified by this consideration for this investigation, as it was used successfully by Perlynn and Kulak to predict the web slenderness limit for compact members.

It appears as though Haaijer and Thurlimann's(10) recommendation of $\alpha = 0.58$ for uniform compression of web plates up to strain-hardening is also applicable to the case of compact and non-compact beam-columns subjected to axial load and moment which did not fail by web buckling. This is due to the behaviour of the material, because it yields in slip-bands(17). Since the material cannot be at strains between the yield strain ε_y, and the strain at the start of strain-hardening ε_{st} (Figure 5.1), $\alpha = 0.58$ appears to apply to any web where the yield strains have been surpassed.

The maximum value of the strain ratio ($\varepsilon_m/\varepsilon_y$) at approximately h/4 of the web was 0.81 (Specimen 6). Hence the supposition that the y/h ratio would not be substantially affected by ignoring the effects of the yield stress having been attained at some location in the web seems to be justified. This is because the web has not reached the yield stress closer than 0.4h, for the worst case, to the point where the total stress is zero. It also appears as if the web in non-compact beam-columns does not have to be stocky enough to prevent failure until the yield stress has been surpassed to a depth of h/4, but rather to a depth of h/6 or h/8.

At this point, it is useful to compare the analytical results with those expected when the specimen design was done. In Appendix I, the specimens were expected to have a value of α of approximately 0.8, while in the analysis, the limit of web slenderness was shown to be $\alpha = \alpha_o = 0.58$. This can be resolved by taking a closer look at the equations used for these calculations. In general, the equations have the following form:

$$\frac{h}{w} \sqrt{Fy} = C \left[1.0 - D(P/Py)^{0.385} \right]^{x} \qquad (5.23)$$

where x = 0.5 if Perlynn and Kulak's approximation for K' vs $\frac{h}{w} \sqrt{Fy}$ is used (Equation 5.13), and x = 1.0 if Equation 5.20 is used.

When the specimen design was done, Perlynn and Kulak's equation was used, where C = 690 and 750, D = 0.695, and x = 0.5. This value of D led to the prediction of α being approximately equal to 0.8.

The analysis, however, indicates that a close approximation to the same curve can be generated by using different values of α and D, for a given value of x. Therefore, the apparent change in values of α between that expected and that obtained can be explained by noting that the value of D in Equation 5.23 varies for the two investigations, for a consistent use of either Equation 5.13 or 5.20.

It is useful to note that the differences in slenderness ratio between P/Py = 0 and P/Py = 1 is approximately the same for both compact and non-compact beam-columns (Figure 5.10). This difference is approximately 280 and can be expressed mathematically by:

$$CD = 280 \tag{5.24}$$

The constants C and D are thus related and seem to be reasonably independent of flange slenderness.

Hence, it appears possible that any flange cross-section (plastic design, compact, non-compact, or other) can have the appropriate web slenderness limit calculated by using Equation 5.23, provided the value of C has been established from an appropriate beam test, and D has been obtained from Equation 5.24. Therefore, once the flange slenderness has been chosen on the basis of the desired amount of rotation, it should be possible to predict any beam-column web slenderness limit by this procedure.

SPECIMEN	P/Py	Mu/My	y/h	σ_{cr}/σ_y	α	K'	$\frac{h\sqrt{F_y}}{w}$	FAILURE
1	0.15	1.16	0.74	0.98	0.76	26.46	639.4	W
2	0.15	0.99	0.76	0.96	0.82	15.87	534.2	W
3	0.30	1.12	0.82	1.00	0.58	38.77	590.7	W&F
4	0.30	1.20	0.81	1.00	0.58	26.48	488.2	F
5	0.70	0.79	0.97	1.00	0.58	27.91	501.2	W&F
6	0.70	1.53	0.95	1.00	0.58	17.87	401.1	F
NC-1•	0.00	1.04	0.70	0.75	1.13	13.33	674.8	W
NC-2•	0.00	1.02	0.70	0.74	1.14	15.41	732.0	W

•From Holtz and Kulak(11)

TABLE 5.1

SPECIMEN TEST DATA

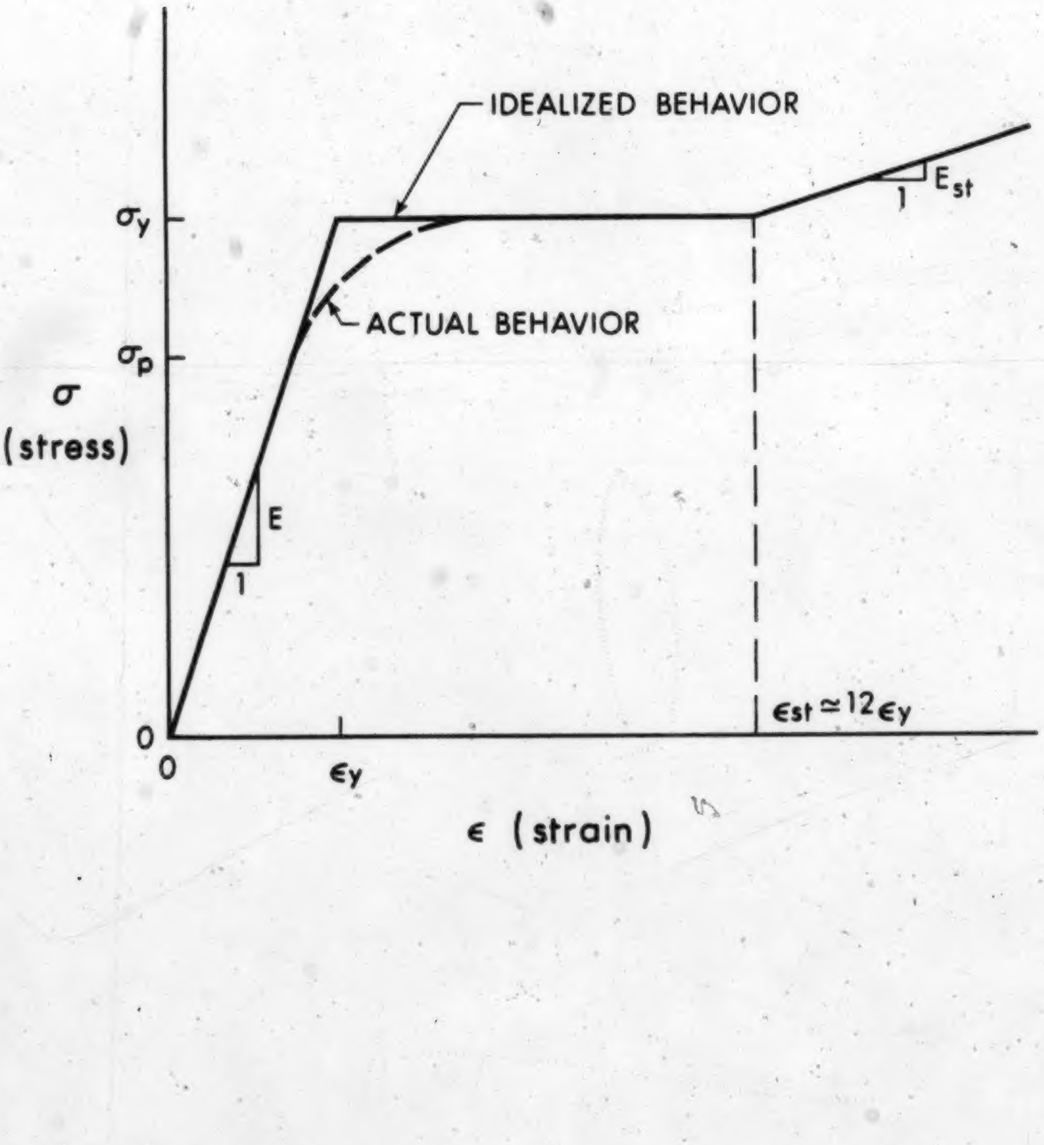

FIGURE 5.1

IDEALIZED STRESS-STRAIN DIAGRAM

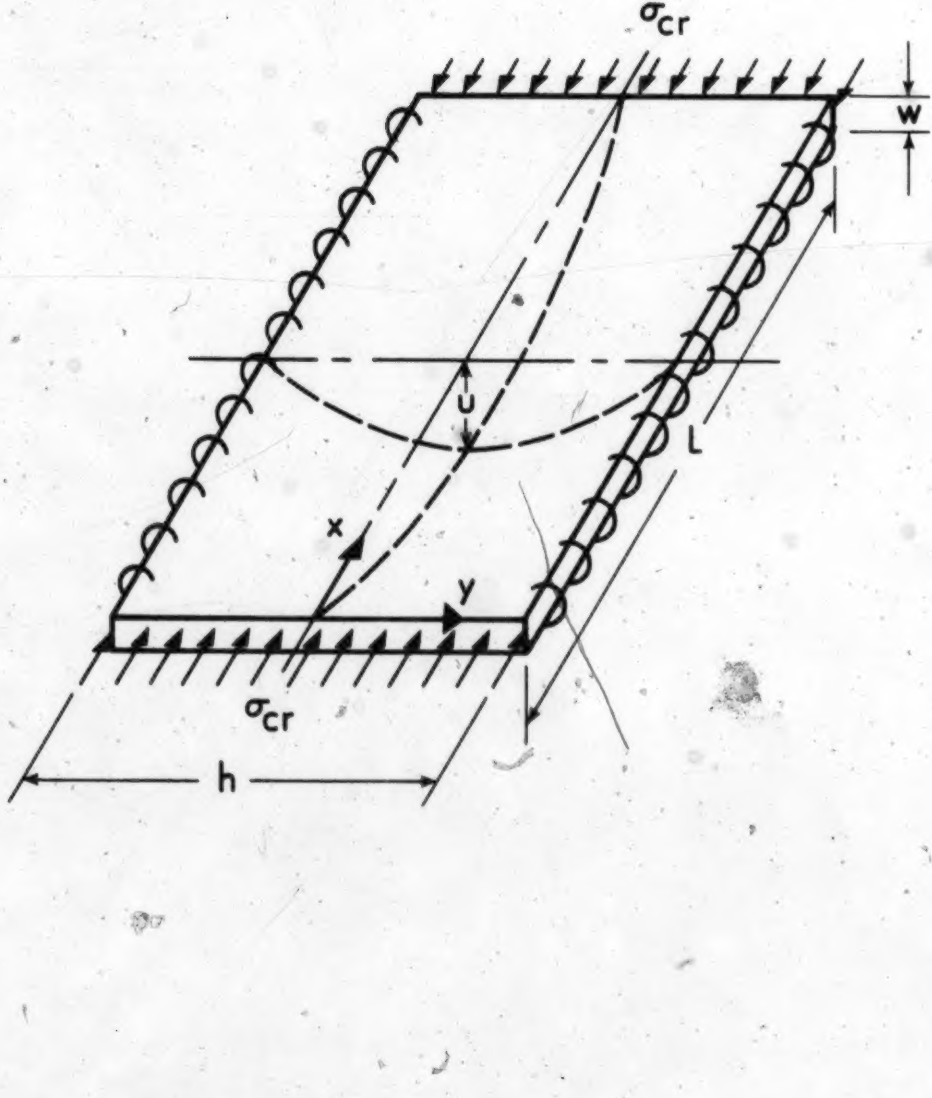

σ_{cr}
w
u
L
x
y
σ_{cr}
h

FIGURE 5.2

PLATE BUCKLING MODEL

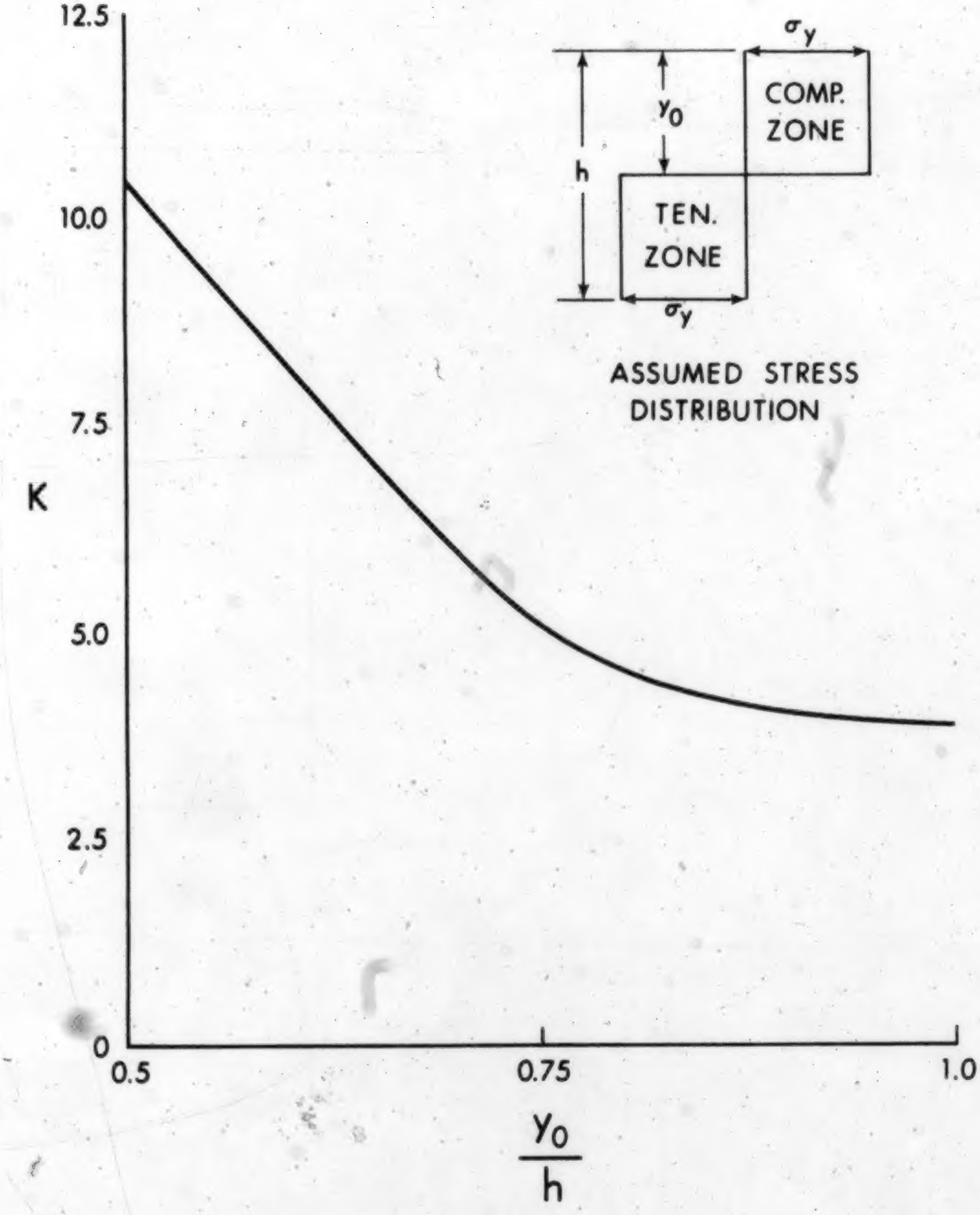

FIGURE 5.3

PLATE COEFFICIENT OF FULLY PLASTIFIED WIDE-FLANGE SECTIONS SUBJECTED TO AXIAL LOAD AND MOMENT

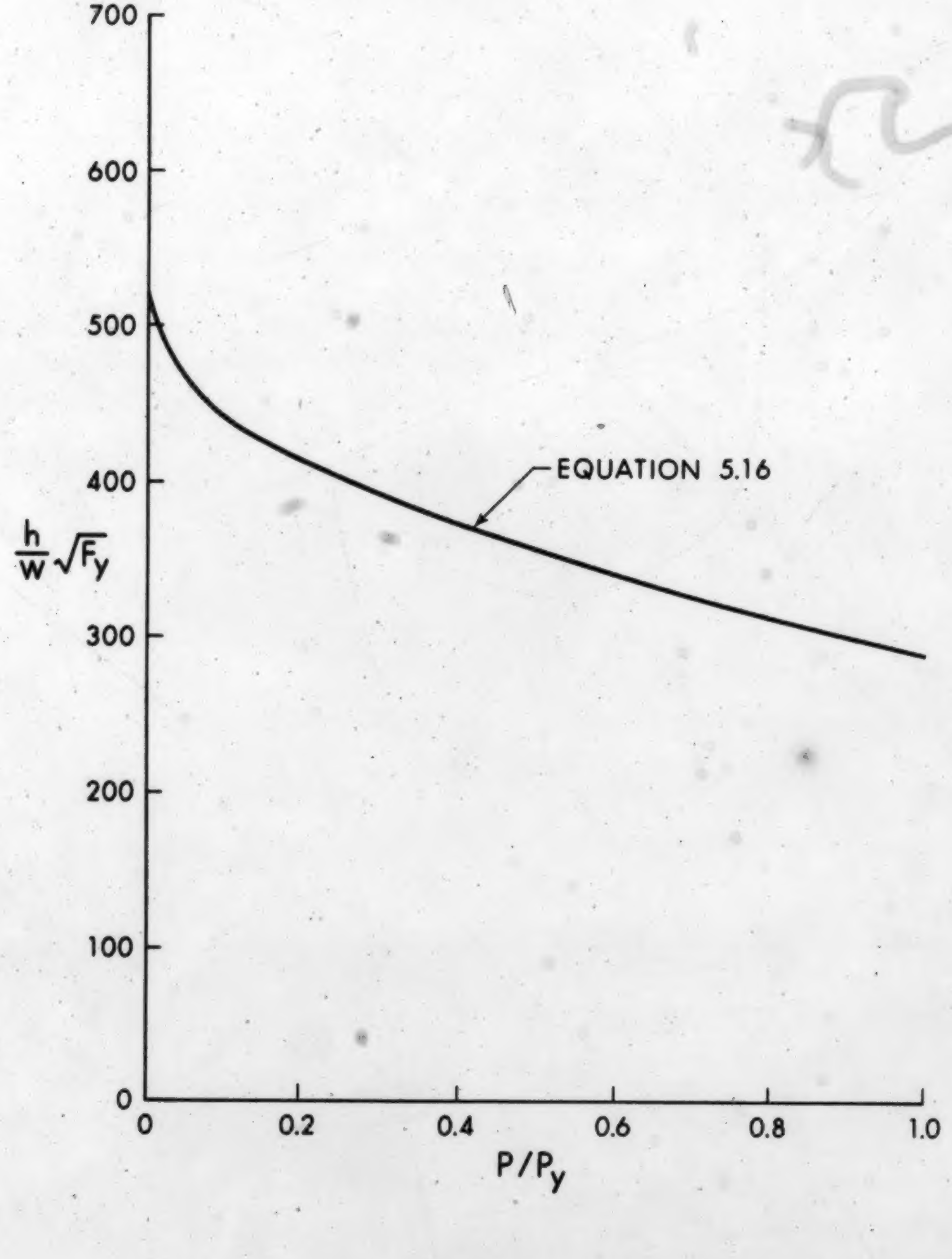

FIGURE 5.4

THE THEORETICAL LIMIT OF WEB SLENDERNESS FOR COMPACT MEMBERS

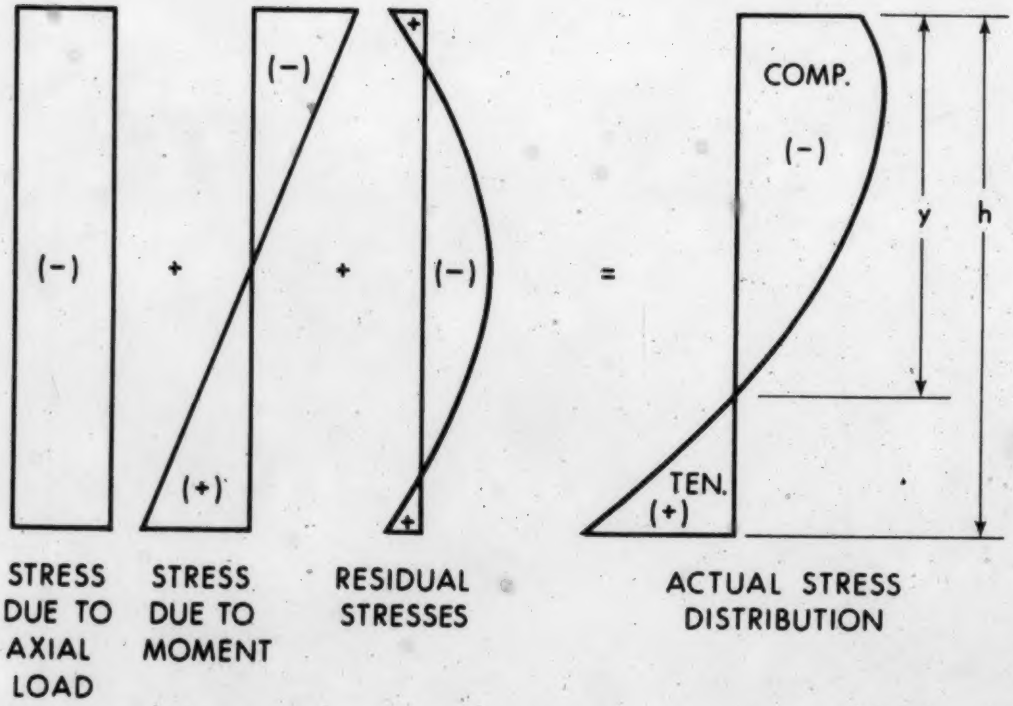
(−)
+
(−)
(+)
+
+
(−)
+
=
COMP.
(−)
y
h
TEN.
(+)
STRESS DUE TO AXIAL LOAD
STRESS DUE TO MOMENT
RESIDUAL STRESSES
ACTUAL STRESS DISTRIBUTION

FIGURE 5.5

ACTUAL STRESS DISTRIBUTION INCLUDING RESIDUAL STRESSES

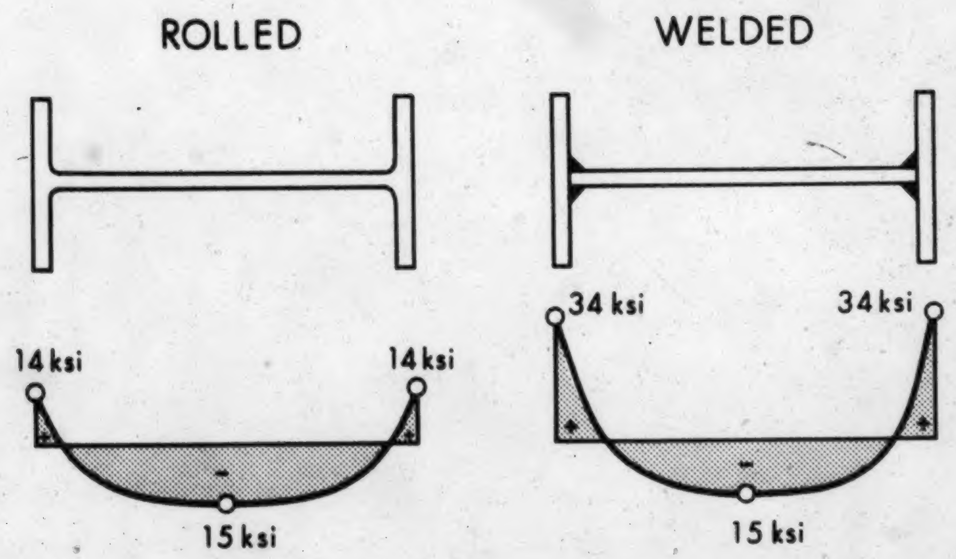
ROLLED
WELDED
14 ksi
14 ksi
+
+
-
15 ksi
34 ksi
34 ksi
+
+
-
15 ksi

FIGURE 5.6

TYPICAL RESIDUAL STRESSES FOR ROLLED AND WELDED MEMBERS

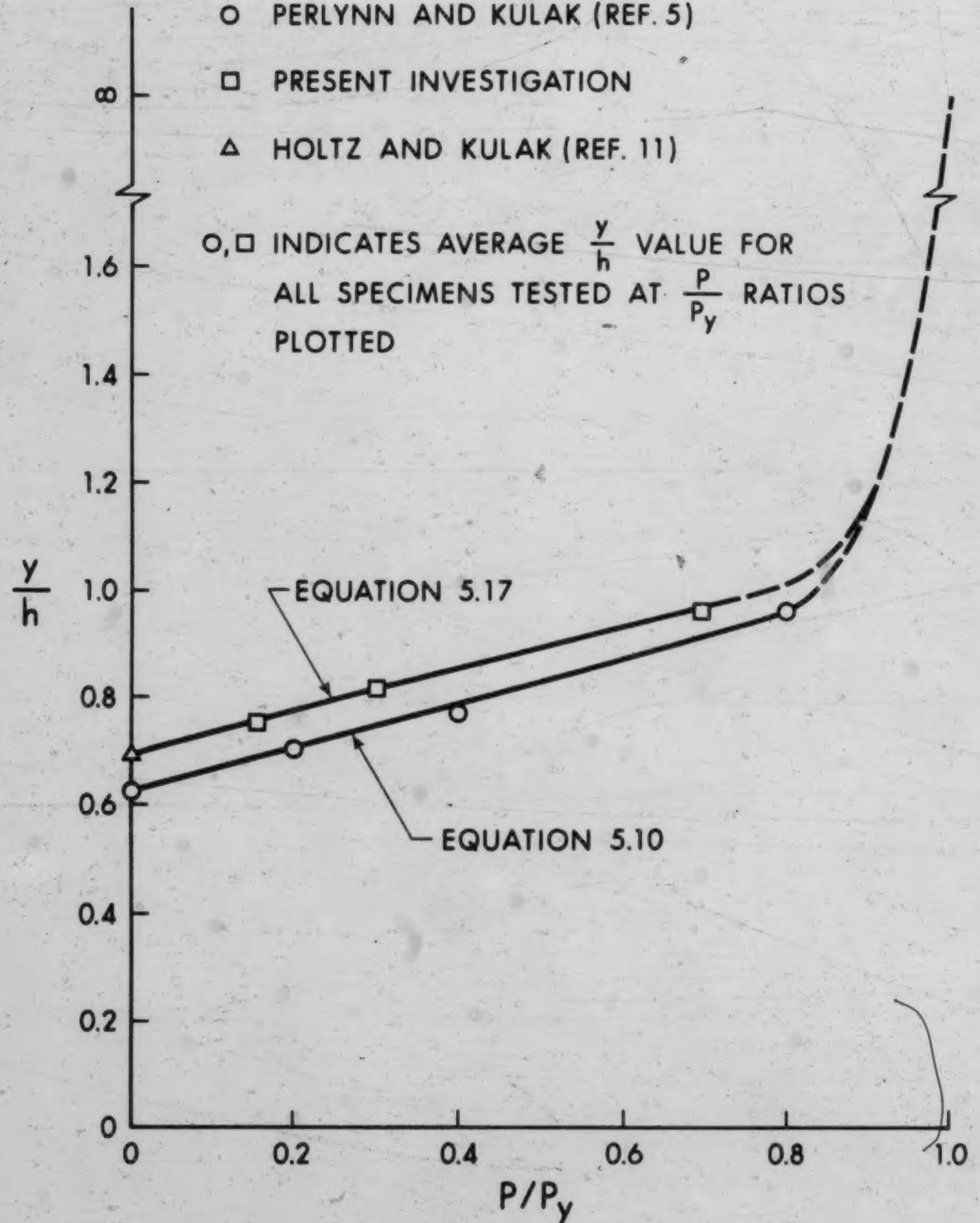

FIGURE 5.7

y/h AS A FUNCTION OF P/Py (COMPACT AND NON-COMPACT)

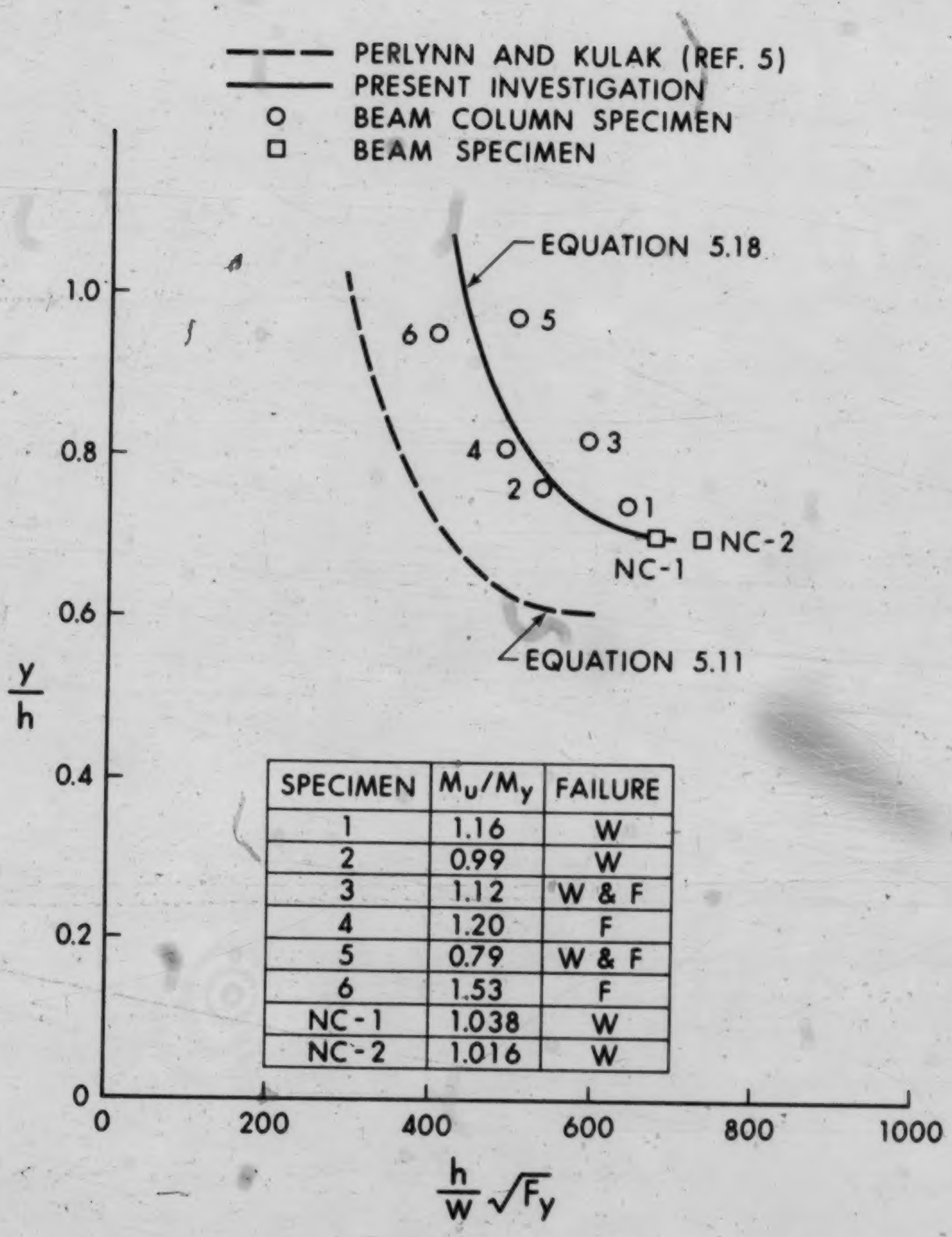

SPECIMEN	M_u/M_y	FAILURE
1	1.16	W
2	0.99	W
3	1.12	W & F
4	1.20	F
5	0.79	W & F
6	1.53	F
NC-1	1.038	W
NC-2	1.016	W

FIGURE 5.8

y/h AS A FUNCTION OF $\frac{h}{w}\sqrt{Fy}$ (COMPACT AND NON-COMPACT)

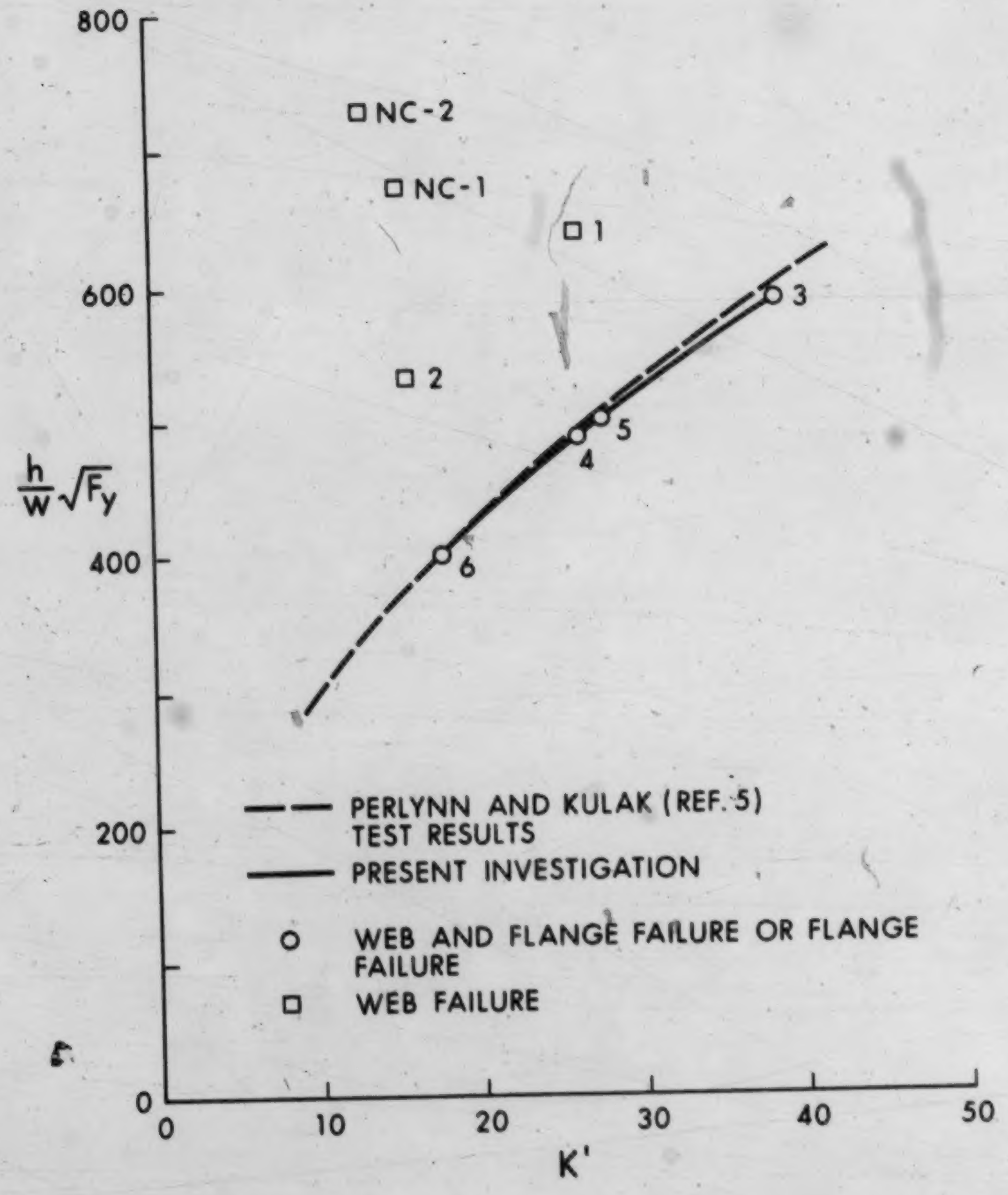

FIGURE 5.9

K' AS A FUNCTION OF $\frac{h}{w}\sqrt{Fy}$ (COMPACT AND NON-COMPACT)

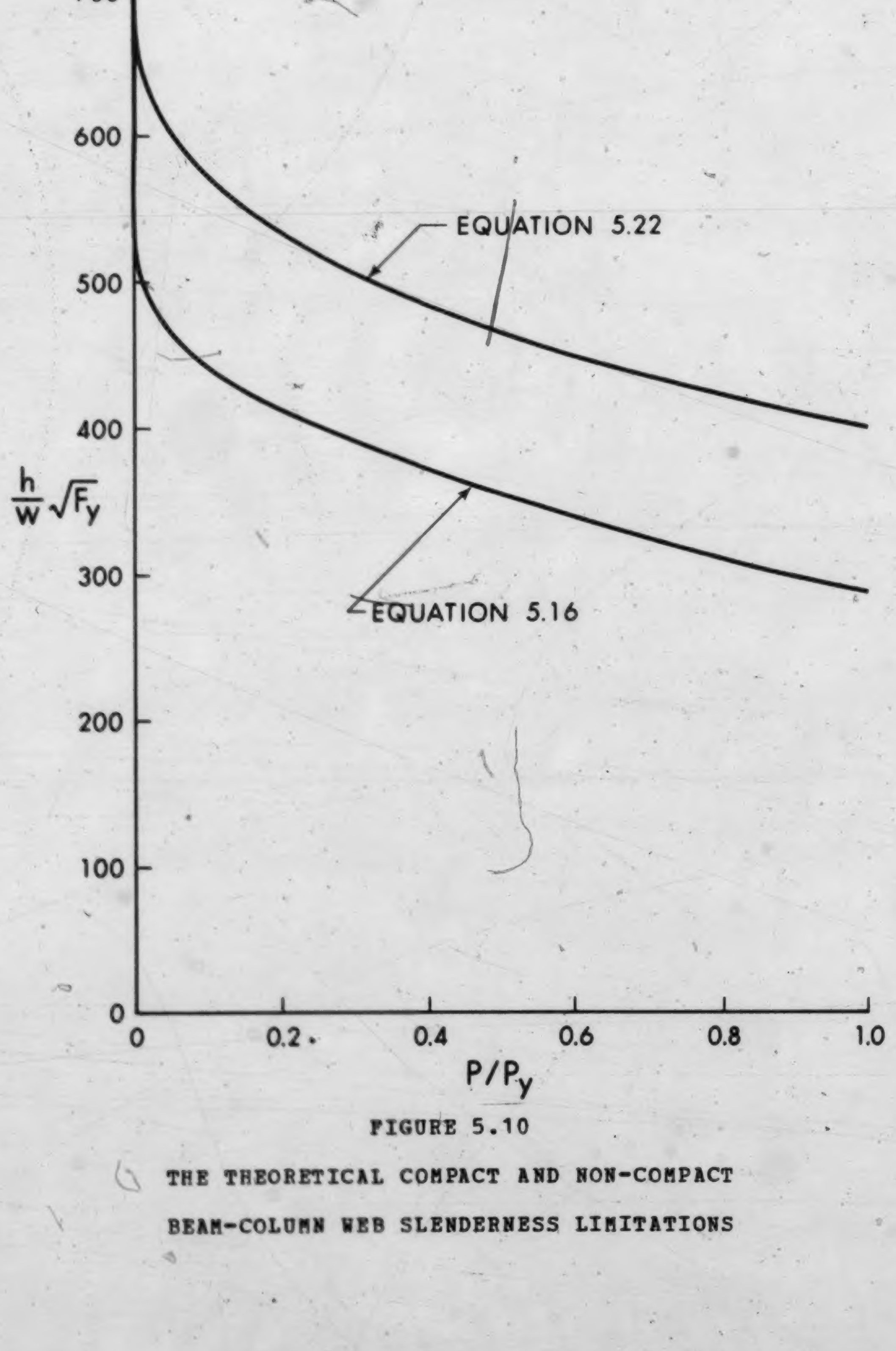

FIGURE 5.10

THE THEORETICAL COMPACT AND NON-COMPACT BEAM-COLUMN WEB SLENDERNESS LIMITATIONS

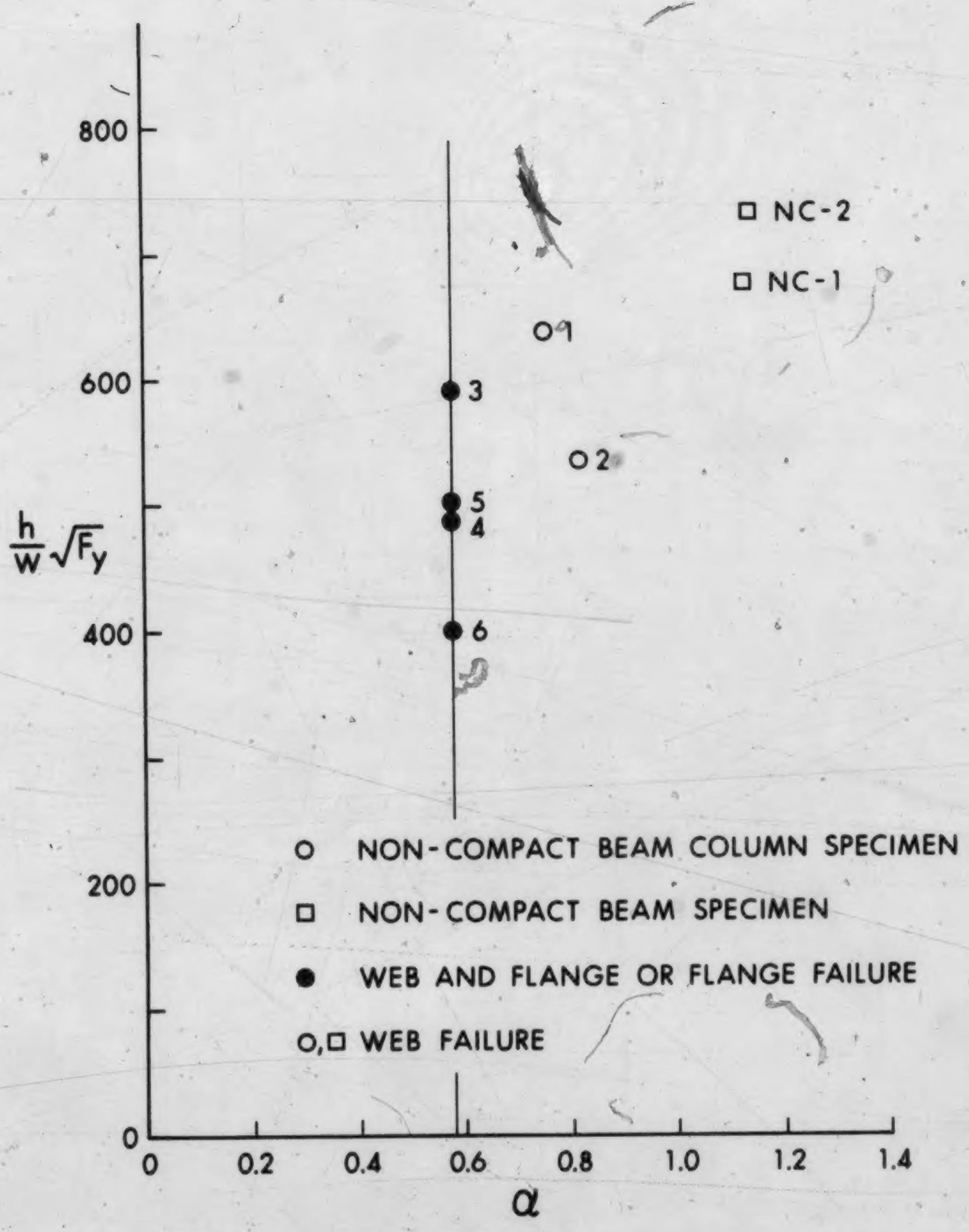

FIGURE 5.11

ALPHA AS A FUNCTION OF $\frac{h}{w}\sqrt{Fy}$

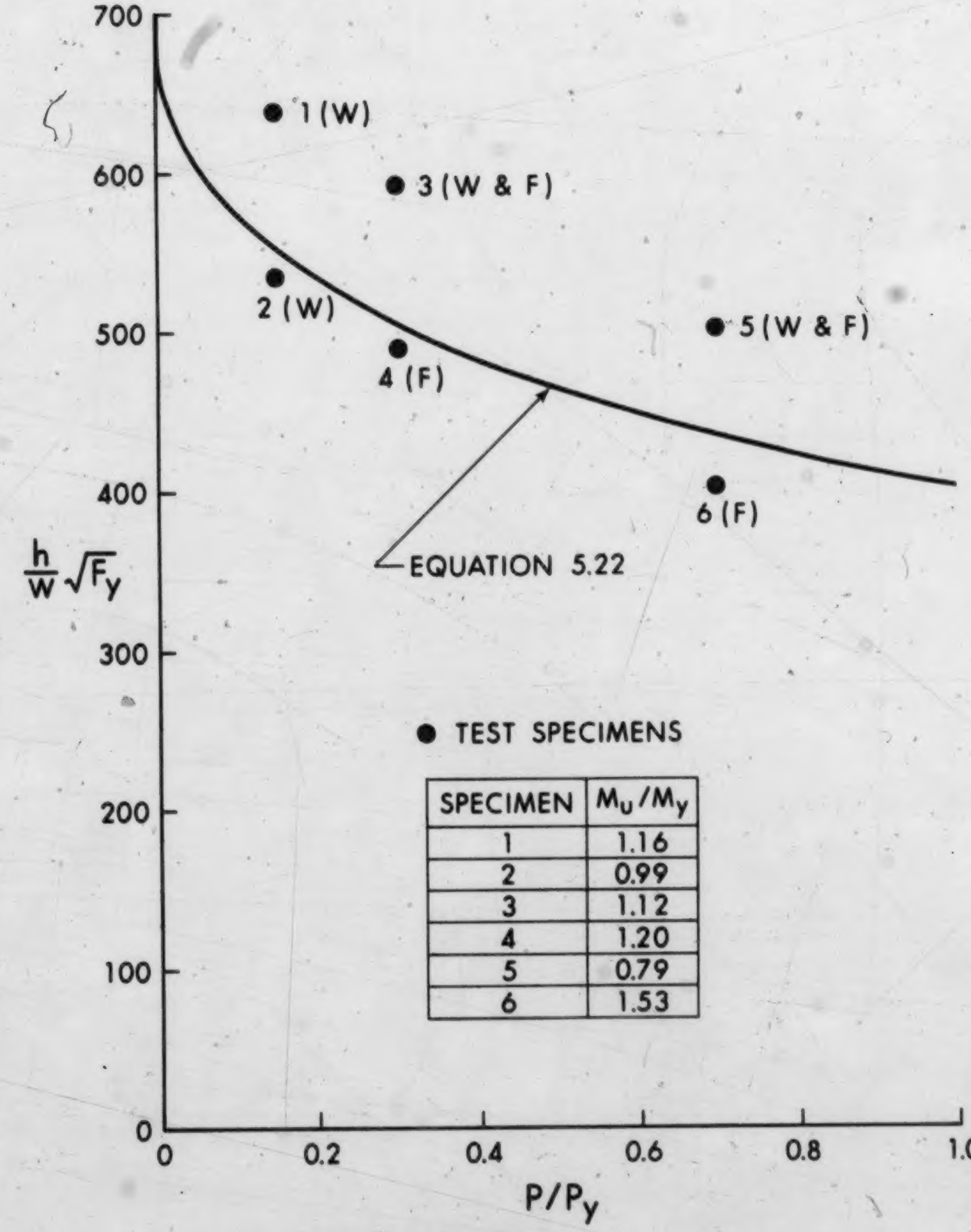

SPECIMEN	M_u/M_y
1	1.16
2	0.99
3	1.12
4	1.20
5	0.79
6	1.53

FIGURE 5.12

TEST SPECIMENS AND

THE NON-COMPACT WEB SLENDERNESS LIMITATION

CHAPTER VI

SUMMARY, CONCLUSIONS, AND RECOMMENDATIONS

6.1 Summary

In order to determine whether or not the web slenderness limits for non-compact beam-columns could be revised upwards, a total of six specimens were tested. All of the specimens had flanges proportioned such that the CSA Standard S16-1969 specification for non-compact flanges was just satisfied, and had webs that were more slender than permitted by the current S16.1 and S16.2 standards. Two tests were conducted at each of three P/Py ratios, to encompass a wide range of beam-column design.

The deflections, rotations, loads, and strain gauge readings were all taken by a minicomputer serving as a data acquisition device. These data were then used to evaluate the specimen behaviour, including the determination of which plate element of the specimens buckled first, causing specimen failure.

The specimens failed by web buckling, flange buckling, or a combination of both. Failure itself is caused by the first plate to deflect significantly.

In two of the three test series at the different P/Py ratios, the more slender specimen of the two failed at a lower Mu/My ratio than did the stockier section. However, for the specimens tested at P/Py = 0.15, the more slender specimen failed at a higher Mu/My ratio than the stockier section. This discrepancy has not been resolved.

The two web buckling theories previously developed for compact beam-columns(5) were re-developed, using the results of the present investigation. The theories, allowing for the differences between compact and non-compact members, adequately describe both types of beam-column behaviour. Furthermore, some of the conclusions previously postulated for compact members were extended to non-compact members.

A generalized web buckling theory has been developed which makes it possible to determine any beam-column web slenderness limit, provided the maximum web slenderness is known for a beam with the same flange proportions.

6.2 Conclusions

The main conclusion that this investigation has brought forward is that the web slenderness of non-compact beam-columns may be relaxed significantly. Hence, non-compact members will be used more efficiently in the future.

An important theoretical conclusion relates to the earlier work of Perlynn and Kulak in which it was noted that, for compact beam-columns, if α , the plate buckling modulus, is greater than 0.58, web buckling will invariably occur before flange buckling or simultaneous web and flange buckling. This investigation has shown that this conclusion is also valid for non-compact members. Extending this conclusion, if a specimen has not failed by local buckling when the strain (including the residual strain) at any point in the web has reached the yield strain, it appears that it will not fail by web buckling. This is equivalent to defining α_o as the value of α at the first occurrence of yielding.

Another conclusion of interest is the apparent lack of effect the specimen's proportions have on the revised plate buckling coefficient, K'. For six separate studies, four of which were considered by Perlynn and Kulak, and the other two in this investigation, all indicated that specimens failing by web buckling plotted erratically above a smooth curve formed by joining the points plotted for the specimens failing by simultaneous web and flange buckling or flange buckling. This smooth curve is another representation of the straight line corresponding to $\alpha = 0.58$ in Figure 5.11.

6.3 Recommendations

Since it has been determined that the web slenderness limits of non-compact beam-columns may be increased, it remains to alter the theoretical result, (Equation 5.22), such that it may be easily used for design purposes. This equation is:

$$\frac{h}{w}\sqrt{Fy} = 690\,[1 - 0.425\,(P/Py)^{0.385}] \qquad (6.1)$$

As previously noted, it is considered that this curve is slightly unconservative in the region of specimen 2. This will be taken into account, in proposing a limitation suitable for design use.

To maintain continuity between this investigation and the previous design approximations, a bi-linear design approximation will be proposed. This approximation is:

For $0 \leq P/Py \leq 0.15$,

$$\frac{h}{w}\sqrt{Fy} = 690\,[1 - 1.69\,(P/Py)] \qquad (6.2)$$

For $0.15 \leq P/Py \leq 1.0$,

$$\frac{h}{w}\sqrt{Fy} = 535\,[1 - 0.28\,(P/Py)] \qquad (6.3)$$

It is hoped that equations of this kind, based on this investigation, will be incorporated into future building standards. These equations, along with the theoretical limit, (Equation 6.1), and the present web slenderness limitations for non-compact beam-columns are shown in Figure 6.1.

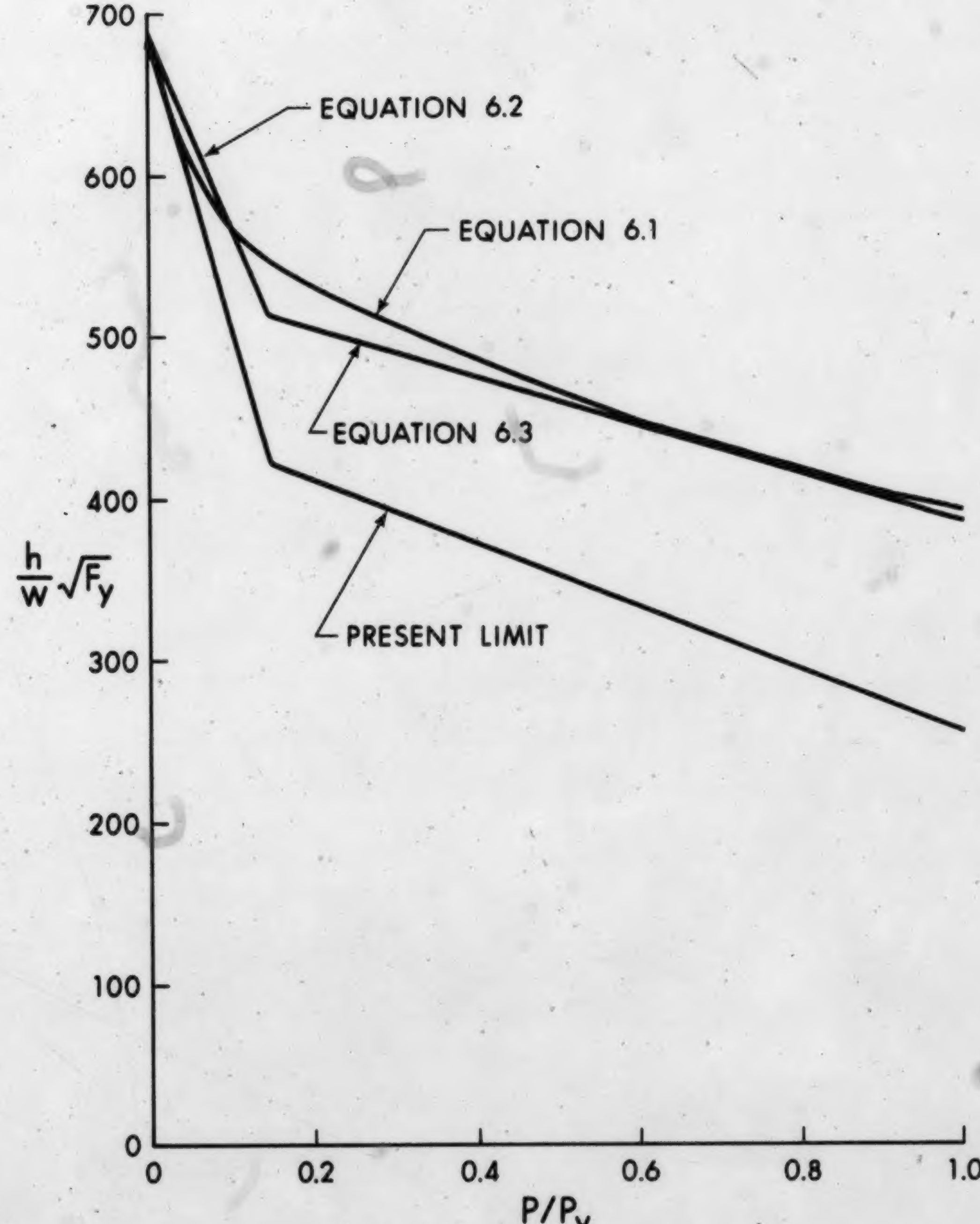

FIGURE 6.1

THE BI-LINEAR DESIGN APPROXIMATION

NOMENCLATURE

A = constant

A = total specimen area

Aw = specimen web area

b = width of flange

B = constant

C = constant

C = maximum beam web slenderness for a given flange slenderness

D = constant

D = EI/(1 - ν^2) for idealized plate buckling model

Dx = Ex/(1 - $\nu_x\nu_y$)

Dy = Ey/(1 - $\nu_x\nu_y$)

Dxy = ν_yDx

Dyx = ν_xDy

e = eccentricity of eccentric load (P_2)

E = Young's Modulus = 30000 ksi for Perlynn and Kulak(5)

E = Young's Modulus = 29600 ksi for present investigation

Ex = Young's Modulus in x-direction

Ey = Young's Modulus in y-direction

Fy = 44.33 ksi = yield stress of web material

Gt = tangent shear modulus

h = width of plate in plate buckling model

h = height of web

h_t = total height of specimen = 2t + h

H = (Dx + Dy + 4Gt)/2

I = moment of inertia

K = Timoshenko's(2) plate buckling coefficient

K = Haaijer and Thurlimann's(10) plate buckling coefficient for a fully-plastified wide-flange section

K' = modified plate buckling coefficient taken from beam-column tests

l = length of plate in plate buckling model

M = moment per unit length required for a unit rotation for plate buckling model

M = applied moment = P_2 X e

Mpc = plastic moment (reduced for axial load)

My = yield moment (reduced for axial load)

Mu = ultimate moment held by specimen

n = $2(\alpha_p - \alpha_o)/(\alpha_p(\alpha_p^2 - 1))$

P = applied axial load = $P_1 + P_2$

P_1 = concentric load applied by testing machine

P_2 = eccentric load applied by eccentric load jack

Py = Fy X A = specimen yield load

t = thickness of flange

u = plate mid-point deflection in plate buckling model

w = thickness of plate in plate buckling model

w = thickness of specimen webs

x = constant

x = Cartesian coordinate

y = Cartesian coordinate

y = distance to neutral axis from compression side of web

yo = distance to neutral axis of fully-plastified wide-flange section from compression edge of web

α = plate buckling modulus

α_o = 0.58 = alpha at the first occurrence of yielding

α_o = alpha at the point of strain-hardening

α_p = $\sqrt{\sigma_y/\sigma_p}$ = alpha at the proportional limit

β = B/A = Mh/2DyI = coefficient of restraint against rotation

δ = maximum initial web deflection

Δ = maximum strong-axis deflection of specimen at Mu

ε_{cr} = maximum strain in web when the ultimate moment is reached

ε_m = maximum compressive strain in web

ε_m = maximum compressive strain in flange

ε_{st} = strain at the beginning of the strain-hardening range as known on a stress-strain diagram

ε_y = yield strain of web plate material

σ_{cr} = maximum stress in web when ultimate moment is reached (not greater than σ_y)

σ_p = σ_y - σ_r = stress at proportional limit

σ_r = 15 ksi = maximum compressive residual stress in web

σ_x = uniform compressive stress applied to edge of plate elastically restrained against rotation along the unloaded edges

σ_y = 44.33 ksi = Fy

ν = 0.3 = Poisson's ratio for steel

ν_x = Poisson's ratio in the x-direction

ν_y = Poisson's ratio in the y-direction

REFERENCES

1. "CSA S16-1969 Steel Structures for Buildings", Canadian Standards Association, Rexdale, Ontario, 1969.

2. Timoshenko, S., and Gere, J., "Theory of Elastic Stability", Second Edition, McGraw-Hill Book Co. Inc., New York, N. Y., 1961.

3. "Specification for the Design, Fabrication and Erection of Structural Steel for Buildings", American Institute of Steel Construction, New York, N. Y., 1969.

4. Haaijer, G., "Plate Buckling in the Strain-Hardening Range", Journal of the Engineering Mechanics Division, ASCE, Volume 83, No. EM2, April 1957.

5. Perlynn, M. J., and Kulak, G. L., "Web Slenderness Limits for Compact Beam-Columns", Structural Engineering Report No. 50, Department of Civil Engineering, University of Alberta, September 1974.

6. "CSA S16.1-1975 Steel Structures for Buildings - Limit States Design", Canadian Standards Association, Rexdale, Ontario, 1975.

7. "CSA S16.2-1975 Steel Structures for Buildings - Working Stress Design", Canadian Standards Association, Rexdale, Ontario, 1975.

8. Bleich, F., "Buckling Strength of Metal Structures", McGraw-Hill Book Co., Inc., New York, N. Y., 1952.

9. McGuire, W., "Steel Structures", Prentice-Hall Inc., Englewood Cliffs, N. J., 1968.

10. Haaijer, G., and Thurlimann, B., "On Inelastic Buckling in Steel", Proceedings, ASCE, Volume 84, No. EM2, April 1958.

11. Holtz, N. M., and Kulak, G. L., "Web Slenderness Limits for Non-Compact Beams", Structural Engineering Report No. 51, Department of Civil Engineering, University of Alberta, August 1975.

12. "CSA G40.21-1973 Structural Quality Steels", Canadian Standards Association, Rexdale, Ontario, 1973.

13. American Society for Testing and Materials, "Standard Specification for Structural Steel-Designation A36-67", Philadelphia, Pa., 1967.

14. Yarimci, E., Yura, J. A., and Lu, L. W., "Techniques for Testing Structures Permitted to Sway", Fritz Engineering Lab Report No. 273.40, Lehigh University, Bethlehem Pa., 1966.

15. American Society for Testing and Materials, "Test Methods for Compression Members", ASTM Special Technical Publication No. 419, August 1967.

16. "CSA W59.1-1970 General Specification for Welding of Steel Structures (Metal-Arc Welding)", Canadian Standards Association, Rexdale, Ontario, 1969.

17. Nadai, A., "Theory of Flow and Fracture of Solids", McGraw-Hill Book Co., Inc., New York, N. Y., 1950.

18. Handelman, G. H., and Prager, W., "Plastic Buckling of a Rectangular Plate Under Edge Thrusts", National Advisory Committee for Aeronautics, Technical Note No. 1530, August, 1948.

19. Lundquist, E. E., and Stowell, E. Z., "Critical Compressive Stress for Flat Rectangular Plates Supported along all Edges and Elastically Restrained against Rotation along the Unloaded Edges", National Advisory Committee for Aeronautics, Technical Report No. 733, 1942.

20. Lukey, A. F., and Adams, P. F., "Rotation Capacity of Wide-flange Beams under Moment Gradient", Structural Engineering Report No. 1, Department of Civil Engineering, University of Alberta, May 1967.

21. Brockenbrough, R. L., and Johnston B. G., "United States Steel Design Manual", United States Steel Corporation, ADUSS 27-3400-02, November 1968.

APPENDIX I

DESIGN OF THE TEST SPECIMENS

It was decided, that because of the availability of test results for compact beam-columns(5), and test results for non-compact beams(11), testing two specimens at each of three different P/Py ratios would be sufficient to closely determine the maximum web slenderness limits for non-compact beam-columns.

The test results for the non-compact beams provided a means for estimating the maximum web slenderness ratio. This was done by determining the value of α from Perlynn and Kulak's(5) Equation 5.16 corresponding to the non-compact beam results. This equation is:

$$\alpha = \frac{h}{100w}\sqrt{Fy}\sqrt{\frac{0.01241}{1 - 0.695(P/Py)^{0.3846}}} \qquad (A1.1)$$

For P/Py = 0, Equation A1.1 becomes:

$$\alpha = 0.001114\ \frac{h}{w}\sqrt{Fy} \qquad (A1.2)$$

Substituting Holtz and Kulak's test result for non-compact beams of $\frac{h}{w}\sqrt{Fy} = 690$ in Equation A1.2 yields

$\alpha = 0.77$. This is the same value recommended by Haaijer and Thurlimann(10) to guarantee that web buckling will not occur for plates uniformly compressed up to the yield stress.

Having this value gives a reasonable indication of where the limit of web buckling might be. However, it was expected that the value of α would be somewhat higher than this for the case of non-compact beam-columns because of the effects of residual stresses, and the fact that not all the web is subjected to the yield stress. Somewhat arbitrarily, a value of $\frac{h}{w}\sqrt{Fy} = 750$ was chosen for $P/Py = 0$ to obtain a second value of α. Using the same procedure as before results in $\alpha = 0.84$.

By back-substituting the value of α in Equation A1.1, a unique relationship can be obtained for web slenderness as a function of P/Py. Figure A1.1 shows the two boundaries which are obtained by this procedure.

It was considered that it would be useful to incorporate the compact beam-column test results into the specimen design, if possible(5). An inspection of those test specimens indicated that specimen BC-9 failed at $M/Mpc = 0.9$, or at about the yield moment. While the flanges of their specimens were compact, and so the test result could not be used directly for this investigation, this specimen was still of some interest because it failed by web buckling, and its slenderness was only slightly below that of the curve corresponding to $\alpha = 0.77$ at $P/Py = 0.8$. Hence it was decided to design three of the specimens to be below the curve $\alpha = 0.77$ by the same amount as specimen BC-9 was at $P/Py = 0.8$. Similarly, the other three specimens were designed to be this amount above the curve corresponding to $\alpha = 0.84$. As mentioned in Chapter 3, it was hoped to gain some insight into beam-column behaviour in general, so the P/Py ratios chosen for the specimens were slightly different from those used in Perlynn and Kulak's testing program. In the end, P/Py ratios of 0.15, 0.3, and 0.7 were used to obtain results useful for a large range of beam-column design.

Once the position of the specimens had been determined with respect to web slenderness and P/Py ratios, the actual design was done. It was decided to use 1/4 in. plate for the webs. This was considered to be a reasonable thickness; thicker plates would require using very large loads for the tests, and thinner plates would be more affected by the residual stresses due to the welding of the flanges and mill rolling. It was also felt that thinner plates could have more pronounced out-of-straightness which could seriously affect the test results, particularly with respect to the critical buckling stress. Once the thickness was chosen, the value of "h" was determined, assuming the steel that the specimens would be fabricated from would have a yield stress of 44 ksi.

For the design of the flanges, the nominal yield stress was again used. As with the web plates, it was possible to choose both the width and thickness of the flange plates as only the ratio is of concern in local buckling problems for usual plate proportions. It was decided to use plate slightly thicker than the plate for the webs, mainly for the reason that in most structural wide-flange shapes the web is usually thinner than the flanges. Again, because of loading criteria, relatively thin plate had to be used for the flanges. Flanges were proportioned so that the CSA S16-1969 Standard was just satisfied for non-compact members. In this way, the most critical flange proportion for this member classification would be tested. The final flange size was chosen to be 5/16 in. by 9-1/2 in. This corresponds to $b/2t = 15.20$ which is slightly over the allowable by S16-1969 of $100/\sqrt{F_y} = 15.08$ for steel of yield strength 44ksi. The location of the specimens with respect to the curves corresponding to the two values of α are also shown in Figure A1.1.

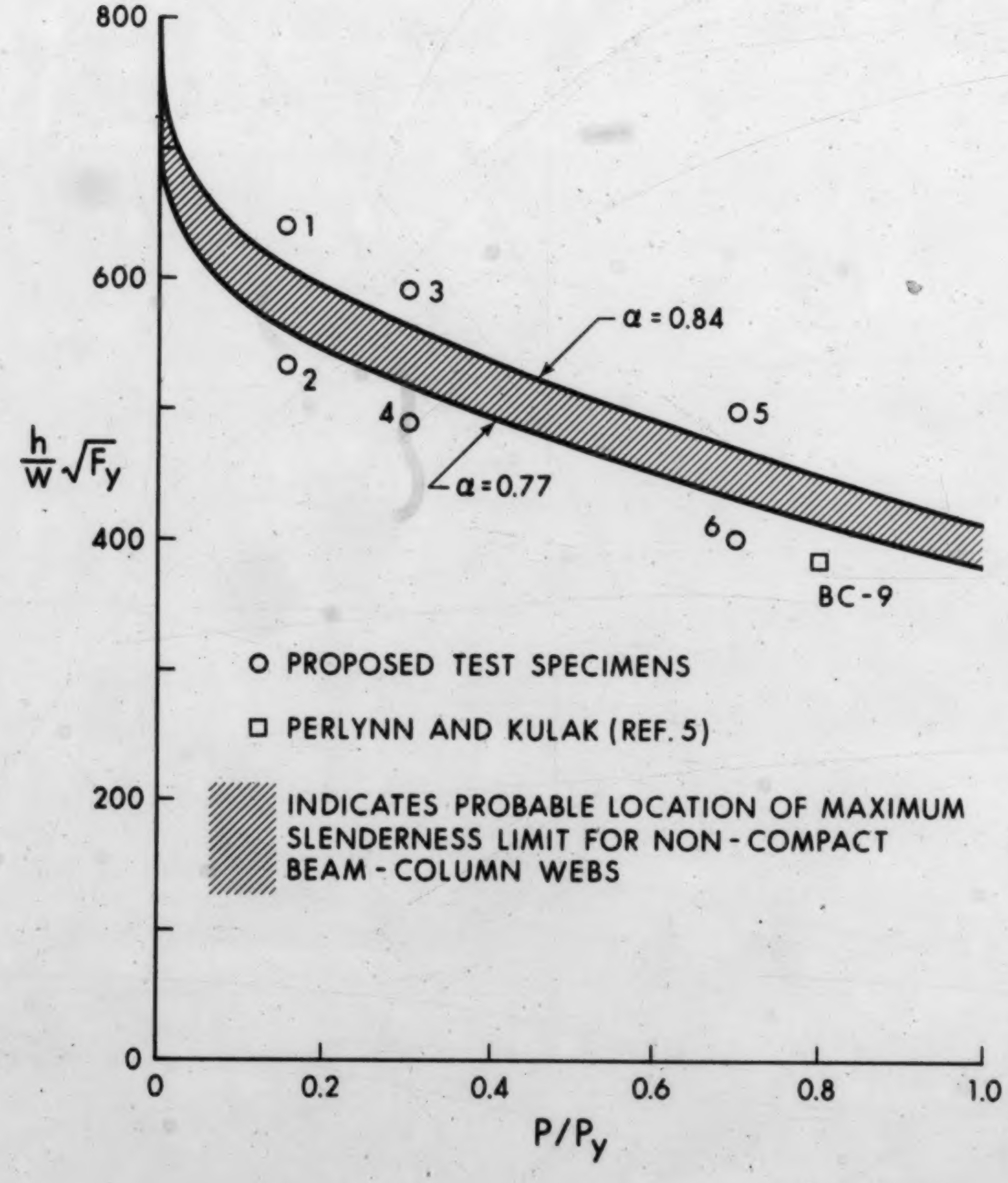

FIGURE A1.1

LOCATION OF THE TEST SPECIMENS

APPENDIX II

THE DEFLECTION MEASURING APPARATUS

A2.1 Introduction

This device made it possible to record many readings over a short period of time and store them for later processing. As a result, it was possible to plot accurate deflections of the web and the compression flange for a number of load increments. This in turn made the process of determining which plate element buckled first easier to do, and minimized the possibility of data misinterpretation.

A2.2 The Trolley

The apparatus itself was moved up and down by a motorized trolley (Figure 3.6). The trolley travelled about one inch per second, and was designed to follow the edge of the specimen's tension flange in such a way that the tension flange could be considered as datum for the positions of the grid points of the web. Because the tension flange was considered as datum, this provided a means for measuring compression flange deflections. The trolley was moved by a motor powering a drive gear along a gear rack which was fastened to the ends of the tension flange by two special clamps. Because of the stud used for lateral (weak-axis) bracing, it was necessary to put four wheels along the side of the trolley to keep it in proper position with respect to the edge of the tension flange. Two of these ran against the edge of the flange and the other two ran against a bar suspended between the same flange clamps as the gear rack. This system provided a means of preventing the trolley from creeping off the edge of the flange. To maintain proper tracking of the gear rack, the motor and drive gear were mounted on a plate sliding in a dovetail groove, with a wheel also mounted on the opposite side of the rack so as to keep the gear rack and drive gear properly meshed. This setup also allowed for rack deflections, as the dovetail plate was spring loaded.

In order to keep track of the vertical position of the trolley, it was fitted with a ten-turn potentiometer which was attached to one of the wheels running along the edge of the flange (Figure 3.6). The voltage across the potentiometer changed as the trolley moved, and the resulting analog signal was used by the minicomputer to sense where the trolley was, and, hence, when it was correctly positioned to take a reading. The trolley was also equipped with microswitches at both ends which touched spring loaded bumpers mounted on the tension flange clamps and prevented the apparatus from running off the ends of the specimen.

The trolley also carried the side-rack on which the deflection measuring apparatus was mounted. After one vertical set of readings, the apparatus was moved over to the next position manually and the next vertical string of readings taken. After measurement of the web was completed, the apparatus was turned 90° on a bracket mounted on the side rack and the compression flange readings were taken (Figure 3.7).

A2.3 The Apparatus

The apparatus itself operates on an optical feedback system. A light powered by a well-filtered power supply is housed along with a photocell in a container at the end of a flexible tube containing many strands of fiber optics. The light is positioned such that about 85% of the strands are able to transmit the light. The other 15% of the strands are used for the photocell.

The principle of operation is to shine a light via the fiber optics onto the surface being measured. Depending upon the reflectivity of the surface and on the angle between the probe and the surface, some light is reflected back up the tube in the 15% of the fiber optics connected to the photocell. The output of the photocell varies as the amount of light which strikes it varies. This output is amplified and modified by an electronic circuit to control the motor of the apparatus. The motor operates so as to correct for the reading of the photocell in such a way that an initial predetermined analog signal is maintained (Figure A2.1). This predetermined reading takes the form of deciding on a suitable distance for the probe to run above the surface it is measuring before any readings are taken. The correction is automatically made by means of a motor moving the probe either closer or farther away from the surface being measured. Hence the probe appears as if it is keeping the same distance between it and the surface it is following.

The portion of the flexible tubing doing the actual movement over the deflected surface is housed in a small pipe to make it rigid.

The shaft of the motor is connected so as to both move the probe and turn a potentiometer over which a regulated voltage is maintained. This potentiometer acts as a voltage divider and the resulting change in voltage from it was used to determine the deflections.

The initial probe height, and hence the initial photocell reading, was adjusted beforehand along with the damping of the probe, and its sensitivity. Because flat white paint proved to be ideal for making these adjustments, and for reflecting a reasonable but not excessive amount of light, the specimens were painted on the side the measurements were taken before the tests were performed. All readings were read into storage by the minicomputer for later processing.

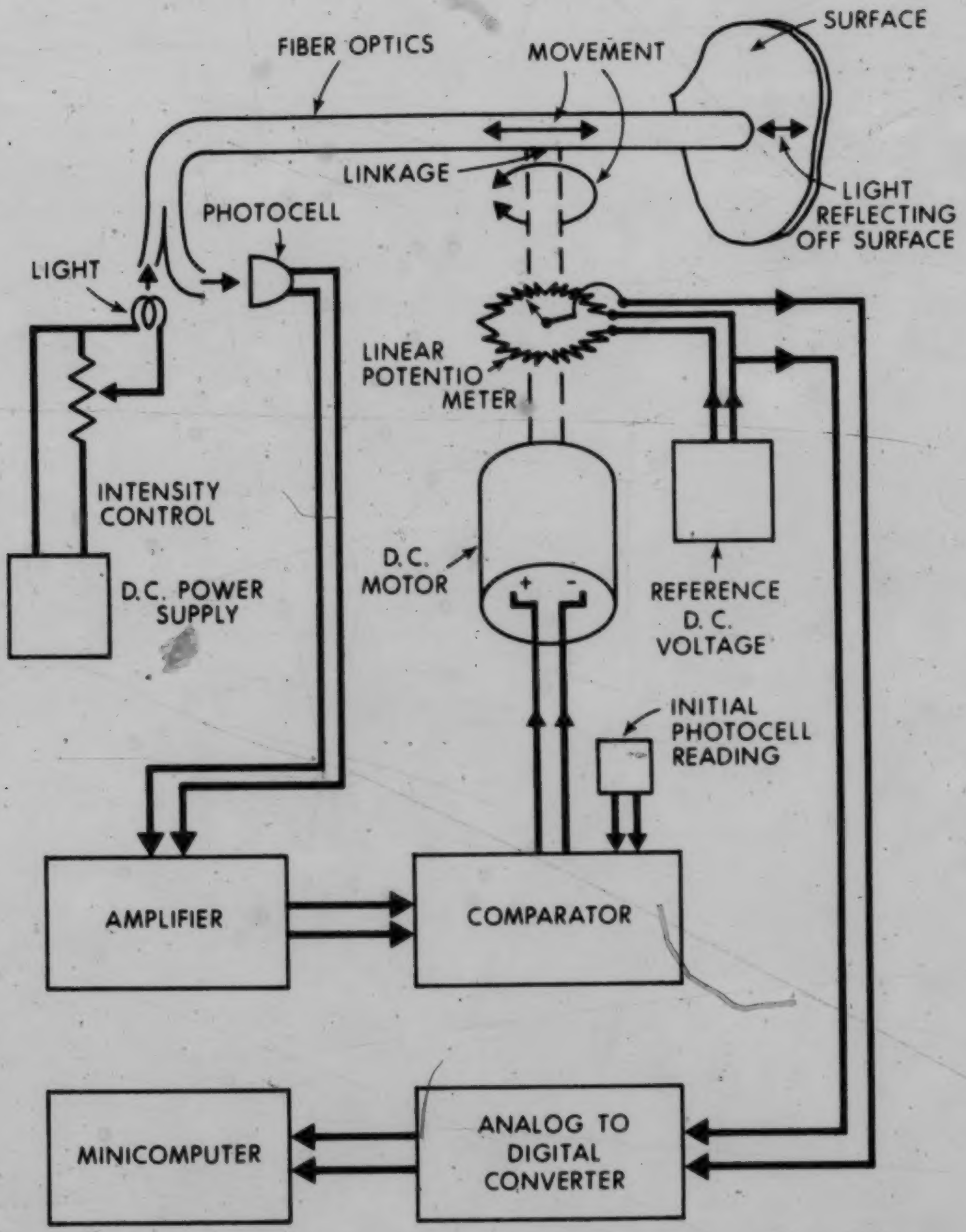
SURFACE
FIBER OPTICS
MOVEMENT
LINKAGE
PHOTOCELL
LIGHT
REFLECTING
OFF SURFACE
LIGHT
LINEAR
POTENTIO
METER
INTENSITY
CONTROL
D.C.
MOTOR
REFERENCE
D.C.
VOLTAGE
D.C. POWER
SUPPLY
+
-
INITIAL
PHOTOCELL
READING
AMPLIFIER
COMPARATOR
MINICOMPUTER
ANALOG TO
DIGITAL
CONVERTER

FIGURE A2.1

BLOCK DIAGRAM OF DEFLECTION MEASURING DEVICE